

# **Influence of Suspensor Development on Embryogenesis and its Cell Fate Specification in *Arabidopsis thaliana***

## **Dissertation**

der Mathematisch-Naturwissenschaftlichen Fakultät

der Eberhard Karls Universität Tübingen

zur Erlangung des Grades eines

Doktors der Naturwissenschaften

(Dr. rer. nat.)

vorgelegt von

**Yashodar Babu**

aus Tumkur/ India

Tübingen

2014

Tag der mündlichen Qualifikation: 14 October 2014

Dekan:

Prof. Dr. Wolfgang Rosenstiel

1. Berichterstatter:

Prof. Dr. Gerd Jürgens

2. Berichterstatter:

Prof. Dr. Rita Gross-Hardt

*A first step into my scientific career.*

## Acknowledgements

First and foremost I wish to thank my advisor, Dr. Martin Bayer. He has given me a wonderful opportunity to do PhD in his group. He has been supportive since the days I began working on cloning the construct for a pollen marker. Later I started to characterize *NMA* and I was also involved in mapping the mutation in *nma-1*. He gave full freedom and support, when I said that I wanted to link cell wall with cytoskeleton and also try to understand the cell elongation in *Arabidopsis* by studying *nma*. He continuously supported me all throughout my PhD. Considering my research interests he provided me a second project to identify the components of SSP-signaling during embryogenesis. He supported me both technically and also helped me to design new experiments throughout my PhD. He helped me to transform from a curious student into a proper researcher. But there is no end for a learning process; I will always remember him as one of my earlier Guru (teacher) in my life.

I want to thank my project instructor Prof. Gerd Jürgens. He has always been inspirational to me. His questions towards my research work have helped to realize the potential and also to think in a broader manner. I am grateful to his kind and generous gestures. I thank my PhD supervisor Prof. Rita Gross-Hardt. She helped me to understand my research questions in deeper thoughts.

I also want to thank to Dr. Christopher Grefen who has helped to understand and establish split ubiquitin based yeast two hybrid assays. His optimistic thoughts have encouraged me to conduct my assays and to analyse the results. He was very kind to share the vectors and yeast strains for these assays. I thank Dr. Matthias Flötenmeyer for the electron micrographs of immuno-gold labelling. I also want to thank Dr. Masahiko Furutani who helped me with immuno-staining and sharing his ideas about life and research.

I thank Ancilla Neu, who helped me to purify the NMA protein from *E.coli*. Her experience and advice was immense and she was involved for almost one year with biochemical characterization of the NMA protein. I also thank Prof. Ulrike Zentgraf for providing me some of the yeast vectors and strains.

Daniel and Jixiang were being wonderful as my dear friends and colleagues. They always backed me with their experience and knowledge. I am grateful for the cheerful moments in the lab provided by each and every person in the lab. Agnes has been a very good colleague who worked with me in the NMA project and also a wonderful friend. Martina is also another wonderful friend and colleague who helped in lab and with other things. Ole and Patric has helped me both scientifically and also as a friend. I also want to thank Thomas and Melanie for their help and support.

I want to thank my wife for her never ending support and encouragement. I am grateful for her belief in me and for motivating me. I am also grateful to my parents for their support. And I thank everyone who has helped me to complete my PhD.

## Table of Contents

<b>Acknowledgements</b> .....	<b>2</b>
<b>Table of Contents</b> .....	Error! Bookmark not defined.
<b>Zusammenfassung</b> .....	<b>5</b>
<b>Summary</b> .....	<b>7</b>
<b>3. Introduction</b> .....	<b>8</b>
3.1. Embryogenesis in <i>Arabidopsis thaliana</i> .....	<b>8</b>
3.2. Suspensor morphology and function .....	<b>8</b>
3.3 Suspensor cell fate determination during embryogenesis in <i>Arabidopsis thaliana</i> .....	<b>12</b>
3.4 Plant cell wall .....	<b>12</b>
3.5 Polygalacturonases and plant development .....	<b>16</b>
<b>4. Aim of this study</b> .....	<b>18</b>
<b>5. Results</b> .....	<b>19</b>
<b>Chapter I: Characterization of <i>NIMNA</i> function during early embryogenesis of <i>Arabidopsis thaliana</i></b>	
5.1. <i>NIMNA</i> is involved in cell elongation during early embryogenesis in <i>Arabidopsis thaliana</i> .....	<b>19</b>
5.2. Reciprocal crosses and haplo-insufficiency of <i>NMA</i> .....	<b>23</b>
5.3. Mapping the <i>nma-1</i> mutation .....	<b>24</b>
5.4. Gene annotation and other alleles of <i>NMA</i> .....	<b>25</b>
5.5. Developmental delay in <i>nma</i> and <i>ssp</i> embryos .....	<b>27</b>
5.6. Immuno-gold labeling with LM19 and LM20 .....	<b>31</b>
5.7. Adult plant phenotype of <i>nma</i> .....	<b>34</b>
5.8. Expression analysis of <i>NMA</i> .....	<b>36</b>
5.9. Cell-autonomous effect of <i>NMA</i> .....	<b>38</b>
5.10 Attempts to biochemically characterize <i>NMA</i> .....	<b>40</b>
5.11. Transient expression of <i>NMA</i> variants in <i>Arabidopsis</i> protoplasts .....	<b>44</b>
<b>Chapter II: Studying the SSP signaling cascade in <i>Arabidopsis</i> embryogenesis</b>	
5.12. MPK3/6 target search by generating phospo-mutants .....	<b>46</b>
5.13. Split Ubiquitin System (SUS) Yeast two hybrid screen to identify interaction partners of YDA and MPK3/6 .....	<b>49</b>
5.14 cDNA library construction and screening for interacting proteins of YDA and MPK6 .....	<b>56</b>
<b>Discussion</b> .....	<b>61</b>
6.1 <i>NMA</i> and suspensor cell elongation .....	<b>61</b>
6.2 SSP signaling cascade in <i>Arabidopsis</i> embryogenesis .....	<b>64</b>
<b>Materials and Methods</b> .....	<b>67</b>
<b>References</b> .....	<b>74</b>
<b>Appendix</b> .....	<b>83</b>
<b>Curriculum vitae</b> .....	<b>85</b>

## Zusammenfassung

Der pflanzliche Suspensor ist eine extra-embryonale Struktur, die den sich entwickelnden Embryo in die Samenhöhle hinausschiebt. Ihm werden verschiedene Funktionen zugeschrieben, unter anderem Nährstoff- und Hormontransport. Allerdings sind die Entwicklung des Suspendors und seine Rolle in der Embryogenese noch wenig verstanden. In einem vorwärts-gerichteten genetischen Ansatz, der auf Mutationen mit paternalem Effekt ausgerichtet ist, haben wir die *nma-1* Mutante identifiziert, die einen Defekt in der Streckung der Suspensorzellen zeigt. *nma-1* wurde einem Locus zugeordnet (At2g33160), der für eine putative Exopolygalacturonase kodiert. Diese Mutante weist einen Phänotyp mit kurzem Suspensor auf, und die Embryonen der *nma* Mutanten entwickeln sich langsamer als die von Wildtyp Pflanzen. Dies legt nahe, dass Suspensorlänge ein bestimmender Faktor für das Voranschreiten der embryonalen Entwicklung ist. Dies haben wir an einer zweiten Mutante mit kurzem Suspensor Phänotyp, *short suspensor (ssp)* ebenfalls nachgewiesen. Des Weiteren zeigen wir, dass die Funktion von NMA für die Streckung der Suspensorzellen zellautonom ist. NMA wurde in einem Screening nach paternalen Effekten isoliert und wir konnten weiterhin zeigen, dass der Beitrag des paternalen Allels zur Streckung der Suspensorzellen größer ist, als der des maternalen Allels. Dies deutet auf ungleiche parentale Einflüsse hin. Insgesamt weisen diese Ergebnisse eine Rolle für NMA in der Suspensorzellverlängerung und dessen Auswirkung auf die Embryogenese von *Arabidopsis* nach. Diese Arbeit zeigt, dass der Suspensor in *Arabidopsis* zusätzlich zu den bekannten Funktionen eine strukturelle Rolle in der embryonalen Entwicklung besitzt.

Neben der Rolle des Suspendors in der Embryogenese wurden die Komponenten des molekularen Mechanismus zur Bestimmung des Zellschicksals im Suspensor untersucht. Das Zellschicksal von Suspensorzellen wird in *Arabidopsis thaliana* von einem Signalweg bestimmt, der auf YODA (YDA) basiert. YDA ist eine mitogenaktivierte Protein-Kinase-Kinase-Kinase, an deren Aktivierung nach der Befruchtung mutmaßlich SSP beteiligt ist. YDA besitzt eine bekannte Funktion in der Entstehung von Stomata, aber über die Beteiligung des YDA Signalwegs an der Embryogenese ist wenig bekannt. Um mehr Elemente dieses Signalwegs zu identifizieren, haben wir einen Screen nach Phosphomutanten und split-Ubiquitin

basierte yeast-3-hybrid Experimente durchgeführt. Zusätzlich haben wir Proteine aus dem YDA Signalweg, die eine bekannte Funktion in der Stomataentwicklung haben, und ausgewählte andere Proteine auf physische Interaktion mit YDA getestet. Die neu identifizierten Interaktionskandidaten werden das Wissen über die Festlegung des Zellschicksals im Suspensor und die frühe embryonale Entwicklung in *Arabidopsis* erweitern.



## Summary

In plants, suspensor is an extra-embryonic structure that protrudes developing embryo into the seed cavity and they were ascertained with various functions including nutrient and hormone transport. However, the development of suspensor and its role in embryogenesis is not well understood. In a forward genetic screen for paternal effect mutants, we identified *nma-1* mutant which shows defects in suspensor cell elongation. The mutation in *nma-1* was mapped to a locus (At2g33160) which encodes for a putative exo-polygalacturonase. In consequence to the short suspensor phenotype, *nma* mutant embryos develop slower when compared to WT, suggesting suspensor length is one of the determinants for the developmental progression of the embryo. This result was also verified in another mutant with a short suspensor phenotype, *short suspensor (ssp)*. In addition we show that the NMA function in suspensor cell elongation is cell autonomous. As it was isolated from a paternal effect screen, and we were further able to show that the contribution of paternal allele of *NMA* towards suspensor cell elongation is stronger than the maternal allele suggesting the unequal parental contributions. These findings demonstrate the role of *NMA* in suspensor cell elongation and its effect on *Arabidopsis* embryogenesis. This study provides evidence describing the structural function of suspensor, in addition to its known functions.

Besides the role of suspensor in embryogenesis, we also report a study to identify the components of the molecular mechanism which specifies the suspensor cell fate. In *Arabidopsis thaliana*, suspensor cell fate is determined by a pathway mediated by YODA (YDA), a mitogen activated protein kinase kinase kinase, and SSP is assumed to be involved in YDA activation upon fertilization. In addition, YDA was also shown to function in stomata development. However little is known about the components of the YDA pathway involved in embryogenesis. Therefore, we performed a phospho-mutant screen and split ubiquitin based yeast three hybrid screen to identify components of this pathway. Additionally, we tested known proteins in this pathway which were previously shown to function in stomata development and other selected proteins for protein-protein interaction with YDA. Novel potential candidates isolated will broaden our knowledge about cell fate determination of suspensor and early embryo development.

### 3. Introduction

#### 3.1. Embryogenesis in *Arabidopsis thaliana*

In multi-cellular organisms, the fertilization event initiates embryogenesis and the subsequent cell divisions will lay the foundation for the basic body plan. Double fertilization is observed in flowering plants where the pollen tube delivers two sperm cells; one of them fusing with the haploid egg cell and another with the diploid central cell.

In *Arabidopsis thaliana*, where cell divisions are stereotypic during early embryogenesis, the zygote elongates nearly threefold and divides asymmetrically to produce two daughter cells with very distinct cell fates (Mansfield and Briarty 1991; Meinke et al., 1991). This asymmetric cell division is thought to occur based on the zygotic polarity (Ueda et al., 2011). Afterwards, the apical cell undergoes stereotypic cell divisions resulting in the pro-embryo, which constitutes most parts of the mature embryo and seedling. Meanwhile, the basal cell undergoes several rounds of cell division resulting in a file of cells. Only the uppermost suspensor cell contributes to parts of the root meristem whereas the other cells remain extra-embryonic (Scheres et al., 1994). This cell file is called suspensor because it suspends the embryo in a seed cavity while attaching it to the inner cells of the seed (Yeung and Meinke, 1993).

#### 3.2. Suspensor morphology and function

Suspensors or suspensor-like structures called foot can also be found in lower plant embryos including mosses and bryophytes (Wardlaw, 1955). It is tempting to speculate that it is one of the ancient embryonic structures and has evolved since the land plant lineage diverged from green algae around 450 million years ago (Sanderson 2003). Morphologically suspensors vary from vascular single cell to complex multicellular structures. Simple files of multicellular suspensors are observed in *Arabidopsis*, *Capsella bursa-pastoris* and *Diplotaxis eruroides* as well as other members of the Brassicaceae family (Fig. 1). Interestingly, suspensors in the Orchidaceae family usually are only an elongated single cell (Raghavan, 2006). Some members of the Loranthaceae family have a multi-seriate suspensor which extends into the style (Raghavan, 2006). In certain members of the Fabaceae, a possible correlation was noticed between the proliferated suspensor morphology and the reduced proportion of endosperm (Nagl, 1976). In an extreme case of suspensor

adaptation, some members of the Crassulaceae, Fumariaceae, Orchidaceae, Podostemaceae, Rubiaceae, Trapaceae and Tropaeolaceae families developed suspensors which are modified to haustoria-like structures for absorption and translocation of nutrients into the growing embryo (Raghavan, 2006).

The diverse suspensor morphologies prevailing in different plant families might suggest their evolution according to the adaptation of the plants. In addition to their morphological diversity, the subcellular features are also different in different suspensor types. Ultrastructural analysis of suspensors in *Stellaria media* embryogenesis revealed that it contains highly differentiated plastids, microbodies and mitochondria suggesting concentration of organelles in the suspensor compared to the pro-embryo (Newcomb and Fowke 1974). In general suspensors are marked by two specialized subcellular features which are existence of specialized plastids and lack of a cuticle layer (Raghavan, 2006).

Besides all these differences among suspensor types, these are commonly structures which are suspending the embryo in the seed cavity and are attached to the maternal tissue suggesting that their main function could be to serve as a channel for nutrients and hormones to the developing embryo. Sucrose is the main transportable carbohydrate found in plants (Ward et al., 1998) and in *Arabidopsis thaliana* SUCROSE TRANSPORTER 3 (SUC3) was shown to be up-regulated in the suspensor suggesting that the suspensor could be involved in sucrose transport to the pro-embryo (Stadler et al., 2005). Radioactive labeling experiments with  $^{14}\text{C}$ -putrescine and  $^3\text{H}$  in ovule cultures of scarlet runner bean (*Phaseolus coccineus*) demonstrated that these labels were transported to the embryo through the suspensor (Nagl, 1990). In another study the suspensor was shown to translocate  $^{14}\text{C}$ -sucrose from the endosperm to the embryo (Yeung, 1980). Mutant embryos in *vacuoleless1* (*vcl1*) show the presence of autophagosomes and it was speculated that this is due to starvation of the embryo because of inadequate nutrient flow through suspensor cells. Additionally, suspensors in the *vcl1* mutant show defects in cell elongation and the embryos show abnormal cell divisions (Rojo et al., 2001). All these experiments suggest that suspensor function is critical for transport of nutrients at early stages of at least *Arabidopsis* embryogenesis.

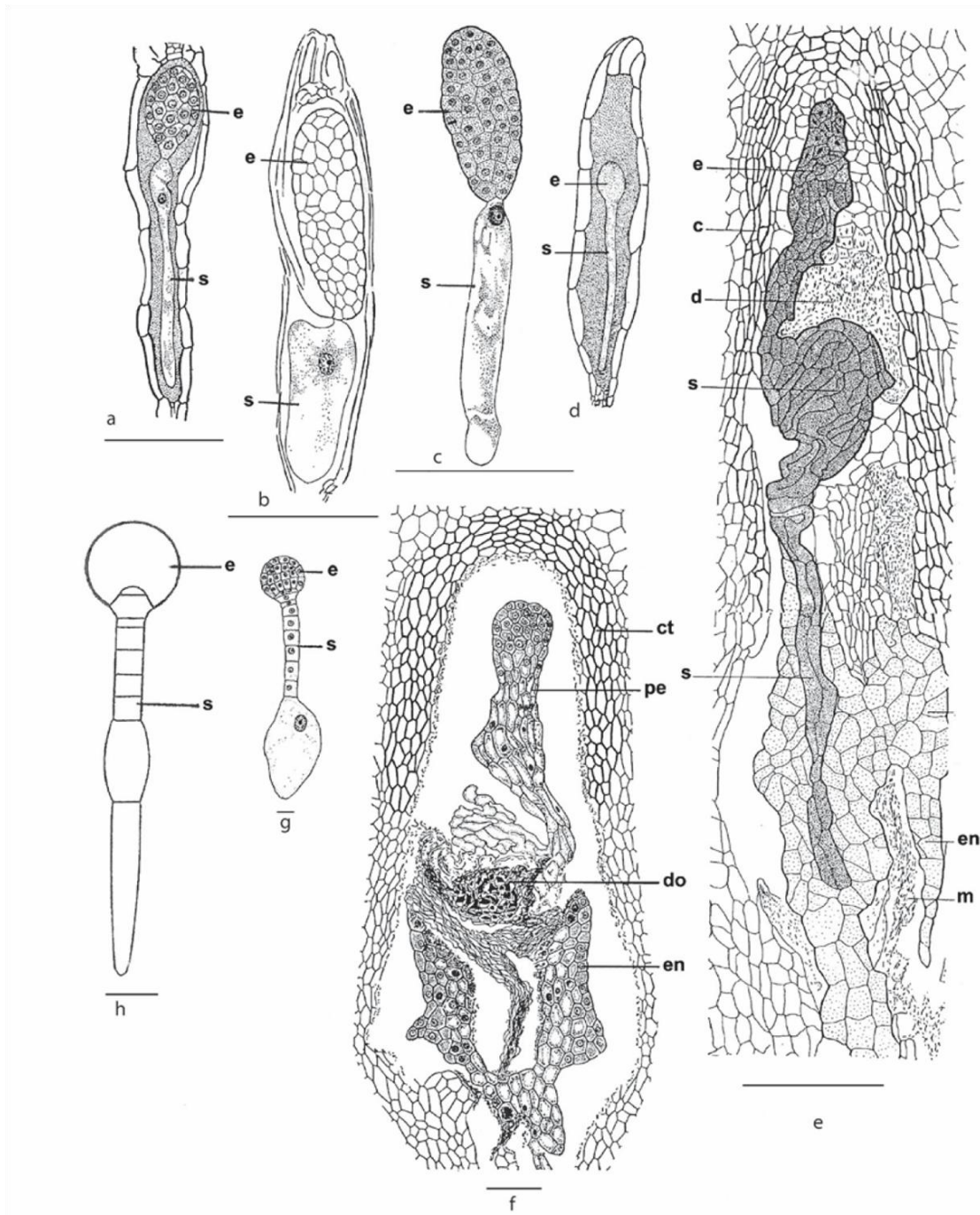


**Figure 1. Suspensor morphology in different plant families.** Orchidaceae, unicellular suspensor of *Bulbophyllum mysorense* (a), *Dendrobium barbatulum* (b), *Spathoglottis plicata* (c) and *Peristeria elata* (d). Loranthaceae, embryo-suspensor complex of *Macrosolen cochinsiensis* (e) and *Peraxilla tetrapetala* (f), respectively. Brassicaceae, filamentous suspensor of *Capsella bursa-pastoris* (g) and *Diplotaxis eruroides* (h). c Collenchyma, ct collenchymatous tube, d degenerated ovary cells, do degenerated ovarian tissue, e embryo, en endosperm, f fruit wall, m degenerated cells of the mamelon (a structure which arises from the base of the ovary and terminates at the point of the style), pe proembryo, s suspensor. Scale bars a-c, e 100µm (bar in a also applies to d); f 7µm; g 10µm; h 40µm. The figure is modified from Swamy 1949, Maheshwari and Singh 1952 and Raghavan, 2006.

In various studies, plant hormones were also shown to be present in suspensors of different plant species (Raghavan 2006). In certain species, gibberlic acid (GA) was shown to be synthesized and in other species to be only transported through the suspensor (Kawashima and Goldberg 2009). In a different study, *P. coccineus* embryos were shown to be dependent on suspensor for GA biosynthesis and transport in early stages (Piaggese et al., 1989). Furthermore, GA biosynthesis intermediates such as kaurene and ent-7 $\alpha$ -hydroxykaurenoic acids were identified in suspensor cells of *P. coccineus* and it was also shown that GA could be synthesized from exogenous precursors in suspensor cells (Ceccarelli et al., 1979, 1981a, 1981b). GA biosynthesis in the suspensor has been reported in the Fabaceae family, in *Arabidopsis thaliana* however the endosperm was shown to be the main synthesis site (Hu et al., 2008).

Transport of auxin, another plant hormone regulating many developmental processes in plants, was shown to be facilitated by PIN FORMED (PIN) auxin efflux carrier proteins providing directionality and cell specific accumulation of the hormone (Petrasek et al., 2006; Yang and Murphy 2009). In *Arabidopsis thaliana* PIN7 was shown to localize to the apical plasma membrane of suspensor cells and thereby it was proposed that at early embryonic stages auxin is transported to the pro-embryo via the suspensor (Friml et al., 2003). At later stages localized accumulation of auxin in the pro-embryo together with accompanying polarization of PIN1 towards the suspensor would eventually lead to auxin flow redirection and establishment of an auxin maximum in the hypophysis precursor cell (Robert et al., 2013; Friml et al., 2003). Altogether, the suspensor was shown to be involved in transport of both GA and auxin and in some cases even synthesis of GA (Friml et al., 2003; Piaggese et al., 1989; Ceccarelli et al., 1979, 1981a, 1981b), suggesting that it is indeed a channel for hormone transport during early stages of embryo development.

At later stages of embryo development the suspensor undergoes programmed cell death (PCD) (Nagl 1976). In Scarlet runner bean suspensor DNA degradation was shown to occur during PCD as a typical hallmark (Lambardi et al., 2007) and also that cysteine protease mClI-Pa functions during PCD (Bozhkov et al., 2005a). PCD is crucial for embryo development, since failure to activate it leads to abnormalities or even embryo arrest (Bozhkov et al., 2005b).

### **3.3 Suspensor cell fate determination during embryogenesis in *Arabidopsis thaliana***

The first step for establishment of apical and basal cell fate is acquisition of zygote polarity. In *A. thaliana* *WUSCHEL RELATED HOMEODOMAIN (WOX) 8* and possibly *WOX9* gene activation by *WRKY DNA BINDING PROTEIN 2 (WRKY2)* is thought to establish zygote polarity (Ueda et al., 2011). Additionally, in *yda* loss of function alleles the zygote fails to elongate and the basal cell fate is altered whereas *yda* gain of function embryos show altered apical cell fate during embryogenesis (Lukowitz et al., 2004). In the embryo, YDA is activated by an interleukin receptor associated kinase IRAK/Pelle-like kinase SHORT SUSPENSOR (SSP) upon fertilization. SSP mRNA is thought to be delivered through sperm cells to the egg cell during fertilization and is then translated in the resulting zygote (Bayer et al., 2009). MITOGEN ACTIVATED PROTEIN KINASE KINASE 4/5 (MKK4/5)-MITOGEN ACTIVATED PROTEIN KINASE 3/6 (MPK3/6) module were shown to act downstream of YDA during stomata development (Wang et al., 2007; Lampard et al., 2008). The double mutant of *mpk3*<sup>-/-</sup> and *mpk6*<sup>-/-</sup> is embryo lethal which suggest that they also function in embryo development. However, the phosphorylation targets of MPK3/6 in the YDA pathway during embryogenesis have not yet been determined and detailed information on SSP signaling and its components are still missing.

### **3.4 Plant cell wall**

Unlike in animals, plant cells are surrounded by a highly complex and dynamic structure called cell wall. The plant cell contains many solutes creating an internal osmotic pressure ranging from 0.1 to 3.0MPa (Somerville et al., 2004) which the cell wall resists by creating a homogenous turgor pressure and still allows for modifications which allow expansion of the cell (Schopfer 2006). Cell division along with cell wall dynamics determines the morphology of the tissue. Cell division in plants ends with accumulation and extension of cell wall materials in the plane of division. In some cells including fiber cells the primary cell wall is strengthened by deposition of a second layer called secondary cell wall. The each daughter cells formed by a symmetric cell division ends up with the same or larger volume as the mother cell which is achieved by expansion of the daughter cells through loosening and stiffening wall reactions facilitated by the cytoskeleton (Schopfer 2006). Additionally, the plant cell wall can be also modified in response to several developmental and environmental stimuli (Caffall and Mohnen 2009).

The composition of cell walls differs and thereby provides a potential for modification and control of the cell shape. The main constituents are polysaccharides, structural proteins and phenolic compounds and among the polysaccharides cellulose, hemicelluloses and pectins are the major classes of the primary cell wall in *Arabidopsis* (Fig. 2) (Cosgrove 2005; Somerville et. al, 2004). In general, the cell wall is a highly cross-linked structure of various networks such as pectin-pectin, pectin-xyloglucan, pectin-phenolic compound, pectin-protein and xyloglucan-cellulose networks (Fig. 2) (Caffall and Mohnen 2009). In order to understand the dynamics of the cell wall during cell elongation knowledge of these networks and their structure is of fundamental importance. Cellulose microfibrils forms a backbone of the cell wall in plants.

Cellulose is build up of unbranched microfibrils of  $\beta$ -1,4-glucose residues which are interconnected to other cellulose chains by hydrogen bonding and van der Waals forces (Nishiyama 2002). The exact length of fibril is not defined but could range between 500-15,000 units of glucose (Brett 2000). Naturally occurring cellulose chains in plants align parallel to each other (Sugiyama et al., 1991) and their molecular weight is lighter in the primary cell wall when compared to the secondary cell wall (Brown 2004; Brett 2000). Synthesis of cellulose is achieved by a multimeric complex comprised of CELLULOSE SYNTHASE (CESA) proteins residing directly at the plasma membrane and secreting the microfibrils (Ha et. al, 1998; Delmer 1999). As cellulose microfibrils are deposited transversely to the direction of elongation, during cell expansion they re-orient parallel to the direction of elongation. Additionally, these fibrils are strengthened by synthesis of new fibrils which orient in multiple angles against the existing strain (Anderson et al., 2010). The orientation of the fibrils is coordinated with cortical microtubules (Baskin et al., 2004). Interestingly, perturbation of the parallel alignment between cortical microtubules and nascent cellulose microfibril revealed that modifications in pectin influence the deposition of cellulose microfibrils and/or the maintenance of their orientation parallel with the cortical microtubules (Yoneda et al., 2010).

Hemicellulose consists of branched polymers of  $\beta$ -1,4-linked pyranosyl residues with O-4 in the equatorial position (ONeill and York 2003). Depending on the residues in the backbone and side chains, different types of hemicelluloses are identified in nature such as xylans, mannans, xyloglucan and arabinogalactan. Xyloglucan is the



most abundant hemicellulose in dicots and is known to interact with cellulose networks increasing their expansibility (Whitney et al., 2006; Chanliaud et al., 2002). Generally, both in monocots and dicots hemicelluloses are more abundant in secondary cell walls than in the primary cell wall (Caffall and Mohnen 2009).

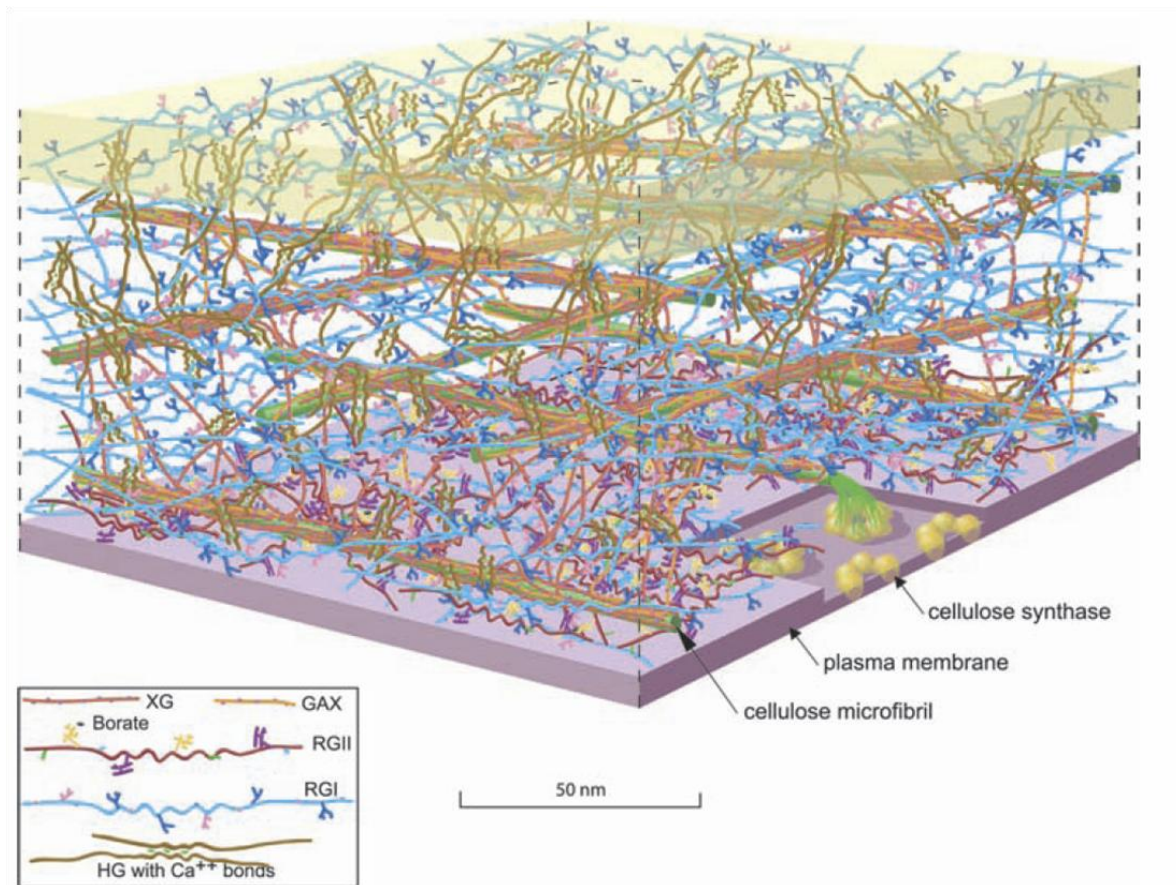


**Figure 2. Model representing the polysaccharides in the cell wall of an *Arabidopsis* leaf cell.** The structural backbone of the cell wall consists of cellulose microfibrils and hemicelluloses. Pectins (HG, XG, RGI and RGII) form a matrix interconnecting each other and hemicelluloses. The figure is an elaboration of a model originally presented by McCann and Roberts. The figure was rendered by Abbey Ryan and published in Somerville et al., 2004.

Unlike cellulose, pectins are complex polysaccharides which are linked to other pectins and wall molecules forming a pectin network structure. The complexity of this network and modulation of the crosslinks are major determinants of strength, flexibility and functionality of the primary cell wall (Caffall and Mohnen 2009). Pectins were also shown to crosslink hemicelluloses, phenolic compounds and proteins, thus providing structural and functional complexity to the cell wall. Also, pectins were shown to be important for many functions including cell elongation, control of cell



strength, cell adhesion, regulating stomata function and defense response (Caffall and Mohnen 2009).

Pectins are polymers mainly composed of galacturonic acid in their backbone. They are most abundant in the primary cell wall and middle lamella providing developmental flexibility to the cell. Pectins can be grouped into five structural classes depending on their complexity which are homogalacturonan (HG), apiogalacturonan (AGA) and xylogalacturonan (XGA), rhamnogalacturonan I (RGI) and rhamnogalacturonan II (RGII). Homogalacturonan (HG) is a linear polymer of  $\alpha$ -1,4-linked-D-galacturonic acid that represents more than 60% of pectin in the plant cell wall (Ridley et al., 2001). Apiogalacturonan and xylogalacturonan are HG substituted by D-apiose and D-xylose respectively. Rhamnogalacturonan I has alternating galacturonan and rhamnose residues, while the rhamnogalacturonan II structure is highly complex with 12 different types of glycosyl residues (Caffall and Mohnen 2009).

Homogalacturonan represents around 23% of the *Arabidopsis* leaf walls and is often referred to as pectin in the literature (Zablackis et al., 1995). The galacturonic acid (GalA) residues of HG can be methyl-esterified at the C-6 carboxyl group or acetylated at the O-2 or O-3 positions although the functional significance of acetylation of GalA in HG and in RG-I residues is not clear (Caffall and Mohnen 2009). Methyl-esterification is tightly regulated by the plant in a developmental and tissue-specific manner (Wolf and Greiner 2012). Pectin methyltransferases (PMT) act while pectins are synthesized in the Golgi apparatus (Lennon and Lord 2000; Li et al., 1997). During plant development these marks are removed by pectin methylesterases (PME) and contrastingly, the PME activity can also be blocked by PME inhibitors (Jolie et al., 2010). A low level of pectin methyl esterification is often correlated with wall extensibility. In that respect, demethylesterification might lead to either consolidation of the cell wall by cross-linking with  $\text{Ca}^{2+}$  or degradation of the pectin polysaccharides allowing cell separation and cell elongation events (Wolf and Greiner 2012).

After analysis of 291 amino acid sequences of glycosyl hydrolases, they were classified into the so called family 28 which by then only consisted of four polygalacturonases (PG) and one exo-polygalacturonase (exo-PG) (Henrissat 1991). All family 28 glycosyl hydrolases act by a general acid catalysis mechanism in which

two amino acid residues participate in a single-displacement reaction resulting in an inversion of the configuration at the anomeric carbon atom of the hydrolyzed glycoside (Sinnott, 1990). The family includes five types of enzymes depending on the substrate specificity: (i) endo-polygalacturonase (endo-PG) or polygalacturonase (PG; EC 3.2.1.15) which randomly hydrolyses pectins while (ii) exo-polygalacturonase (EPG; EC 3.2.2.67) hydrolyses one GalA residue at a time from the non-reducing end; (iii) exo-poly- $\alpha$ -galacturonosidase (EPGD; EC 3.2.1.82) hydrolyses two GalA residues also from the non-reducing end; (iv) rhamnogalacturonase (RG; EC 3.2.1.171) hydrolyses  $\alpha$ -1,2 glycosidic bonds between GalA and rhamnose and (v) endo-xylogalacturonan hydrolase (XGH; EC 3.2.1.-) randomly hydrolyses glycosidic bonds between GalA and xylose (Caffall and Mohnen 2009).

Plant pathogens secrete pectate lyase (EC 4.2.2.2) which is important for their pathogenesis. Pectate lyase cleaves by  $\beta$ -elimination of the GalA residues and this produces C4-C5 unsaturated bonds at non-reducing ends of the polysaccharides (Pickersgill et al., 1994). Pectate lyase-like (PLL) genes with strong amino acid sequence homology with the PelC isoform of bacterial pectate lyases has been reported to be also present in plants (Wing et al., 1989; Marín-Rodríguez et al., 2002; Palusa et al., 2007; Zhang 2003). PLL promoter activity in *Arabidopsis* was mainly observed in abscission zones (AZs) or dehiscence zones (DZs) suggesting that they might be involved in cell-separation.

### 3.5 Polygalacturonases and plant development

As homogalacturonans represent a major proportion of pectins, degradation of this polysaccharide will essentially contribute towards loosening the pectin matrix cross-linking with each other and hemicelluloses. In bacteria and fungi the sequence identity in endo-polygalacturonases is low (4.7 and 8.9%) while in exo-polygalacturonases it is much higher (23.7% and 36.7%). However, the active sites of all these PGs are well conserved arguing for a similar type of catalytic reaction (Markovic and Janecek, 2001). The GH 28 family protein structure resembles a conventional right-handed parallel  $\beta$ -helix topology. An endo-polygalacturonase isolated from *Erwinia chrysanthemi* displays a tunnel-like structure; this allows the enzyme to bind the substrate randomly. Whereas in an exo-polygalacturonase isolated from *Yersinia enterocolitica* (YeGH28), a loop has been inserted blocking the

other end and rendering it to look like a pocket. The structures of the exo-polygalacturonase (YeGH28) will only allow it to bind to the substrate at non-reducing ends (Abbott and Boraston 2007). Although this loop will allow discrimination of EPG from PG, in plants a clear demarcation is not possible in all cases based on sequence similarities (Markovic and Janecek, 2001). According to this classification system, plant PGs can be divided into five clades based on the evolutionary tree constructed on sequence similarities (A, B, C, D and E) (Markovic and Janecek, 2001). *Arabidopsis* alone contains 59 PGs including EPGs suggesting a high degree of functional redundancy.

The involvement of polygalacturonases in plant development is essential as they control mechanistic properties of the cell. *POLYGALACTURONASE INVOLVED IN EXPANSION1 (PGX1)* was recently shown to be involved in cell elongation in hypocotyls and floral organ patterning in *Arabidopsis thaliana* (Xiao et al., 2014). During cotton cotyledon expansion the activity of endo-PGs was shown to be high during early stages while the activity of exo-PGs peaked at later stages. Additionally, the length of HG polymers was characterized during cotyledon development and indicated that the polymer length is much shorter at early stages arguing that endo-PG activity is required for rapid growth (Zhang et al., 2007). In tomato (*Lycopersicon esculentum*), LeXPG activity was shown to be involved in modifying mechanistic properties of the endosperm and thereby allowing radicle protrusion from tomato seeds. Later the loosening of cell walls by LeXPG1 at the radicle tip and throughout the expanding embryo will potentiate the function of PGs in cell elongation necessary for growth (Sitrit et al., 1999).

#### 4. Aim of this study

In plants the suspensor is formed by a file of cells which are attached to the embryo. The suspensor cell fate acquisition during embryogenesis is poorly understood and its structural impact on early embryogenesis is still unclear. This study focuses on understanding aspects of these questions.

In the first part, we characterized the *nma* mutant with a short suspensor phenotype. The impact of the short suspensor phenotype on embryogenesis has been analyzed by studying the *NMA* phenotype in detail. As the suspensor cells fail to elongate in the *nma* mutant, by studying its function we wanted to gain insights into the mechanism of cell elongation during embryogenesis. As the mutant was isolated from a paternal effect screen, it was interesting to study the parental effect of *NMA* on embryogenesis.

In the second part, we wanted to understand how suspensor fate is determined during early embryogenesis in *Arabidopsis thaliana*. Although this mechanism is poorly understood, it was shown that the SSP signaling cascade is involved in this process through the YDA mitogen activated protein kinase kinase kinase (Bayer et al., 2009; Lukowitz et al., 2004; Wang et al., 2007). Our main aim was to identify components of SSP signaling to improve our understanding of suspensor cell fate specification during early embryo development.

## 5. Results

### Chapter I: Characterization of *NIMNA* function during early embryogenesis in *Arabidopsis thaliana*

An ethyl methanesulfonate (EMS) mutagenesis screen was performed to identify paternal effect mutants. Upon observing the developmental defects in these mutants during embryogenesis we chose to work on a mutant, which was later termed as *NIMNA* (Sanskrit word for sunken or low). *nma-1* mutant embryos show cell elongation defects during early embryogenesis and spectrum of mutant phenotypes were observed in *nma* embryos. Most of the studies described in this chapter are conducted with homozygous *nma* plants. The following chapter deals with the further characterization of this mutant. Most of the work in this chapter has been already published and the figures (including figure legends) were directly taken from the journal article (Babu et al., 2013).

#### 5.1. *NIMNA* is involved in cell elongation during early embryogenesis in *Arabidopsis thaliana*

After fertilization the zygote elongates almost three fold and divides asymmetrically to produce a smaller apical cell and a larger basal cell. The basal cell remains extra-embryonic and after several rounds of cell division results in a file of cells called suspensor (Yeung and Meinke, 1993). In *nma-1* mutants both apical and basal cell remain shorter and wider when compared to *Ler* wild-type (WT, Fig.3). The cells of the basal lineage divide further but fail to elongate resulting in an overall shorter suspensor. As the suspensor cells are shorter but wider in *nma-1*, we measured the area of the uppermost suspensor cell of globular stage embryos and compared it with wild-type expecting that the area/volume would be similar. The area of the uppermost suspensor cell in *nma-1* was comparable to wild-type *Ler* (*nma-1*  $485.9 \pm 97.9 \mu\text{m}^2$ ,  $n = 11$ ; wt *Ler*  $468.3 \pm 74.4 \mu\text{m}^2$ ,  $n = 16$ ; no statistical significance by Mann-Whitney u test;  $P < 0.05$ ) suggesting that the cells elongate rather in the horizontal than the vertical direction.

The apical cell divides several times to form the pro-embryo and later on most parts of the seedling. Until globular stage, the pro-embryo in *nma-1* remains smaller when compared to *Ler*WT (Fig. 3E)

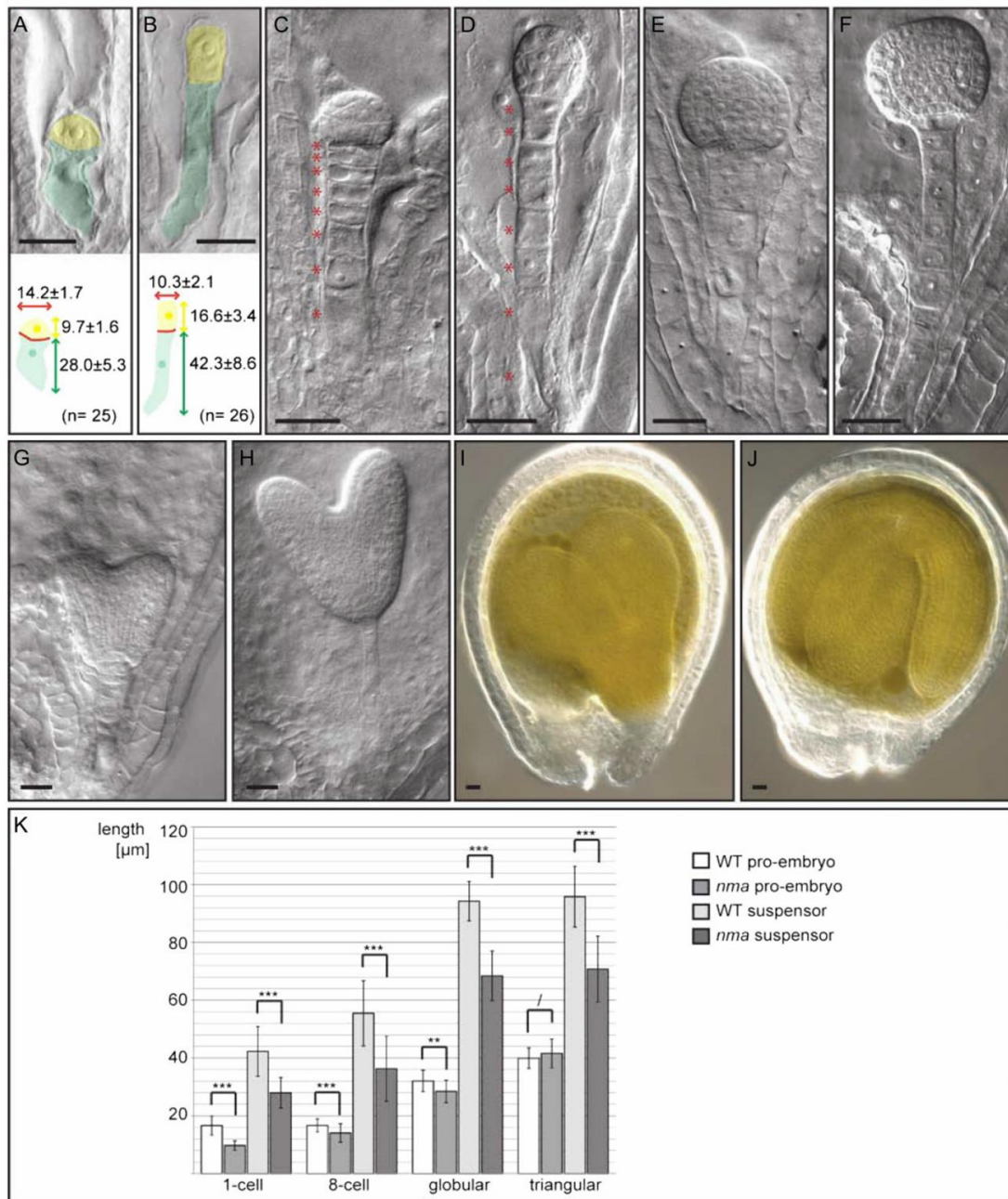


**Figure 3. Embryonic phenotype of *nma* mutants compared to wild-type.** **A** and **B**, *nma-1* (**A**) and WT (**B**) one-cell stage embryos. Apical cells are false colored in yellow; basal cells are false colored in green. Measurements are given as arithmetic mean values with SD in micrometers. **C** and **D**, *nma-1* (**C**) and WT (**D**) 16-cell stage embryos. Suspensor cells are highlighted by accompanying asterisks. **E** and **F**, *nma-1* (**E**) and WT (**F**) late globular stage embryos. **G** and **H**, *nma-1* (**G**) and WT (**H**) heart stage embryos. **I** and **J**, *nma-1* (**I**) and WT (**J**) developing seed 7 dap. Bars = 20  $\mu\text{m}$ . **K**, Measurements of proembryo and suspensor length at different developmental stages. Number of analyzed embryos at one-cell stage: both *nma-1* and WT, n = 26. At eight-cell stage: *nma-1*, n = 101 and WT, n = 98. At globular

stage: *nma-1*, n = 36 and WT, n = 29. At triangular stage: *nma-1*, n = 54 and WT, n = 33. Mean values are shown with SD. Significant differences were determined in pair-wise comparison by Mann-Whitney U test (\* =  $P < 0.05$ , \*\* =  $P < 0.01$ , \*\*\* =  $P < 0.001$ , and / =  $P < 0.05$ ). WT, Wild-Type. This figure is taken from Babu et al., 2013.

At transition stage when the cotyledons are specified and outgrowth is initiated, *nma-1* embryos resemble WT embryos except for the shorter suspensor (Fig. 3G). In addition to cell elongation defects, the pro-embryo shows several defects in development. Around transition stage, the uppermost suspensor cell and at the same time the precursor cell of the hypophysis showed oblique division planes instead of vertical divisions. These oblique divisions occur in about 25% of *nma-1* embryos (n=101) (Fig. 4A) and can also be seen in the third or fourth suspensor cell from the top. In Ler WT, we observed only 6.7% (n = 478) of embryos with similar oblique divisions. Additionally, at early heart stage, in 9.5% *nma-1* embryos (n=303) the suspensor remains extremely short and concomitantly the pro-embryo shows epidermal defects in the cotyledons due to spatial constraints (Fig. 4C). These additional phenotypes might be a secondary effect on embryogenesis because of the shorter suspensor. All mutant embryos recover from these effects and germinate as normal looking seedlings.

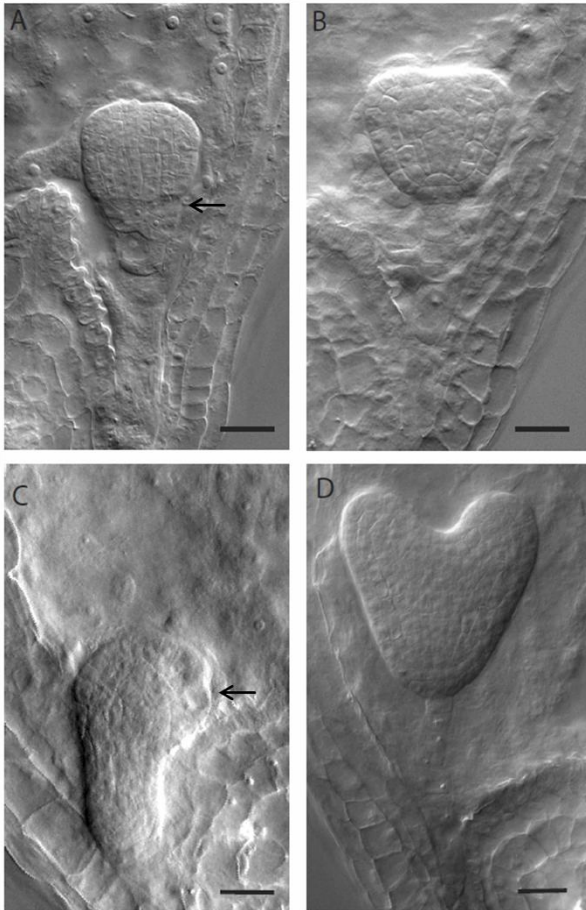


**Figure 4. Other embryonic phenotype of *nma-1*.** **A** and **B**, *nma-1* (**A**) and WT *Ler* (**B**) transition stage embryos, arrow mark indicates oblique division in the uppermost suspensor cell. **C** and **D**, *nma-1* (**C**) and WT *Ler* (**D**) early heart stage embryos, arrow mark indicates bulged epidermal cell in *nma-1* embryos. Scale bars 20 $\mu$ m.

In order to understand if the suspensor phenotype is caused by the physical restraint of the cell wall or because the identity of the suspensor is affected, we introduced a plasma membrane localized suspensor marker *pSUC3:tm-GFP* in *nma* mutant lines (Stadler et al., 2005). We observed proper expression of this marker in the suspensor cells, suggesting that the identity of the suspensor was not affected in *nma-1* mutants (Fig. 5). Although, the suspensor cells are shorter still they retain their identity. This result also implies that NMA may not be involved in SSP signaling cascade in determining the suspensor cell fate.



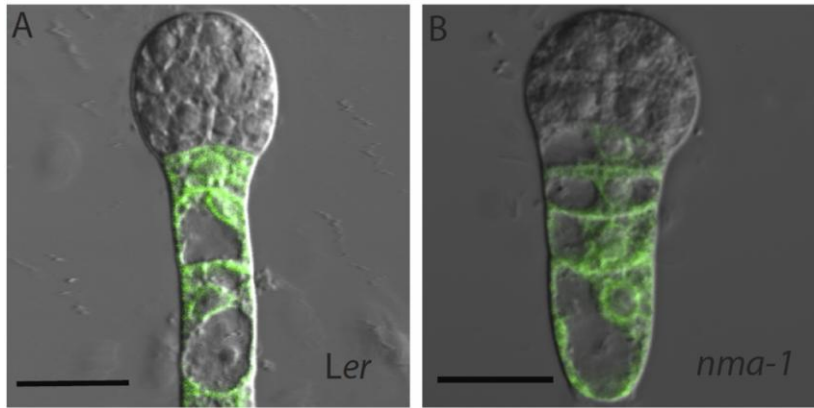


**Figure 5. Localization of suspensor marker *pSUC3::tm-GFP*.** *Ler* WT 16-cell stage embryo (A), *nma-1* 116-cell stage embryo (B). Scale bars 20 $\mu$ m.

## 5.2. Reciprocal crosses and haplo-insufficiency of *NMA*

*SSP* shows a true paternal effect on embryogenesis (Bayer et al., 2009). Both in *ssp* and *nma*, mutations cause a shorter suspensor. As *nma-1* was identified in a paternal effect screen, we conducted reciprocal crosses between *nma* and WT plants. Seeds from these crosses were collected three days after pollination and the suspensor length was measured only from transition stage embryos in order to keep the population uniform. ♀WT x ♂*nma* crosses produced significantly shorter suspensors in comparison to ♀*nma* x ♂WT and to WT x WT ( $P < 0.001$  in Mann-Whitney U-test; Fig. 6). However, *nma* x *nma* produced shortest suspensors among all the crosses. This result indicates that *NMA* has stronger contribution when inherited paternally in suspensor development. Although it is not a true paternal effect, it still reflects dosage dependency of *NMA* in suspensor development with unequal contribution by the parents.

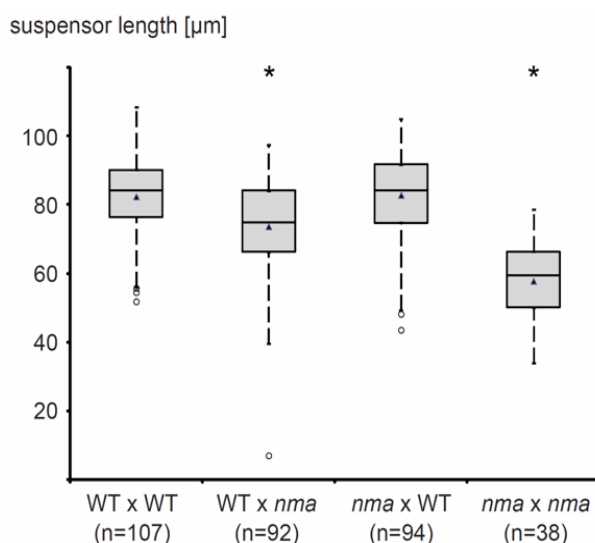


**Figure 6: Measurements of suspensor length after reciprocal crosses of wild-type (*Ler-1*) and *nma-1* mutant plants.** Numbers of measured suspensors are given in brackets. Significant differences to wild-type test crosses (WT x WT) as indicated by Mann Whitney U-test ( $p < 0.001$ ) are highlighted by an asterisk. Boxes represent lower and upper quartiles around median. Mean values are shown as triangles. This figure is taken from Babu et al., 2013.

### 5.3. Mapping the *nma-1* mutation

The mutation in *nma-1* was already mapped to an interval of 153,640bp by Agnes Henschen and Martin Bayer as described below. Rough mapping indicated that the mutation resided on the second chromosome with an interval of 380kbp between markers T32F6 and F4P9. Furthermore, we analyzed 4002 chromosomes to identify any recombination events within this interval. From this screen, we were able to recover 17 F2 plants narrowing the interval down to 153,640bp between markers 255-X (At2g33255) and 5B2-1 (At2g32870) (Fig. 7). Since we could not observe any recombination events in this interval, we amplified and sequenced all annotated coding sequences within this interval. Finally, we mapped the *nma-1* mutation to a G-A nucleotide substitution at position +836bp of the protein coding sequence which resulted in an amino acid substitution G279D in the At2g33160 locus.

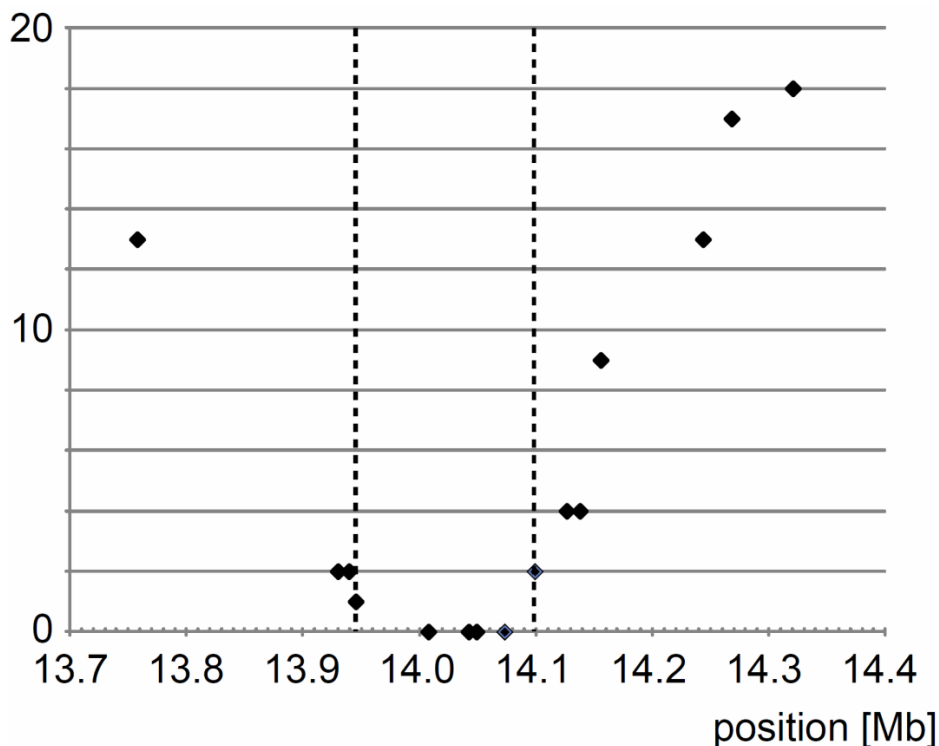


**Figure 7: Fine mapping of *nma-1*.** Numbers of recombinants in a 563kbp genomic interval surrounding the *nma-1* locus on chromosome II are shown. Dashed lines indicate an interval without further recombination events. This figure is taken from Babu et al., 2013.

*NMA* encodes for a putative member of the exo-polygalacturonase family, which are shown to hydrolyse two GalA residues from the non-reducing end of a homogalacturonan (Caffall and Mohnen 2009). The modification of homogalacturonan polymer has been ascertained as a dynamic process and essential for plant growth and development (Caffall and Mohnen 2009).

#### **5.4. Gene annotation and other alleles of *NMA***

The annotation of *NMA* in TAIR as a gene model contained a third exon which encodes for an RNase H fold (Fig. 8C). This model was not supported by either ESTs available or our RT-PCR data. We analyzed the gene model by amplifying the entire coding region from cDNA and we could not get the full annotated sequence. We designed more primers to amplify different parts of the coding sequence. The RT-PCR results indicated that the *NMA* locus has two exons and the second intron is actually the 3' UTR. 3' rapid amplification of cDNA ends (RACE) PCR supported this finding; according to these results, we re-annotated the gene model and the protein model of *NMA* (Fig.8A). According to the amino acid sequence, the signal peptide resides at the N-terminus for extra-cellular localization followed by a cleavage site and polygalacturonases domain (Fig. 8B). The *nma-1* mutation also resides in polygalacturonase domain.

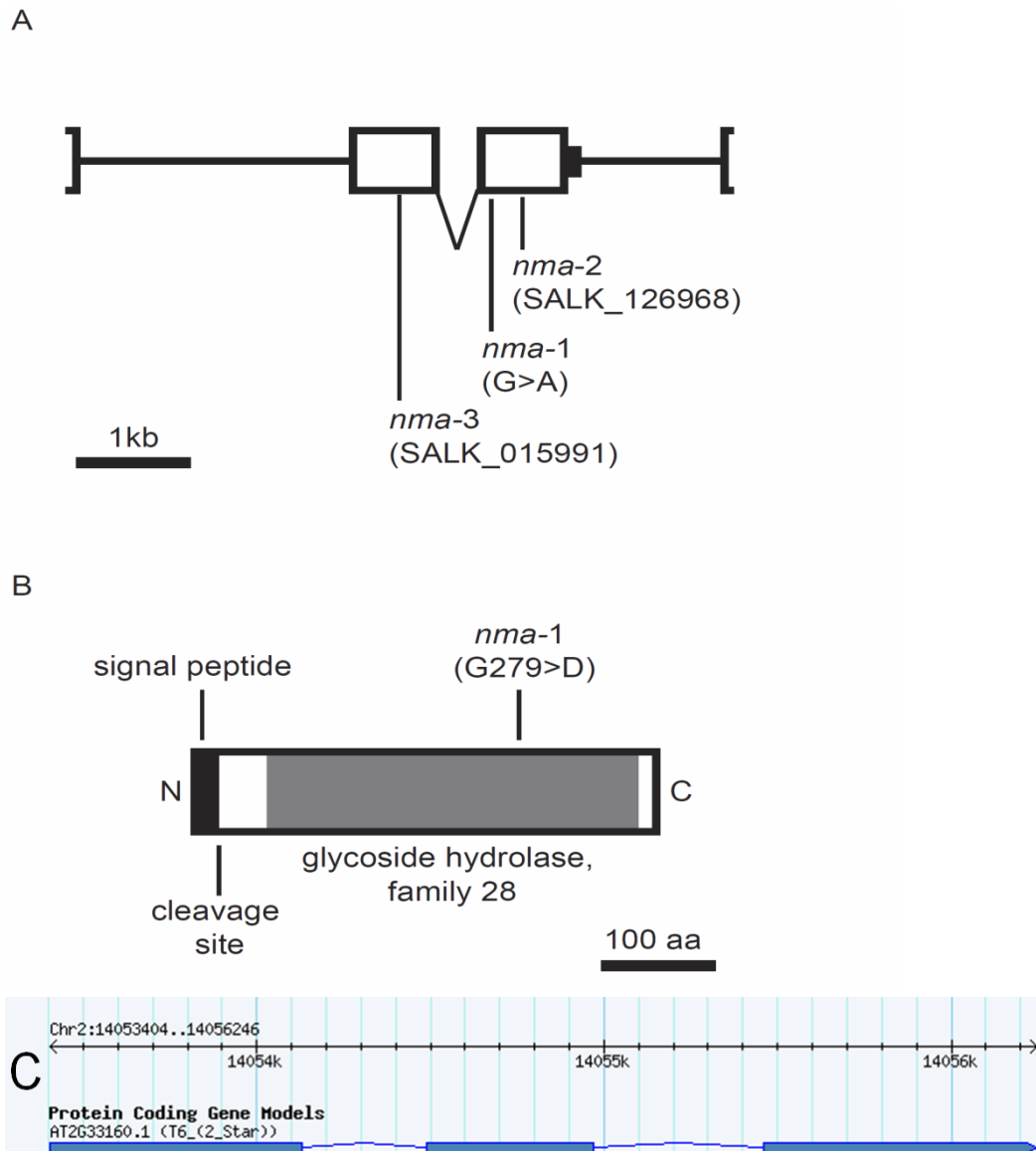


**Figure 8: Graphic representation of the *NMA* gene and protein. **A**, Gene model of the genomic *NMA* locus. Exons are depicted as white boxes, 3'UTR as black box, intergenic regions as line. The position of *nma* alleles are shown below the model. **B**, protein model of *NMA*. The predicted signal peptide is shown in black, the predicted polygalacturonases domain in grey. The position of the *nma-1* substitution is shown on top of the model. **C**, the wrong gene model of *NMA* in TAIR. **A** and **B** is taken from Babu et al., 2013.**

We analyzed two SALK insertion alleles of *NMA*, where the T-DNA were inserted in the first (SALK\_015991/*nma-2*) and second exon (SALK\_126968/*nma-3*) (Fig.8A), both of them showed similar embryonic phenotype as *nma-1* allele. RT-PCR was done to analyze the transcript produced by these two alleles. According to these results, both *nma-2* and *nma-3* alleles produce truncated transcripts. As a result both of these alleles fail to produce functional protein thereby phenocopying *nma-1* which further confirms the mapping of *nma-1* (Fig. 8A and B).

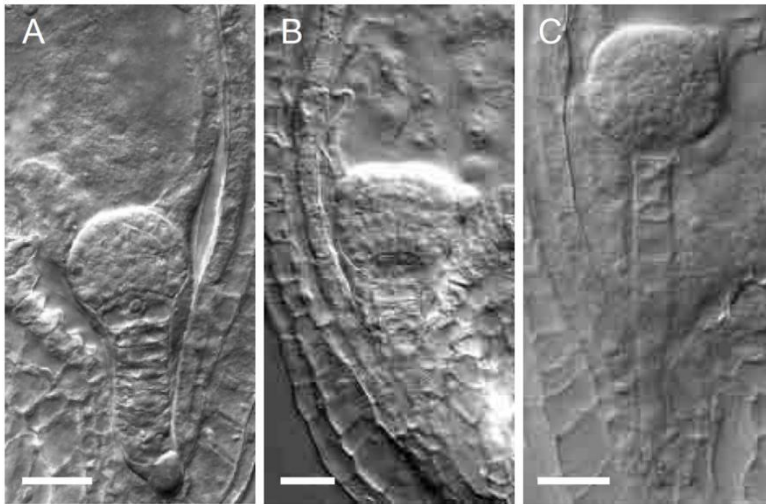


**Figure 9: Embryonic phenotype of T-DNA insertion alleles of *nma*.** A, *nma-2*; B, *nma-3*; C, Col-0 wild-type. Scale bar = 20 $\mu$ m. This figure is taken from Babu et al., 2013.

To provide more supporting evidence of mapping *nma-1*, the full-length *NMA* gene which consists of 2.5kb promoter elements and 2.843kb genomic sequence (genomic version according to old annotation in TAIR) was cloned. This construct (*pNMA::NMA*) was transformed into *nma-1* plants and observed for the complementation. The complementation of *nma-1* will always refer to the rescue of the embryonic phenotype. The complementation can also be quantified by measuring the length of the suspensor at transition stage; as the suspensor terminates to grow after this stage. All 17 T1 plants which were analyzed showed rescue of *nma-1* embryos (Table). Further, the intron was deleted from this construct to resemble the cDNA version of *NMA* and to enable easier genotyping of the transgene, as one of the dCAPS (Derived Cleaved Amplified Polymorphic Sequences) primer anneals to the intron region. Later on, this construct will serve as the backbone for the translational fusions of *NMA*. We observed the complementation of *nma-1* embryo phenotype in 27 T1 plants by this construct (*pNMA::NMA  $\Delta$ intron*).

### 5.5. Developmental delay in *nma* and *ssp* embryos

The impact of suspensor length on developing embryo is poorly understood. We wanted to understand the possible influence of short suspensor on embryogenesis in *nma*. Incidentally while phenotyping, we observed considerable developmental delay in *nma-1* embryos when compared to the WT *Ler* embryos. The experiments were designed to observe the delay in controlled conditions and to measure it quantitatively. The flowers were emasculated on the first day and self-pollinated on the following day. By this way, both *nma* and WT *Ler* were pollinated simultaneously

to achieve common starting point. Four days after pollination, the siliques were dissected and the seeds were collected in such a way to leave out the upper quarter and the lower quarter. This method of collecting seeds will further reduce the bias over the fertilization event which might be affected by the speed of pollen tube growth inside the style of their respective flowers. The seeds were cleared in Hoyer's solution and their embryos were categorized into different developmental stages. The distribution in WT *Ler* was ranging from globular to early torpedo stage and their majority of embryos concentrated between triangular and late heart stage (Fig.10A). The distribution of embryos in *nma-1* was clearly different to wild-type and could be observed between mid-globular and late heart stage and their concentration was high around mid globular to triangular stage (Fig. 10A). Later we attributed numbers to each stage of embryo development and calculated average for the whole population. The average for *nma-1* was ( $2.47 \pm 0.35$ ;  $n = 385$ ) which was significantly lower when compared to WT *Ler* of ( $3.79 \pm 0.33$ ;  $n = 322$ ; Student's t-test,  $P < 0.01$ ; Fig. 10B). These results validate our initial observation about delay in embryogenesis in *nma-1* in comparison to WT *Ler*.

However, to make it clear that this delay in development is caused by short suspensor rather than the loss of NMA function in the pro-embryo it is necessary to analyze an additional mutant with short suspensor. We chose *SHORT SUSPENSOR* (*SSP*) which functions in *YODA* (*YDA*) pathway in determining the suspensor cell fate to further validate our results (Lukowitz et al., 2004; Bayer et al., 2009). *ssp* shows short suspensor phenotype but does not affect the development of the pro-embryo which makes it more suitable for our analysis (Bayer et al., 2009). Similar experiments were conducted now with *ssp-2* which is in Columbia (*Col*) background. Along with WT *Col*, *ssp-2* embryos were categorized four days after self pollination and they also showed a delay in embryo development when compared to WT *Col* (Fig. 10B). We were able to recapitulate similar results with *ssp-2* as in *nma-1*.

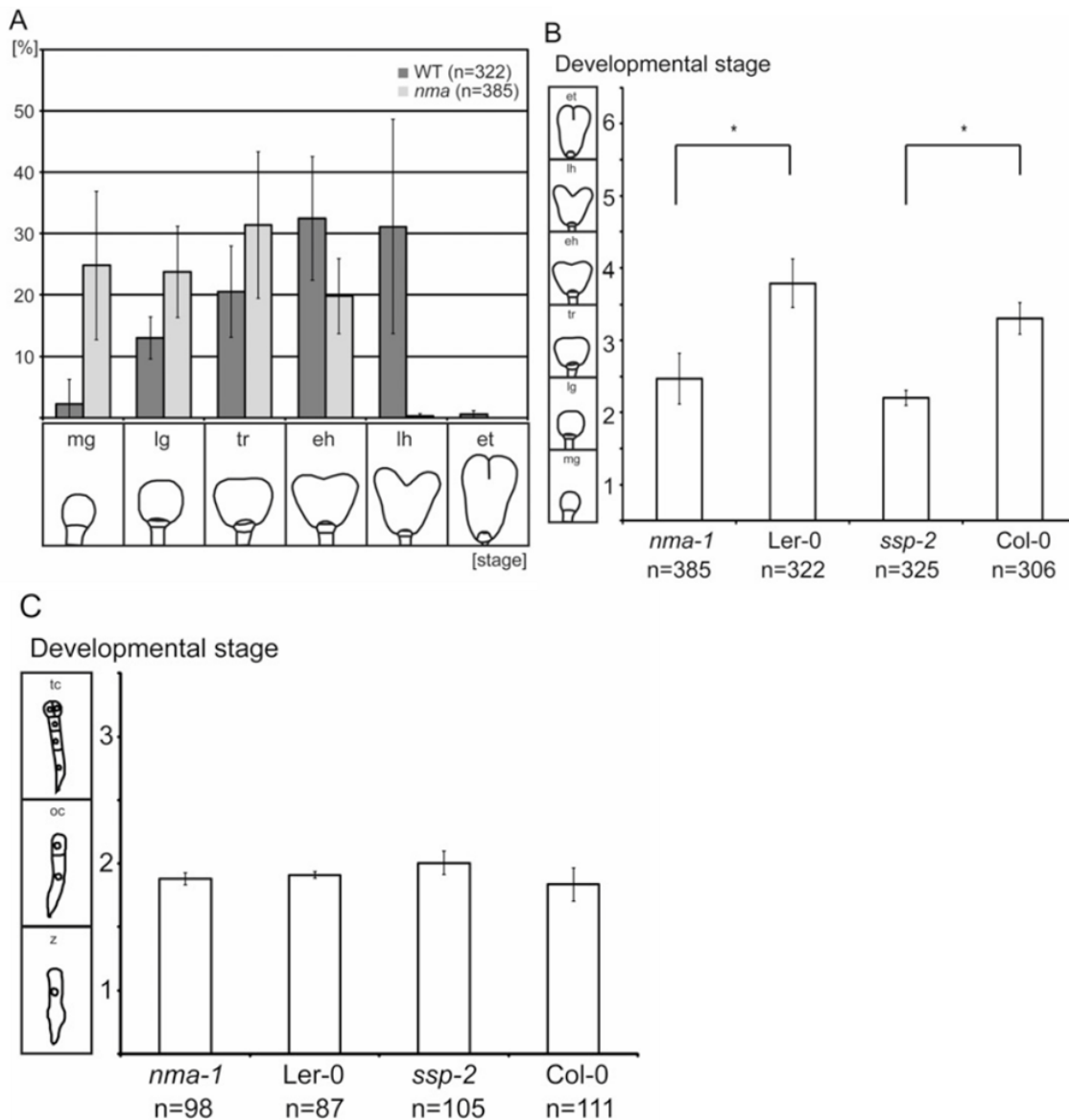


**Figure 10. Developmental stages of embryos.** **A**, Wild-type and *nma* embryos 4 dap were classified into six developmental stages: midglobular (mg), late globular (lg), triangular (tr), early heart (eh), late heart (lh), and early torpedo (et). Schematic depictions of the developmental stage are given below the graphs. Mean values of three independent biological replicates with SD are shown. **B**, Average developmental stage of embryos 4 dap in *nma-1*, *Ler*, *ssp-2*, and Col-0. Embryos were classified in six developmental stages as in Figure 2A. Numerical values were assigned to each stage. Averages and SDs of three biological replicates are shown as bar graphs. Asterisks indicate SDs in pairwise comparison (Mann-WhitneyU test;  $P < 0.001$ ). **C**, Average developmental stage of embryos 30 h after pollination in *nma-1*, *Ler*, *ssp-2*, and Col-0. Embryos were classified in three developmental stages: zygote (Z), one-cell (oc), and two- and four-cell (tc). Numerical values were assigned to each stage. Averages and SDs of three biological replicates are shown as bar graphs. This figure is taken from Babu et al., 2013.

In a time course experiments, describing the starting point and the end point are equally important and it might affect the final interpretation. Although we

simultaneously pollinated in mutant and the WT, the germination of pollen on the pistil and later the fertilization event will define the start point in these experiments with the developmental delay. We conducted additional experiments to analyze these events. *nma-1* and *ssp-2* along with their corresponding WT flowers were emasculated and self pollinated on the next day the seeds were collected 30 hours after pollination from these crosses and their embryos were categorized into three stages, zygote, one-cell stage and two- or four-cell stage. During imaging embryos, distinguishing differences between two and four cell stage embryos was hard, so we combined both stages into one category. We ascertained numerical values for each stage and the average was calculated from this population of embryos. There was no significant delay in embryogenesis 30 hours after pollination either in *nma-1* or in *ssp-2* when compared to their respective WT (*nma-1*/ WT Ler,  $P < 0.05$ ; *ssp-2*/Col-0,  $P < 0.05$  in Mann-Whitney U-test; Fig. 10C).

To provide more supporting evidence for these results on synchronized fertilization event, we analyzed pollen tube growth of *nma-1*. The pollen germination and their growth speed were determined by directly germinating the pollen on growth medium and six hours after germination the length of pollen tubes were measured. The length of *nma-1* pollen tube was  $134 \pm 56 \mu\text{m}$ ;  $n = 189$  and it did not vary significantly with WT Ler  $129 \pm 46 \mu\text{m}$ ;  $n = 146$ ;  $P = 0.79$  in Mann-Whitney U-test. This result suggests that the pollen tube germination and their growth were not affected in *nma-1*.

Additionally, we did a segregation analysis for *nma-1*. To achieve this, reciprocal crosses were performed between heterozygous *nma-1* and WT Ler. The resulting F1 seedlings were genotyped for *nma-1* with an expected segregation ratio of one to one between WT and *nma-1* +/- . With the cross *nma-1* +/- x WT Ler we obtained 90 *nma-1* +/- and 79 WT seedlings while from the other cross WT Ler x *nma-1* +/- we recovered 76 *nma-1* +/- and 97 WT seedlings. The expected segregation ratio and the actual ratio did not vary significantly with chi-square test at 5% level. Segregation analysis was also performed for *ssp* previously (Bayer et al., 2009). These results suggest that pollen tube growth and fertilization events were not affected in *nma-1* and *ssp-2*.

The results describing the delay in embryo development in *nma-1* and *ssp-2* are based on the observation of embryos and categorizing them into different developmental stages. These observations could be misinterpreted by their



morphological appearance and there might be a possibility that they could be categorized into younger stage rather than the actual. To overcome this misinterpretation we repeated the crosses and the seeds were collected at three days after pollination. From this population of the embryos, we calculated the average stage and their microscopic images were acquired at a central plane. These images were used for counting number of cells in the pro-embryo. *nma-1* and *ssp-2* showed fewer cells than their corresponding WT further reinstating the delay in the development (Fig.11). This result also validates the results from earlier experiments conducted to show the developmental delay in *nma-1* and *ssp-2*.

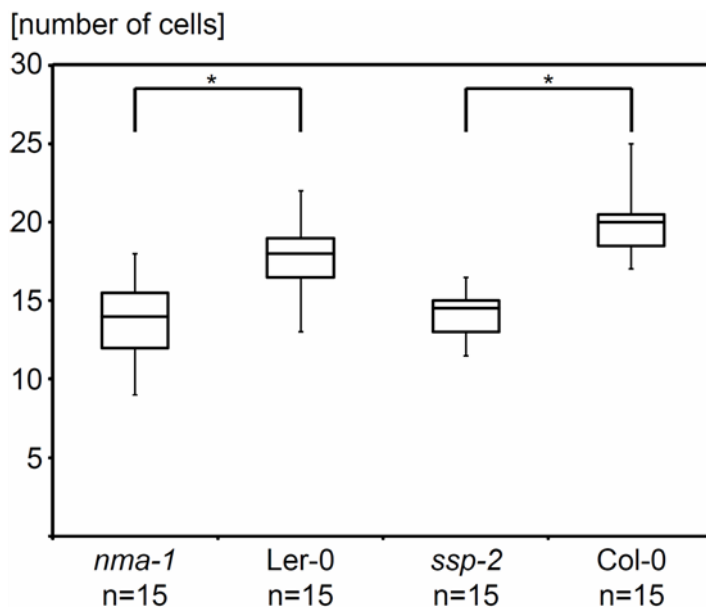
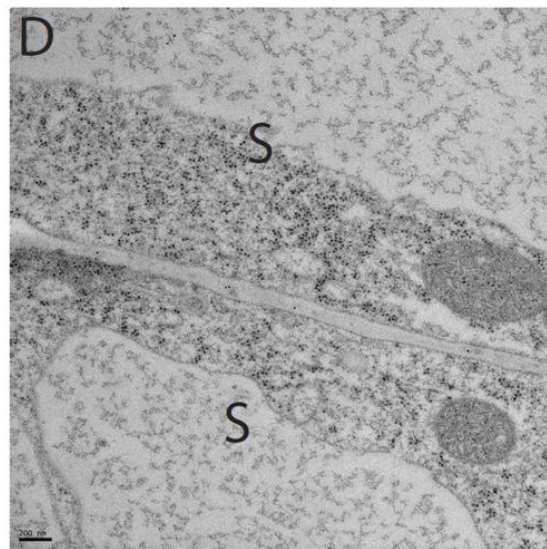
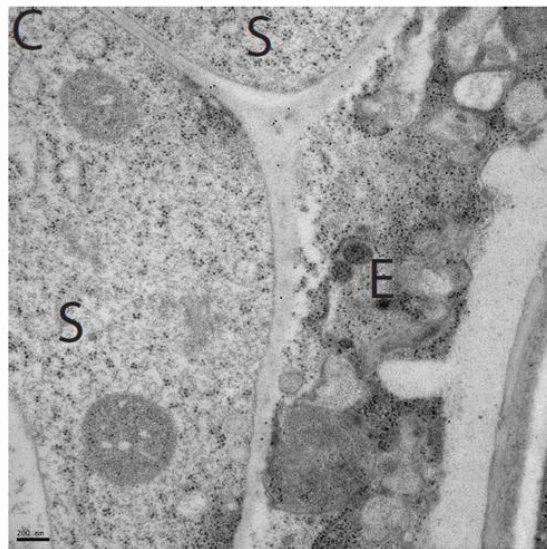
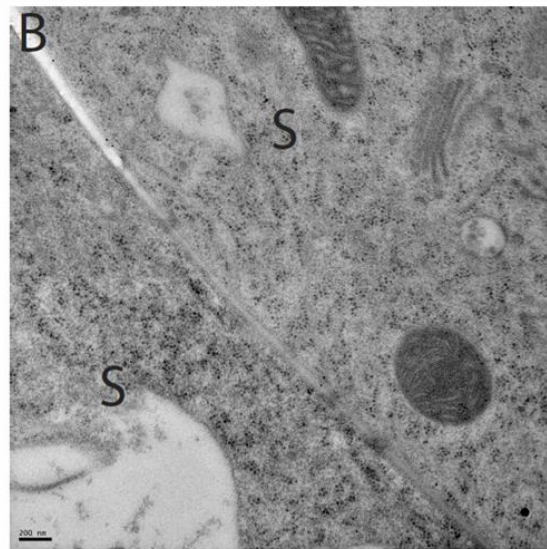
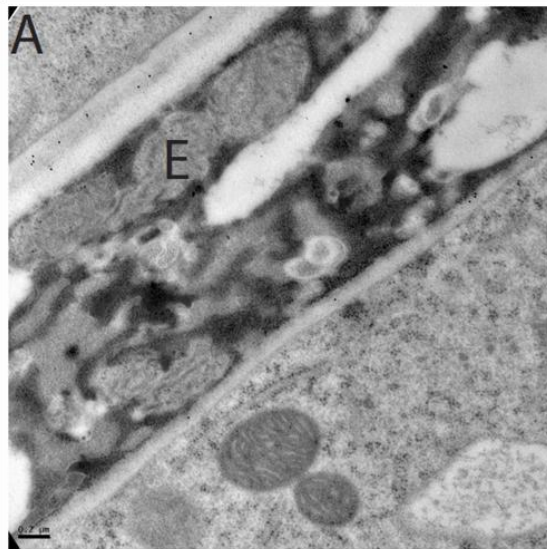


**Figure 11: Number of cells in a central optical section of the proembryo 3 days after pollination.** Significant differences as indicated by Mann Whitney U-test ( $p < 0.001$ ) are highlighted by an asterisk. Boxes represent lower and upper quartiles around median, whiskers indicate maximum and minimum values. The number of examined embryos is given below each genotype. This figure is taken from Babu et al., 2013.

## 5.6. Immuno-gold labeling with LM19 and LM20

After detailed description of *nma-1* phenotype, we performed several biochemical characterizations to understand its function. Since *NMA* encodes for a putative exopolysaccharidase, and loss-of-function mutations cause cell elongation defects we wondered if the pectin composition might be affected. To observe any changes in pectin arrangement in the *nma-1* suspensor cell walls, we labeled the embryos with two specific antibodies called LM19 and LM20, which recognize modifications in un-

esterified homogalacturonans and esterified homogalacturonans, respectively (<http://www.plantprobes.net/index.php>). We made use of immunogold labeling as this method is robust during sample preparation and each gold particle provides detailed information. Methyl-esterification is tightly regulated by plants in a developmental and tissue-specific manner during pectin synthesis and localization (William et al., 2000; Wolf and Greiner 2012). Pectin methyl-esterases remove the methyl-ester groups on pectin polysaccharides thereby rendering them susceptible for action by polygalacturonases. LM19 labeling can recognize these patterns of pectin whereas LM20 should be unchanged after these modifications by polygalacturonases in the primary cell wall arrangements. Detailed analysis of the labeled suspensor cells suggested that there were no significant changes between WT and *nma-1* (Fig. 12A-D). The pattern of arrangement and distribution of the pectin was not altered in *nma-1* when compared to the WT according to the LM19 labeling. However the labeling of LM19 was sparse in between the suspensor cell (Fig. 12B and D) than in the adjacent cell walls of suspensor cells (Fig. 12A and C) both in *nma-1* and WT further suggesting that there is no difference in pectin arrangement also in different location of suspensor cells both in WT and *nma-1*. Congregation of LM19 labeling will indicate the high activity of polygalacturonases, there was no such congregation observed in WT (Fig 12. A and B) in cell walls surrounding suspensor cells further suggesting moderate to low action of polygalacturonases in suspensor cell walls or: antibody unsuited to detect changes made by NMA.



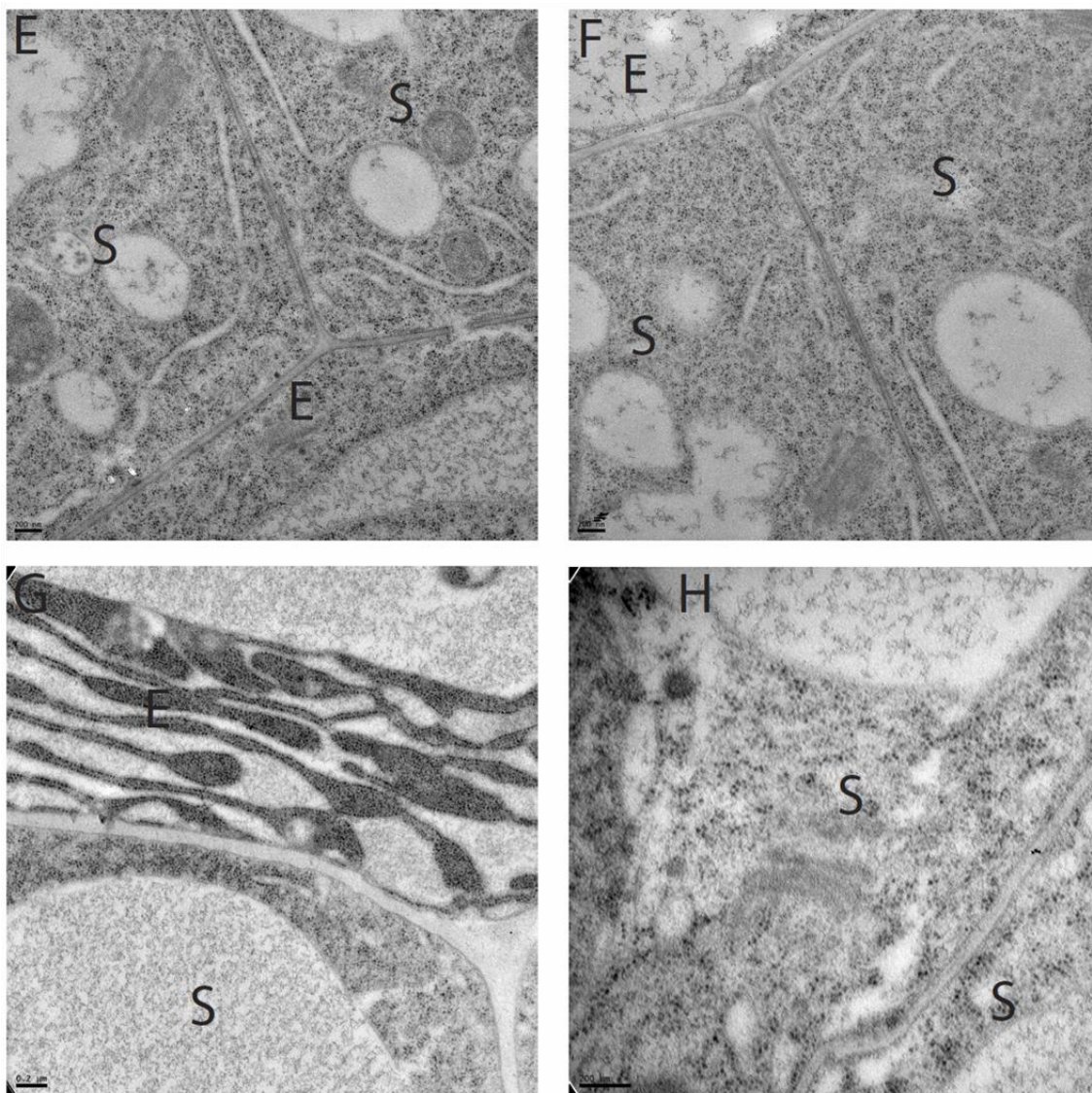


**Figure 12. Immunogold labeling of LM19 and LM20 in the suspensor cell wall.** A-D LM19 labeling, WT embryos (A, B) inside suspensor (right) lateral cell wall (left) *nma-1* (C, D). E-H LM20 labeling, WT (E, F) and *nma-1* (G, H). S, suspensor; E, endosperm surrounding suspensor cells. Scale bar sizes as printed on each figure.

### 5.7. Adult plant phenotype of *nma*

An alternative option for detecting the cell elongation defects is by measuring the plant height and internode length. Both *nma* and Ler WT plants were grown for 6 weeks and possible position effects of growth conditions were avoided by distributing the pots in a random manner in the plant tray. The plant height measurements were conducted on the oldest inflorescence stem but the overall plant height was not affected in *nma-1* compared to WT plants (Fig. 13A). For the internode length measurements, the distance between 3rd and 7th pedicel was measured and divided



by four to give the average internode length. We observed significant differences in internode length between *nma-1* and Ler WT plants (Fig. 13B, Mann-Whitney;  $P < 0.05$ ). Although the internode elongation in *nma-1* mutants was affected, other than this there is no severe or drastic effect of *nma* on post-embryonic plant growth and development.

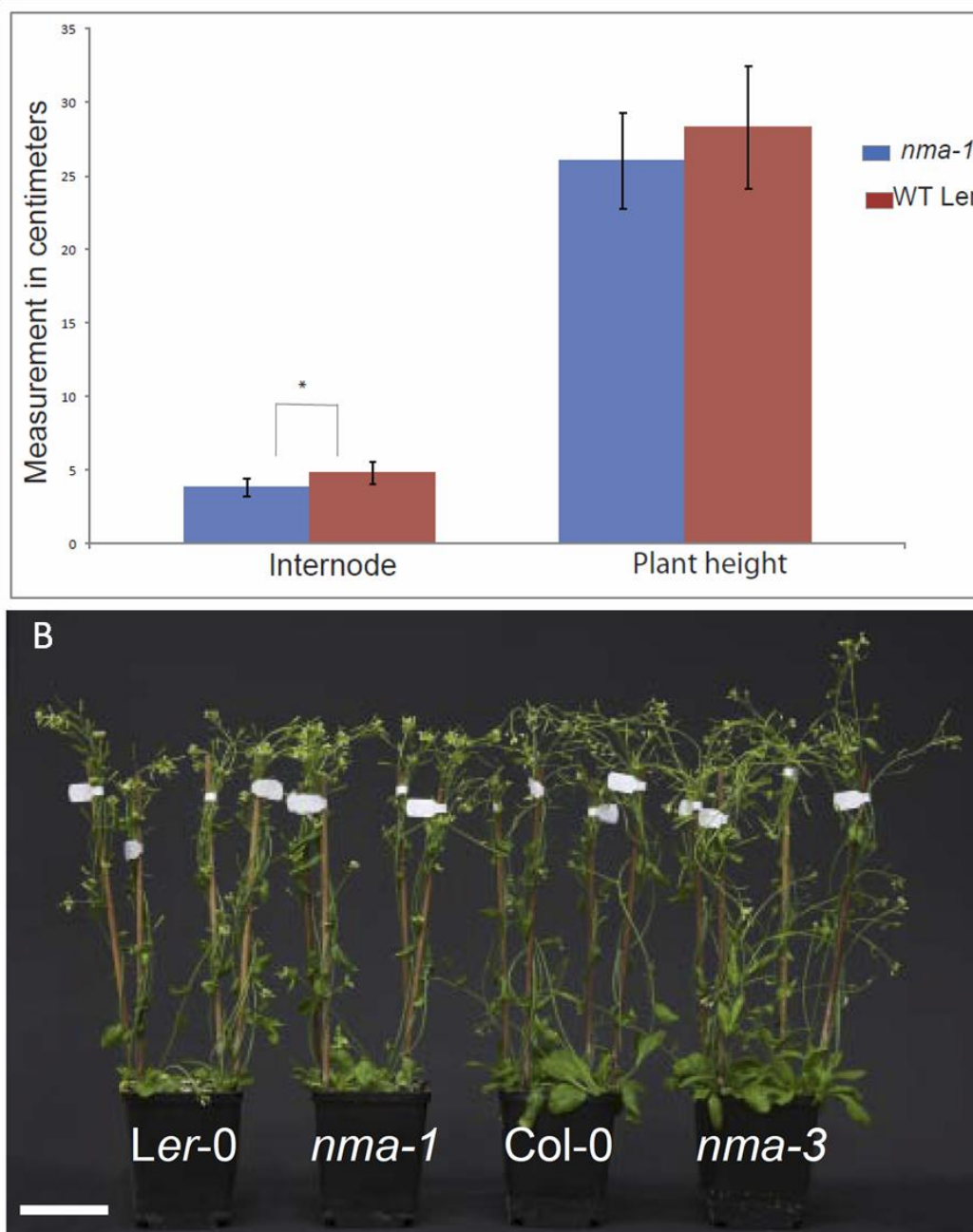


**Figure 13. Adult phenotype of *nma*.** **A**, bar graph depicting internode length and plant height of plants 6 weeks after germination of *nma-1* (blue) in comparison to Ler WT. The distance between 3rd and 7th pedicel was measured and divided by four which gives the average internode length, while the length of the oldest inflorescence stem represents the plant height measurements. Asterisks indicate statistical significance by Mann-Whitney;  $P < 0.05$ . Number of analyzed plants *nma-1* = 23, Ler WT = 26. **B**, six week old plants of *nma-*

1 (Ler-0 background) and *nma-3* (Col-0 background) which were grown in a random manner along with their WT are comparable with respect to adult plant phenotype. Scale bar = 5 cm. **(B)** is taken from Babu et al., 2013.

### 5.8. Expression analysis of *NMA*

We analyzed spatiotemporal expression of *NMA* in detail to understand its functional requirement during plant development. The 2.5kbp upstream region of *NMA* were fused to *3xVenus* and *GUS*, respectively, and expression was analyzed in at least four independent lines for both reporter genes. Seedlings expressing *pNMA::GUS* were stained along with negative controls (WT and *pNMA::3xVenus*). *GUS* staining was observed in the columella cells and in the elongation region of the root. The cotyledons were entirely stained whereas in mature leaves the staining was constricted only to the expanding region. While in inflorescences both the gametophytic tissues and also fertilized seeds showed *GUS* activity (Fig. 14I). The *pNMA::3xVenus* expressing plants were used to study the *NMA* promoter activity at cellular resolution. *NMA* was found to be expressed at very early stages in megasporogenesis and continued even after fertilization (Fig. 14F). We observed its expression in cell lineages of the early female gametophyte (Fig. 14F-H). Among all the female gametophytic cells, the fluorescence was strongest in the central cell and after fertilization the signal persisted in all dividing endosperm cell and got later restricted to the chalazal endosperm cell (Fig. 14D).

In mature pollen, we observed expression in sperm cells along with the generative cell. In embryos, the expression could be observed from one-cell stage to torpedo stage (Fig. 14A). At early stages reporter expression was detected in all cells of the embryo but stronger in suspensor cells (Fig. 14B). Later at heart stage the expression persisted in the suspensor while in the pro-embryo it was restricted to the protoderm, expanding cotyledon, stele, quiescent center and columella cells (Fig. 14C).

To compare *NMA* expression between the different tissues and to provide additional evidence, we did qRT-PCR with all the major tissue-types like root, shoot, rosette leaves, cauline leaves, inflorescence, pollen and siliques. Among all the tissues, inflorescences showed peak levels followed by siliques and pollen, while the vegetative tissues displayed low expression levels (Fig. 15). The results from the promoter-reporter constructs and qRT-PCR used for analysis of *NMA* promoter

activity were consistent and suggested its predominant expression in reproductive tissues.

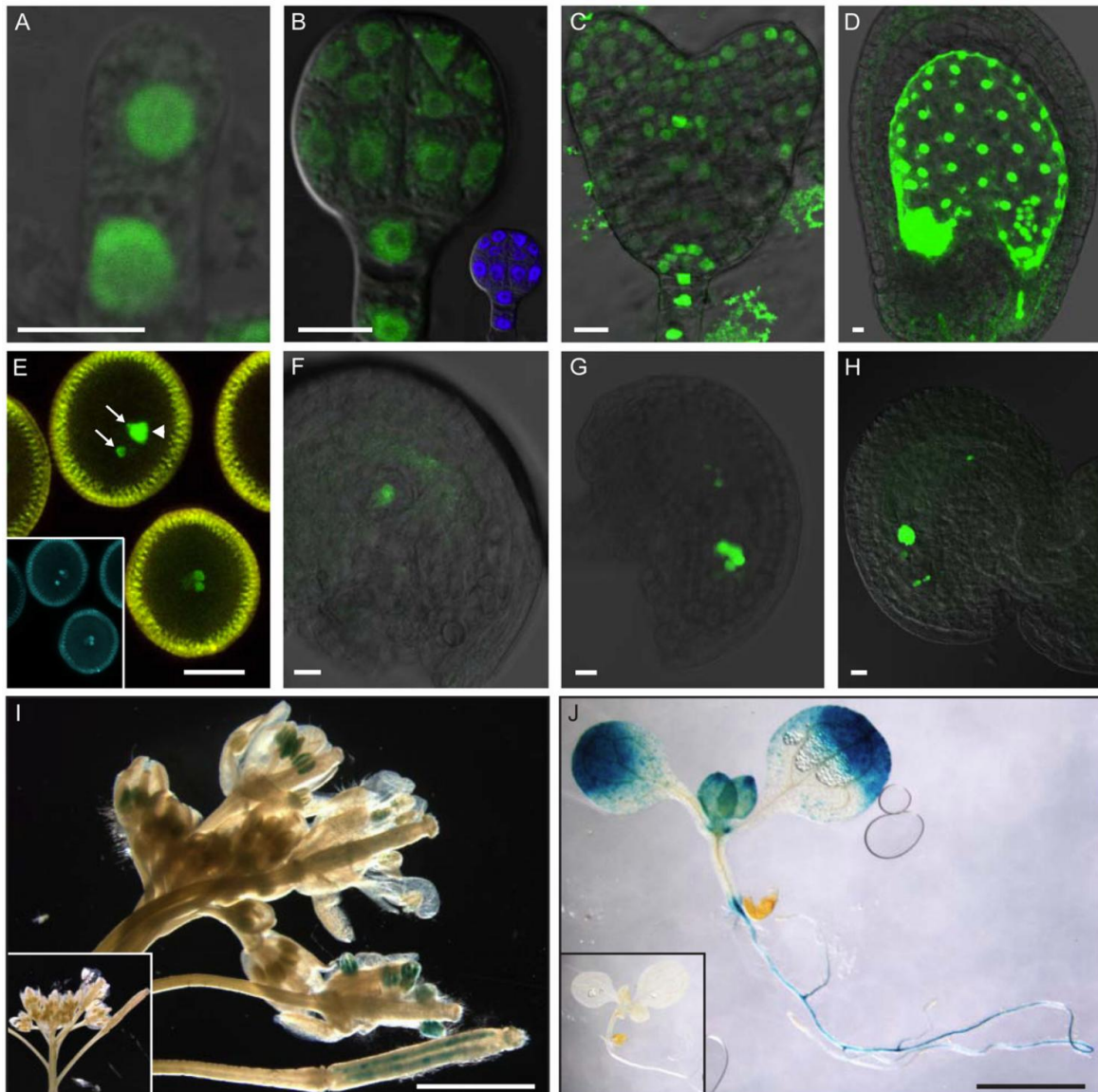


**Figure 14. Expression analysis of *NMA* promoter-reporter gene constructs.** **A to H,** Fluorescence micrographs of transgenic plants carrying a transcriptional fusion of a *NMA* promoter fragment to nuclear-localized triple *Venus-YFP*. **A,** Embryo after the first zygotic division. **B,** Globular-stage embryo, inset shows 49,6-diamidino-2-phenylindole (DAPI) staining. **C,** Heart-stage embryo. **D,** Developing seed 2 dap. **E,** Pollen, arrows mark sperm cell nuclei and arrowhead indicates vegetative cell nucleus; inset shows DAPI staining. **F,** Female gametophyte after meiosis. **G,** Female gametophyte at eight-nuclei stage. **H,** Mature female gametophyte. Bars = 10 mm. **I and J,** GUS activity staining in transgenic plants carrying a transcriptional *pNMA:GUS* fusion construct. **I,** Inflorescence. **J,** Seedling. Insets in **I** and **J** show transgenic control plants without GUS gene. Bars = 2 mm. This figure is taken from Babu et al., 2013.

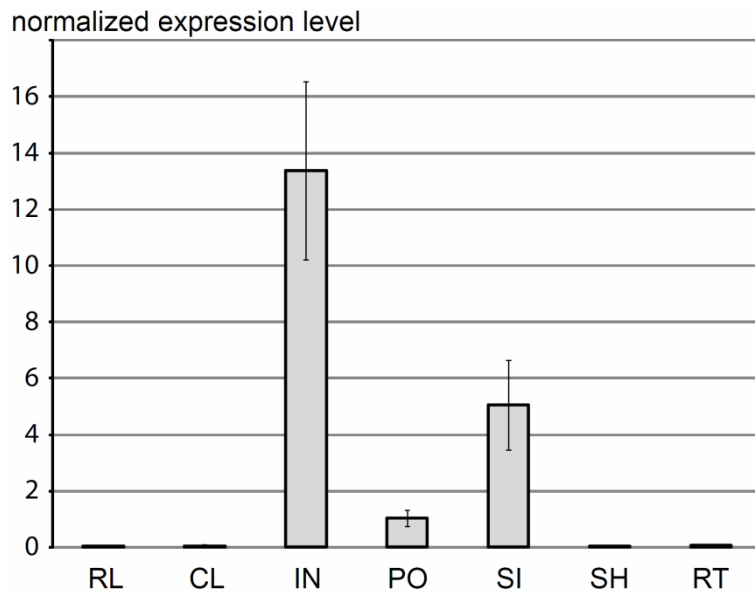


**Figure 15: Quantitative RT-PCR data of *NMA* expression in various tissue types.** RL, rosette leaves; CL, cauline leaves; IN, inflorescences; PO, pollen; SI, siliques; SH, seedling shoot including cotyledons and first leaves; RT, seedling root. Values are normalized to average expression levels in pollen. Mean values of three biological replicates with standard deviations are shown. This figure is taken from Babu et al., 2013.

### 5.9. Cell-autonomous effect of *NMA*

*NMA* is expressed in both fertilization products - embryo and endosperm. Although it is expressed in both tissue types, but only embryo cells are visibly affected in *nma* mutants. Since the embryo is surrounded by endosperm cells which provide space and nutrients, we wanted to clarify whether *NMA* function is cell-autonomous or its function in the endosperm might influence cell elongation in embryos. Therefore, we ectopically expressed it in both of these two tissues by fusing tissue-specific promoter elements from described genes to the *NMA-YFP* coding sequence and we analyzed the ability to rescue the embryonic phenotype of *nma-1*. For endosperm- and embryo-specific expression we used the promoters of SUCROSE PROTON SYMPORTER 5 (*SUC5*) (Baud et al., 2005) and OBF BINDING PROTEIN 1 (*OBP1*) (Skiryicz et al., 2008), respectively (Fig. 16A and B). *SUC5* was later shown to be also expressed in protodermal cells of the torpedo stage embryo (Pommerrenig et al., 2013) but this did not affect our study as we analyzed the rescue phenotype at earlier developmental stages when *SUC5* is not expressed in the embryo. Interestingly, *NMA* function in endosperm cells alone was not sufficient to rescue the cell elongation defects in embryos (Fig. 16C) whereas embryo-specific expression



resulted in WT looking embryos suggesting a cell-autonomous function of NMA (Fig. 16C).

In order to specify its functional requirement within the embryo, we expressed *NMA* only in suspensor cells under the control of the J10 promoter (personal communication Jixiang Kong). The J10 promoter specifically expressed in suspensor cells in seed (Fig. 16B). Expressing *pJ10::YFP-NMA* in *nma-1* plants showed complementation of cell elongation defects in suspensor (Fig.16) but not in pro-embryo cells at earlier stages. This suspensor-specific rescue provided additional evidence that suspensor cells play a role in determining the developmental speed of embryo.

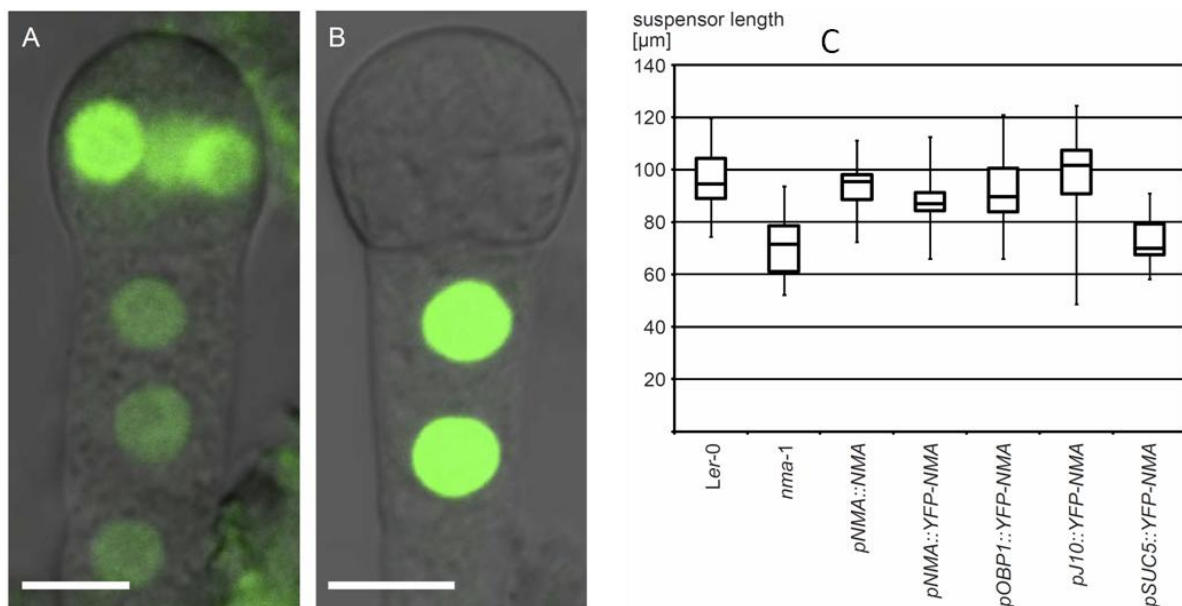


**Figure 16: Complementation assay based on suspensor length and expression of promoter fusions. A, *pOBP1::n3xGFP*. B, *pJ10::n3xGFP*. C, Box plot diagram of suspensor rescue ability. Genotype of representative transgenic lines is given below chart. Boxes represent lower and upper quartiles around median. Whiskers depict maximum and minimum values. Scale bar = 10μm. This Figure is taken from Babu et al., 2013.**

Additionally, similar time-course experiments were conducted to study the rescue ability of plants expressing *pJ10::YFP-NMA*. We grouped embryos into 6 developmental stages and four days after pollination the embryos were analyzed in comparison to *nma-1* and WT. For *pJ10::YFP-NMA* embryos the average stage was  $3.01 \pm 0.09$  ( $n = 374$ ), which was significantly higher than that for *nma-1* embryos  $2.48 \pm 0.29$  ( $n = 500$ , Student's t test  $P < 0.05$ ) (Fig. 17). However, the developmental delay was only partially rescued when compared to WT  $3.61 \pm 0.27$  ( $n = 1102$ ) (Fig.

17). These results suggest that developmental speed in the embryo is determined in a non-cell autonomous way by the suspensor. *YFP-NMA* function in the suspensor rescues the developmental delay but not the cell elongation defects of the embryo proper in *nma-1* plants.

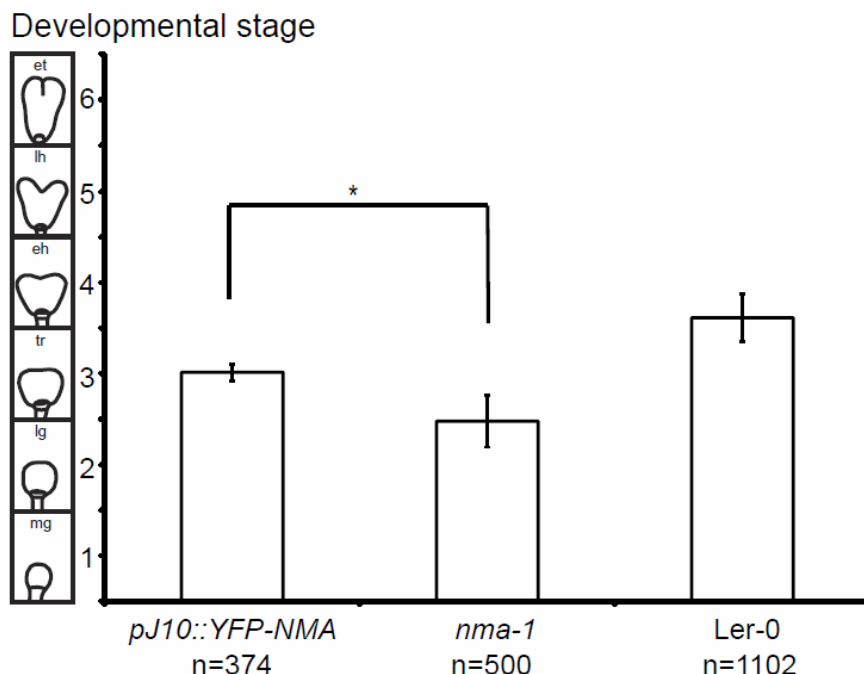


**Figure 17: Average developmental stage of embryos 4 dap in *pJ10::YFP-NMA*, *nma-1*, and *Ler-0*.** Embryos were classified into 6 developmental stages. Numerical values were assigned to each stage. Averages and standard deviations of at least three biological replicates are shown as bar graphs. Asterisks indicate significant differences in pair-wise comparison (t-test;  $p < 0.05$ ). This Figure is taken from Babu et al., 2013.

### 5.10 Attempts to biochemically characterize NMA

*NMA* encodes for a putative exo-polygalacturonase and it is required for cell elongation in early embryogenesis. It is necessary to study its catalytic activity to understand its function in cell elongation. It is difficult to isolate the functional extracellular protein from plants and in addition the expression of *NMA* is very low in the majority of the tissue types. Therefore, we decided to express it heterologously in *E. coli* and isolate the protein. Both mutant and WT alleles of *NMA* were cloned into pETM-20 which harbors IPTG-inducible promoter elements and an N-terminal Thioredoxin (ThxA) and 6X Histidine tag (G. Stier, EMBL). Expressing pETM-20::*ThxA-HIS-NMA* in BL21 *E. coli* cells did not yield soluble protein. We then switched to Rosetta-gami 2 Novagen<sup>TM</sup> host strains which alleviate codon bias and enhance disulfide bond formation in the cytoplasm when heterologous proteins are

expressed in *E. coli*. With the Rosetta-gami 2 cells we were able to obtain soluble NMA protein and we purified it using Ni-Agarose beads. The size of the purified protein was further confirmed by TEV protease cleavage where after cleavage of the His Tag the NMA protein was at of the expected size (42kDa) (Fig. 18).

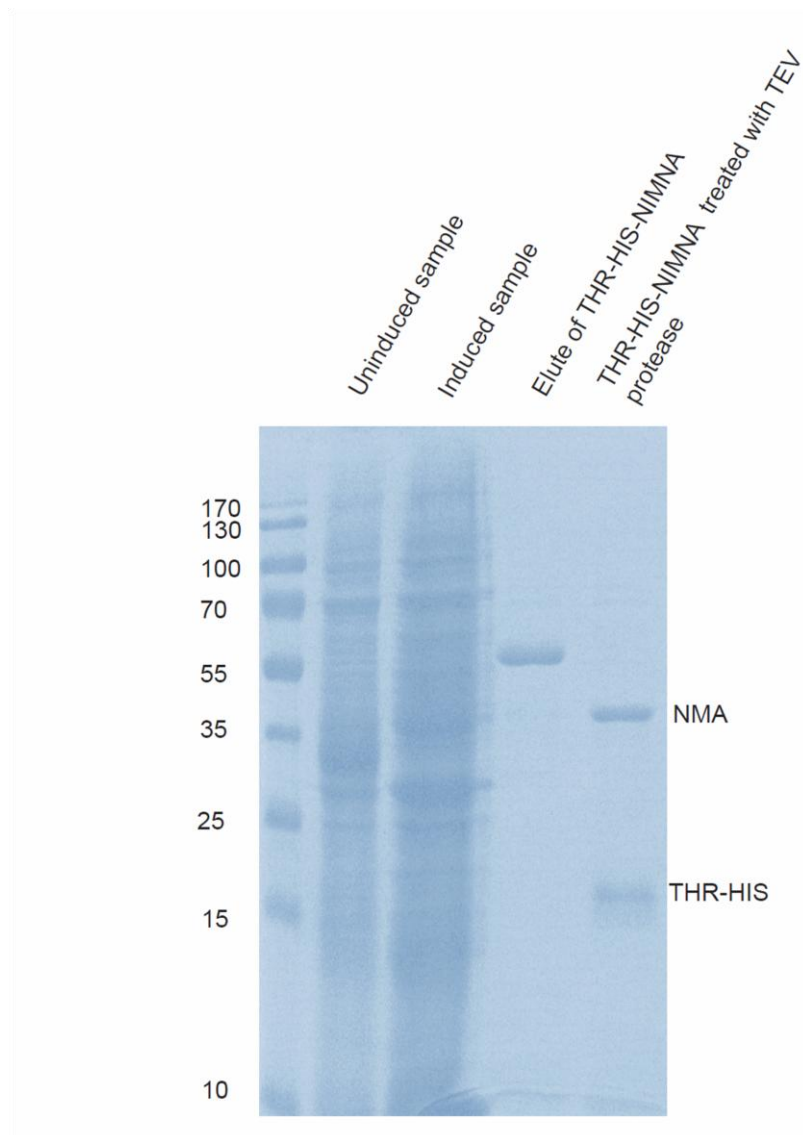


**Figure 18. SDS-PAGE gel picture showing different samples during purification of THR-HIS-NMA.** A sample was loaded before induction of expression of THR-HIS-NMA, after induction, purified elute. A small amount of the protein elute was treated with TEV protease and loaded on the gel.

Initially, we used the 2-cyanoacetamide method (Gross 1982) for detecting the catalytic activity of NMA. We incubated 100µg of His-NMA with 0.4% Polygalacturonic acid (PGA) (Sigma-Aldrich) in sodium acetate buffer pH 5.0 at 30°C. Two hours after incubation the reactions were treated with cold 1.0ml 100mM borate buffer and with 0.2ml of 1% 2-cyanoacetamide. The absorbance was measured to

quantify the released reducing groups at 276nm after blanking the spectrophotometer with a reaction at zero time. Absorbance values were not different between NMA at zero time and four hours after incubation indicating the catalytic activity did not yield any reducing sugars (Tab. 1).

Sample	Absorption at 276nm
Substrate+ Pectolyase (zero time)	0,21
Substrate+ Pectolyase (four hours after incubation)	2,153
Substrate+ NMA (zero time)	0,077
Substrate+ NMA (four hours after incubation)	0,082

**Table 1. Absorption values at 276nm of the samples after PG assay by Cyanoacetamide method.** Zero time was used as a negative control.

Since the absorbance wavelength of reducing sugars was similar to that of proteins, as an alternative we chose the Nelson and Somogyi method for detecting reducing sugars. Here, 500 $\mu$ g of enzyme was incubated with 0.5% PGA substrate in sodium acetate buffer pH 4.5 for at least one hour. The reactions were terminated with equal volume of cupralkaline solution and tubes were immersed into the boiling water for 15 minutes. When the tubes were cooled to room temperature, the catalytic activity was quantified by measuring absorbance at 540nm after addition of half volume of arsenomolybdate solution. We used a Pectolyase from *Aspergillus japonicus* (Sigma-Aldrich) as a positive control and bovine serum albumin (BSA) as a negative control. A curve was plotted between Standard  $\Delta A_{540nm}$  readings and  $\mu$ moles of D-galacturonic acid. We determined the  $\mu$ moles of D-galacturonic acid liberated using the standard curve and enzymatic units were calculated. However, NMA did not show any change in absorption value at 540nm (Tab. 2) and the color changes which indicate the appearance of reducing sugars in presence of copper did not seem to be happening. This result suggests that NMA did not produce any reducing sugar during the assay.

Sample	Absorption at 540nm
Substrate + Bovine serum albumin	0,424
Substrate+ Pectolyase (four hours after incubation)	4,000

Substrate+ NMA (four hours after incubation)	0,048
--	-------

**Table 2. Absorption values at 540nm of the samples after PG assay by Nelson and Somogyi method.** BSA was used as a negative control.

Since nuclear magnetic resonance (NMR) gives us an advantage of monitoring the catalytic reaction over time and enables us to observe the end products directly, we used NMR to study the catalytic activity of NMA. We later used a simple sugar - trigalacturonic acid (TGA) - as a substrate instead of PGA. A spectrum was obtained with TGA in NMR and it was monitored after addition of pectolyase (Sigma-Aldrich) to the reaction. We were able to observe the appearance of end product galacturonic acid peaks after addition of pectolyase.

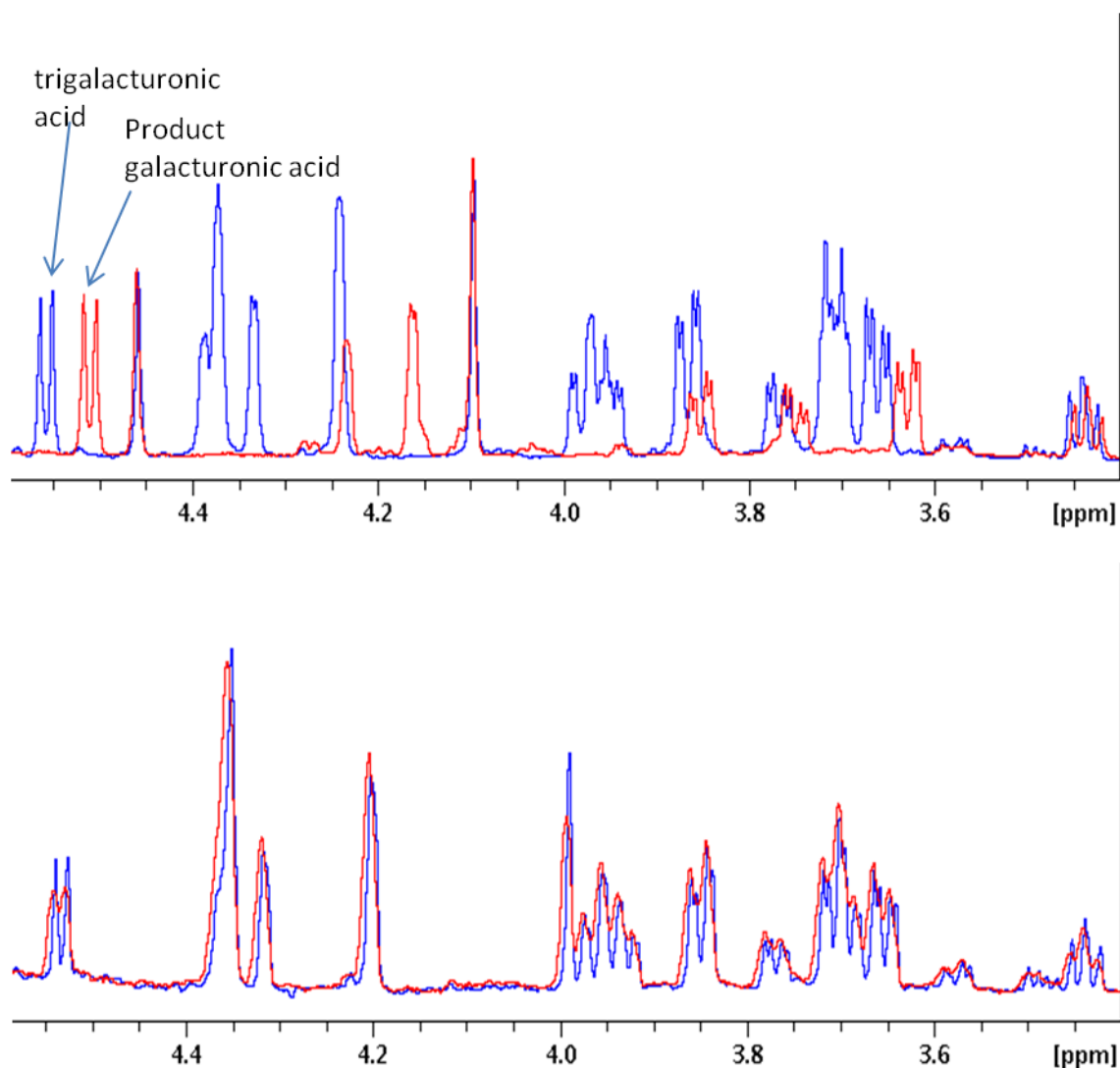


**Figure 18: Proton NMR spectra of trigalacturonic acid.** Upper panel shows spectra of trigalacturonic acid (TGA) alone at zero time (blue) and after addition of pectolyase from *Aspergillus japonicus* (SIGMA-ALDRICH) (red). Lower panel shows spectra of TGA before

(blue) and after addition of THR-HIS-NIMNA (red). End products did not appear even after prolonged incubation when TGA was incubated with THR-HIS-NIMNA.

Although the mode of action is different in pectolyase from exo-PG but we are still expected to see any difference in the substrate spectra. Substrate spectra were also monitored after addition of NMA to the reaction, but even after overnight incubation it was unchanged (Fig. 18). We also used oligo-galacturonic acid (OGA) instead of TGA. Even then there was no NMA activity on the substrate as it did not produce any end products. It can be concluded that the NMA protein purified from Rosetta-gami 2 E.coli was not active, it might need posttranslational modification to be active, and so a eukaryotic organism should be preferred for heterologous expression.

### **5.11. Transient expression of *NMA* variants in *Arabidopsis* protoplasts**

NMA is predicted to be an extracellular protein containing a signal peptide (SP) for plasma membrane localization and a cleavage site (SignalP4.0). To study the subcellular localization of NMA in plants we generated two constructs. One harbors the N-terminal signal-peptide (SP) followed by YFP and *NMA* CDS while the other construct has an N-terminal YFP disrupting the SP. Both of these constructs were expressed under the control of both *NMA* and the *Cauliflower mosaic virus 35S* promoter. These constructs were then transiently expressed in *Arabidopsis* protoplasts but the *NMA* promoter was not strong enough in these cells to be able to observe any YFP signal. *CaMV35S* promoter driven expression of *YFP-NMA* fusions showed localization in the protoplast cells. When the SP was intact, YFP-NMA localized to some of the remnants or newly formed cell walls in the protoplast (Fig. 19A). Previously, pectin was shown to be synthesized in protoplasts during prolonged incubation (Shea et al., 1989; David et al., 1995; Stacey et al., 1995). Three days after transient expression the YFP fluorescence was broadened in newly formed cell wall patches when the SP was intact (Fig. 19D). While the other construct with the disrupted SP localized to the cytoplasm or ER after overnight growth and after three days after transient expression there was no change in the pattern of localization (Fig. 19B and E). The untransformed cells did not show any fluorescence. This result demonstrates that NMA localizes to the cell wall, and when the SP is disrupted it remains in cytoplasm or ER (Fig. 19)

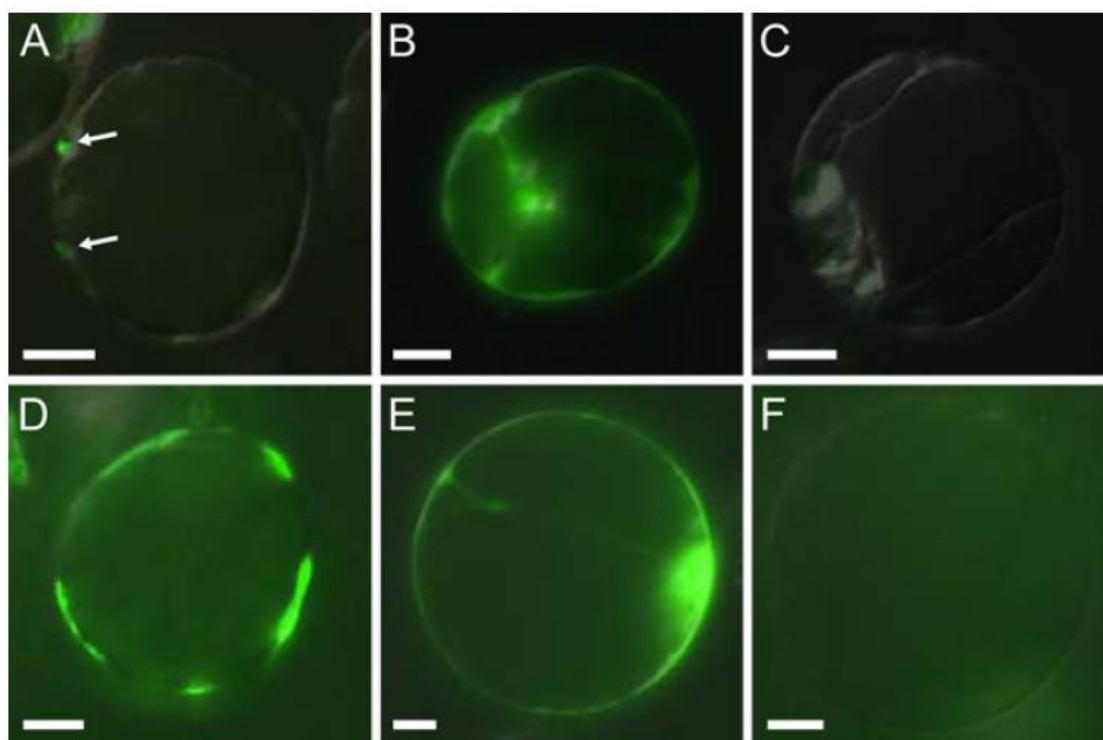


**Figure 19. Transient expression of YFP-NMA fusion proteins in protoplasts.** A to C, 24 h after transformation. D to F, 72 h after transformation. A and D, *p35S:YFP-NMA* fusion construct with intact SP sequence. Arrows in A point to dotted signals on protoplast surface. B and E, *p35S:YFP-NMA dSP* fusion construct with disrupted SP sequence. C and F, untransformed control. Bars = 10 mm. This Figure is taken from Babu et al., 2013.

To further analyze the functional requirement of SP in plants, we transformed both of these constructs under the control of *NMA* promoter into *nma-1* plants. Only the *YFP-NMA* fusion with an intact SP was able to rescue the embryonic phenotype. We were unable to visualize the localization of the protein, which might suggest the low steady-state protein levels of NMA. Western blot on protein extract from the inflorescence tissue of plants expressing YFP-NMA also could not detect the protein further supporting previous results. However in a previous study, certain peptides of NMA protein were detected in extracellular extracts from five day old seedling suggesting its localization in the cell wall (Irshad et al., 2008).

## **Chapter II: Studying the SSP signaling cascade in *Arabidopsis* embryogenesis.**

### **5.12. MPK3/6 target search by generating phospo-mutants**

The YDA mitogen activated protein kinase kinase kinase (MAPKKK) together with SSP mediates signaling during zygote elongation and in determining extra-embryonic cell fate (Lukowitz et al., 2004; Bayer et al., 2009). MPK3 and MPK6 act downstream of YDA in stomata development and they were also shown to phosphorylate SPCH, a bHLH transcription factor, *in vitro* (Wang et al., 2008; Lampard et al., 2009; Lampard et al., 2008). MPK3 and MPK6 were also implicated to play a role in embryo development (Bush and Krysan 2007; Wang et al., 2007; López-Bucio et al., 2014). The preferred sequence motif for phosphorylation by MPK3 and MPK6 was determined by positional scanning the random peptides by Sörensson et al., (2012) (Fig. 20). Candidate genes were selected based on their expression in the embryo, their function and/or also if they contained the phosphorylation sequence. Additionally, we also analyzed SCREAM1 (SCRM1) and SCREAM2 (SCRM2) as they are downstream components of the ERECTA family signaling during stomata development which is in turn also mediated by the YDA pathway (Kanaoka et al., 2008; Bergmann et al., 2004). Phospho-mimic and non-phosphorylatable versions of these candidates were generated by mutating serine residues into aspartic acid and alanine, respectively. We reasoned that these mutations would render the proteins as dominant versions and constitutive expression of these versions would not produce viable seedlings. Additionally, expression of these candidate genes under their native promoter elements did not appear convenient to study due to their variable expression levels also in other tissue types. Considering all these conditions we expressed the candidate genes under the control of the Upstream Activator Sequence (UAS) enhancer elements (Fig. 20).



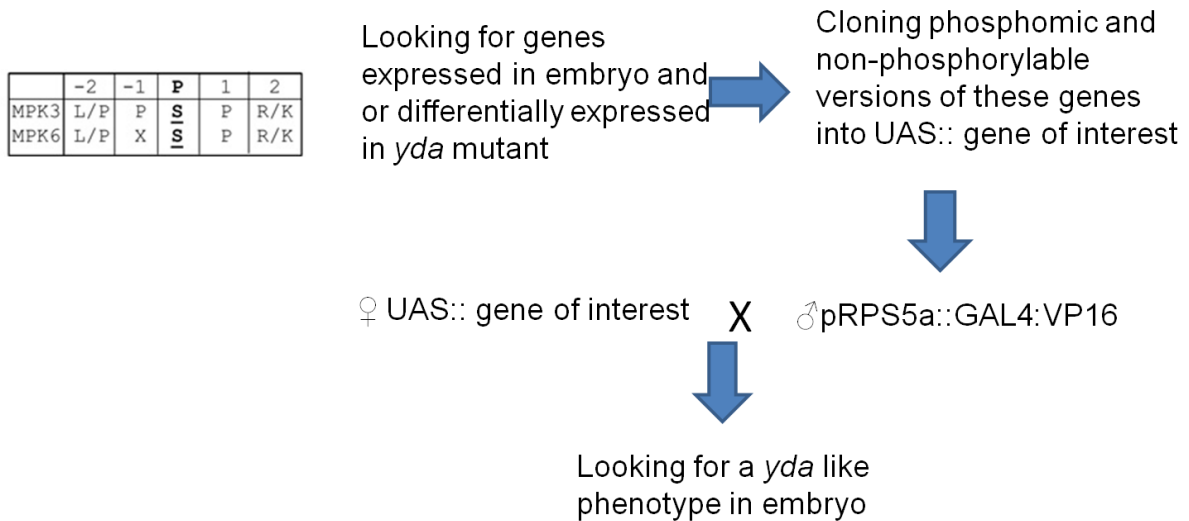
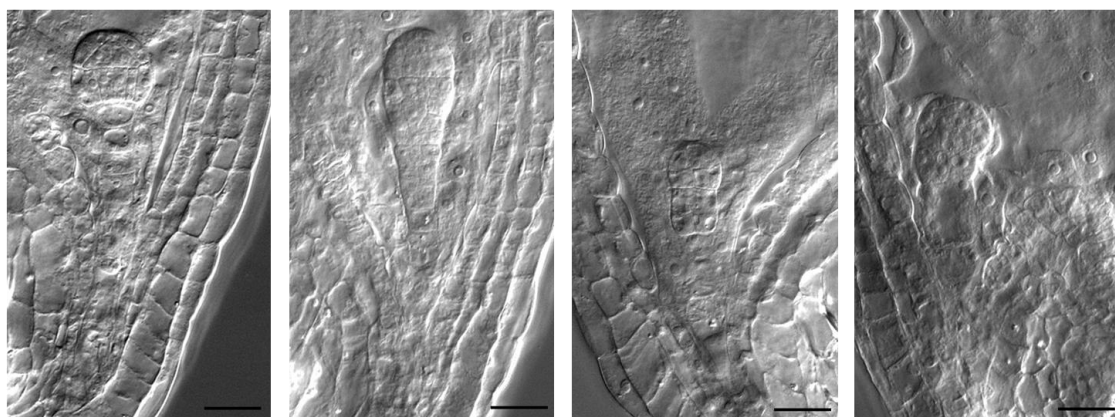


**Figure 20. Schematic representing of phosphor-mutant screen.** MPK3 and MPK6 target phosphorylation amino acid consensus (Sörensson et al., 2012).

Along with the mutant version, WT alleles were also transformed into WT Col-0 plants. Plants expressing *pRPS5A::GAL4:VP16* were crossed to the T1 plants for over-expression of the various versions of the candidate genes. Three days after pollination the embryos from these crosses were phenotyped. All candidates cloned are provided in table 3. Only two of the candidate genes showed effects on embryo development, namely PROTEIN PHOSPHATASE 2C 5 (PP2C5) and PINOID (PID). All three versions of PID (phosphor-mimic, unphosphorylatable and WT) showed periclinal divisions in the protodermal cells of globular stage embryos indicating that they all phenocopy the expected, already published over-expression phenotype (Friml et al., 2004). And again all three versions of PP2C5a showed abnormal divisions in embryo which might suggest that it is not specifically functioning in YDA pathway (Fig. 21). While the mutant versions of some of the candidates including SCRM2 and At5g47070 (protein kinase) showed very weak *ssp*-like phenotype in their phosphomimic versions (Table 3). And mutant versions of other candidates failed to show any effect on embryogenesis (Table 3).

Gene	Predicted protein class	Phenotype observed
SCRM1	bHLH Transcription factor	No phenotype in all three versions
SCRM2	bHLH Transcription factor	No phenotype in WT version, but a weak <i>ssp</i> -like phenotype in S>D version
NULP1	bHLH Transcription factor	No phenotype in S>D and S>A versions
At5g47070	Receptor like cytoplasmic kinase	No phenotype in WT version, but a weak <i>ssp</i> -like phenotype in S>D version
At2g32850	Protein Kinase	No phenotype in all three versions
At3g24790	Protein Kinase	No phenotype in all three versions
At2g40180/PP2C5	Protein Phosphatase	All three Versions show <i>yda</i> phenotype
PID	Protein Kinase	All three Versions show over-expression phenotype
At1g63100	GRAS Transcription factor	No phenotype in all three versions

**Table 3. Genes which were analyzed in phospho mutant screen.**



♀ WT x ♂  
pRPS5A::GAI4-VP16

♀ pUAS::PP2C5a x ♂  
RPS5A::GAI4-VP16

♀ pUAS::PP2C5a S55A x ♂  
pRPS5A::GAI4-VP16

♀ pUAS::PP2C5a S55D x ♂  
pRPS5A::GAI4-VP16

**Figure 21. F1 embryos of phosphomutants of PP2C5a crossed with RPS5A effector lines.** Abnormal divisions can be observed in embryos from all three crosses. Scale bar 20µm

### **5.13. Split Ubiquitin System (SUS) Yeast two hybrid screen to identify interaction partners of YDA and MPK3/6**

Since studying SSP signaling in embryogenesis by the above mentioned approach is laborious and the phospho-mutants generated might not always produce functional protein in plants, we chose to study the protein-protein interaction by a split ubiquitin system (SUS) in a heterologous system (Johnsson and Varshavsky 1994; Obrdlik et al., 2004). In SUS, the interaction will take place on an integral membrane and it uses the ubiquitin (Ub) tag. The Ub protein is split into two halves i.e N-terminal ubiquitin (Nub) and C-terminal Ubiquitin (Cub), which are fused to prey and bait proteins, respectively. Wild type versions of these two halves can naturally re-fuse to form a functional tag without the need of a bait-prey interaction. To overcome this problem isoleucine 13 was mutated to glycine in Nub (NubG) which now requires the close proximity of these two halves to form a functional tag that can only be accomplished by the bait-prey interaction (Johnsson and Varshavsky 1994). Now the functional Ub tag will be recognized by proteases resulting in cleavage of the C-terminal fusion proteins from the bait protein (protein-LexA-VP16). This results in activation of the reporter genes. Since it is a mating-based SUS, bait and prey vectors will be transformed into two different yeast strains; THY.AP4 (MAT $\alpha$ ; ade2<sup>-</sup>, his3<sup>-</sup>, leu2<sup>-</sup>, trp1<sup>-</sup>, ura3<sup>-</sup>; lexA::ADE2, lexA::HIS3, lexA::lacZ) for bait clones and also for bridge clones and THY.AP5 (MAT $\alpha$  ade2<sup>-</sup>, his3<sup>-</sup>, leu2<sup>-</sup>, trp1<sup>-</sup>) for prey clones (Obrdlik et al., 2004). Once these strains are transformed with the respective clones, mating these two strains will combine bait and prey proteins in one diploid cell where the interaction can be assayed by either growth or other methods including an ortho - Nitrophenylgalactopyranoside (o-NPG) assay (Obrdlik et al., 2004).

One of the requirements for the bait to be used in this system is that it should have a plasma membrane or a membrane-localization signal in general as the interaction between bait and prey proteins take place on a membrane inside the yeast cells (Obrdlik et al., 2004). As most of the known proteins in the SSP signaling cascade do not have a membrane-localization signal including YDA, MKK4/5 and MPK3/6, we used a vector, which includes a membrane-localization signal peptide from OST4,

which localizes to ER membranes in yeast (Grefen 2013). As a standard procedure, the bait proteins were tested for background activity, which can be achieved by conducting an interaction assay with the empty prey vectors containing NubG and NubWT, respectively. Another interesting feature of the bait vector is that its expression is under the control of a methionine (Met) repressible promoter element (Met25) (Obrdlík et al., 2004). This feature is helpful in controlling the expression of bait vector and thereby providing more contrasting conditions to identify the interacting protein.

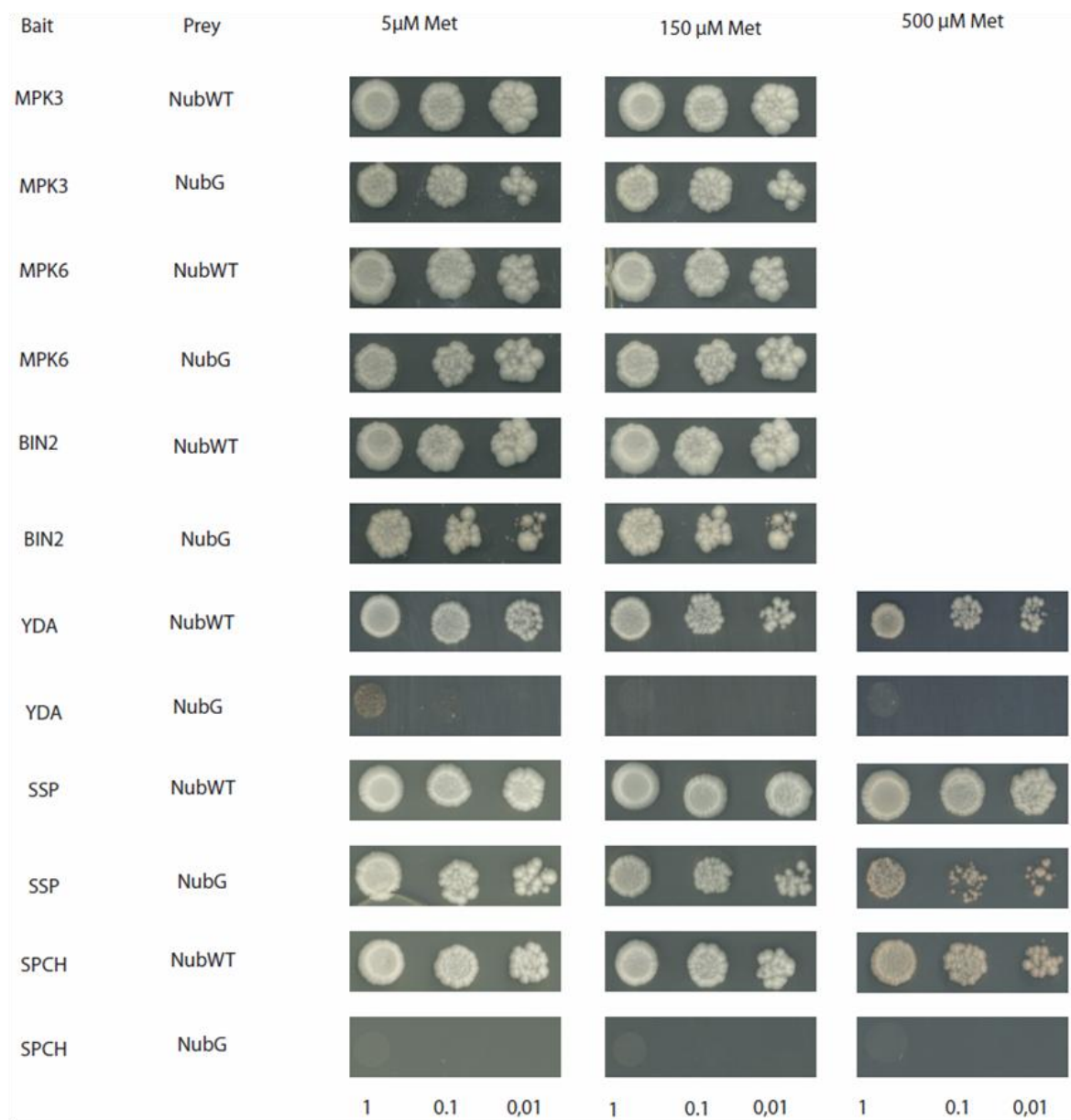
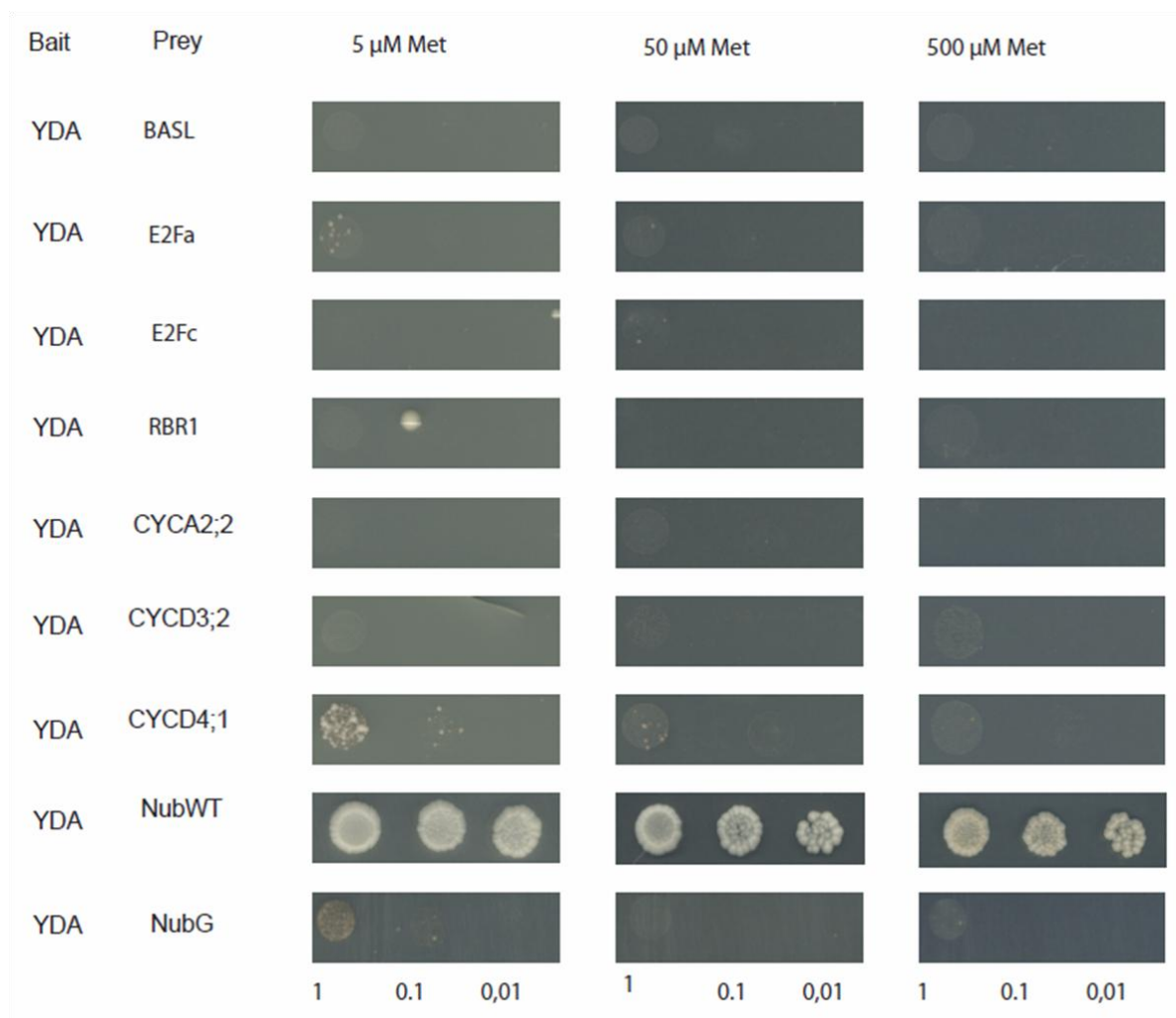


**Figure 22. Bait test for background activity.** Each bait construct was mated with NubWT (positive control) and NubG (negative control) and the mated cells were plated on selective media (-A-H). Positive colonies were re-plated after diluting (1/10, 1/100) onto minimal media with increasing methionine (Met) concentrations (5,150,500 $\mu$ M).

We first tested MPK3, MPK6, BIN2, SSP, YDA and SPCH as baits for background activity. MPK3, MPK6, BIN2 and SSP produced growth on selective plates upon interaction with NubG which suggests the presence of background activity in these bait constructs. The growth of these yeast cells (MPK3, MPK6 and BIN2) did not respond to the increasing Met concentration (up to 1mM Met), which further suggests that these three bait proteins (MPK3, MPK6 and BIN2) are not suitable for screening prey proteins (Fig. 22). YDA on the other hand showed no/very little background activity and could be used for further interaction studies (Fig. 22). As BRASSINOSTEROID-INSENSITIVE 2 (BIN2) was shown to phosphorylate YDA *in vitro* (Kim et al., 2012), we wanted to retest this interaction as a control. We observed interaction of YDA with BIN2 by growth assays and we also observed direct interaction of YDA with MPK3 and MPK6 (Fig. 23) which was not shown before.

To identify further downstream targets of YDA, we decided to perform interaction studies with chosen candidates, which might function in cell elongation and/ or cell fate determination. We ordered entry clones for some candidates from ABRC (Jenny R, cyclin entry clones; Ecker J, other entry clones) and prey clones (Frommer W and Lalonde S, prey clones) depending on the availability, as these SUS vectors (Obrdlik et al., 2004; Grefen et al., 2009; Grefen 2014) are Gateway<sup>TM</sup> compatible. The prey clones include MITOGEN ACTIVATED PROTEIN KINASE PHOSPHATASE 2(MAPKP2), ERECTA, MITOGEN-ACTIVATED PROTEIN KINASE KINASE 4 (MEK4), protein kinases (At5g47070, At5g63370, At3g24790, and At2g32850). However, none of the prey clones ordered showed interaction with YDA (Fig. 23). We subcloned ordered entry clones into the destination vector (prey). CYCLIN D4:1, MICROTUBULE-ASSOCIATED PROTEIN 65-5 (MAP65-5) and E2Fa showed direct interaction with YDA (Fig. 23) and others need to be tested.

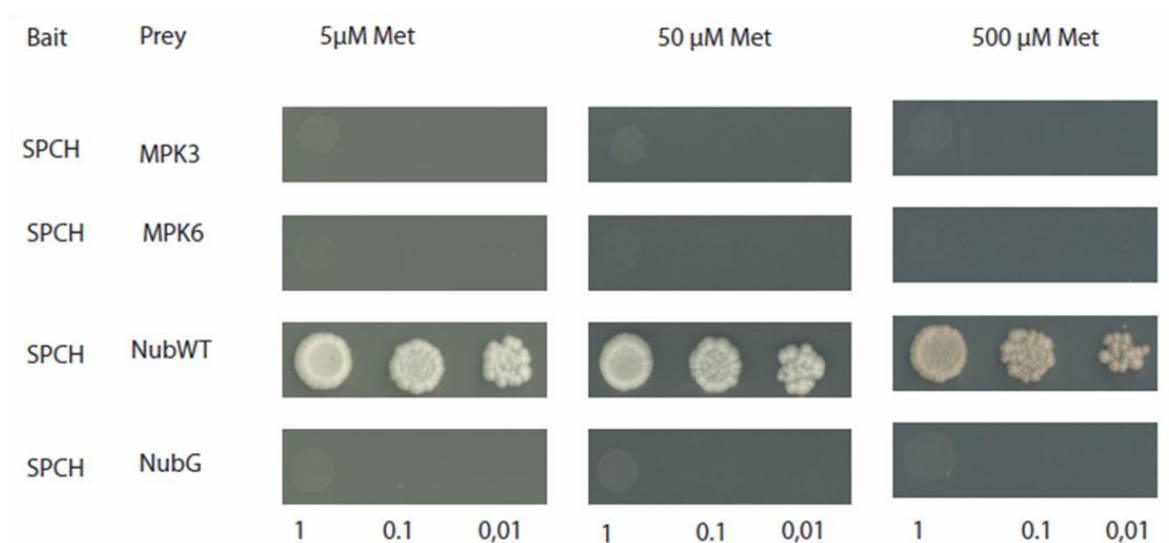




**Figure 23. Split-ubiquitin assay with YDA (bait) and selected candidates.** Each prey construct was mated with YDA and the mated cells were plated on selective media (-A-H). Positive colonies were re-plated after diluting (1/10, 1/100) onto minimal media with increasing methionine (Met) concentrations (5,50,500 $\mu$ M).

Recently, a three component split ubiquitin system was established where a third protein is introduced as a bridge to facilitate or compete or even to enhance the interaction between bait and prey (Grefen 2013). Introducing MPK6 as a bridge might enhance or facilitate the interaction between YDA and potential downstream targets since MPK6 interacts with YDA directly and it was also shown to act downstream of YDA (Wang et al., 2007). We cloned MPK6 into the bridge vector and the previous interaction study was repeated now with YDA and the same candidates in presence of MPK6 (YDA-MPK6). MPK3 and MPK6 were also shown to phosphorylate SPCH *in vitro* (Lampard et al., 2008), so first we analyzed the interaction with YDA and SPCH in presence of MPK6. A very weak interaction was observed between SPCH and YDA in presence of MPK6 (Fig. 25). In contrast, the direct interaction with SPCH (as

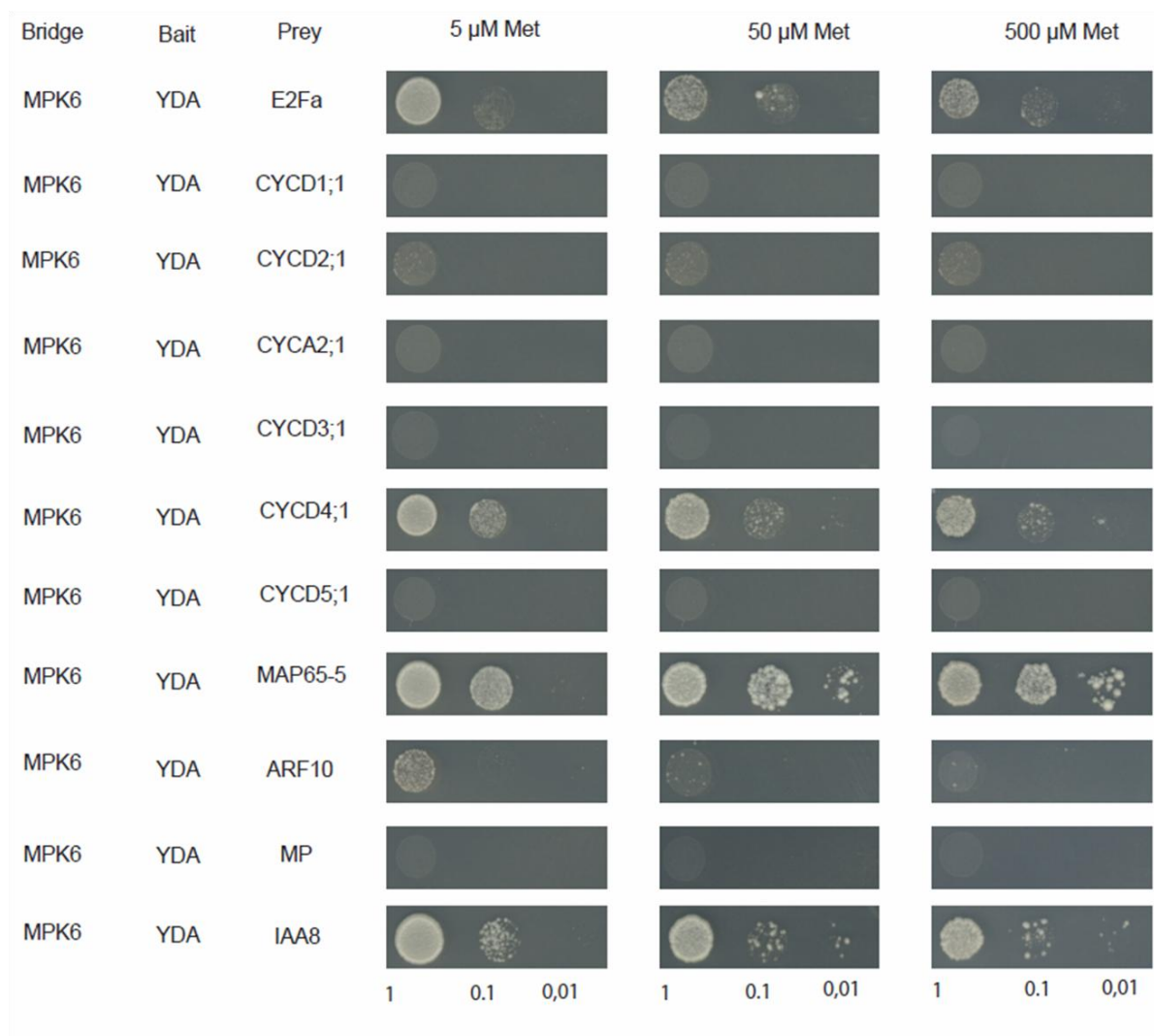
bait) and MPK6 (prey) was not observed (Fig. 24). C-terminal and N-terminal tags on SPCH either as bait or prey might have a role in abolishing or weakening the interaction with MPK6 (prey) or YDA-MPK6 (bait-bridge).



**Figure 24. SPCH protein interaction with MPK3 and MPK6 in split ubiquitin assay.**

When MPK6 was introduced as a bridge some of the candidates now appeared to interact with YDA while the weaker interactions became stronger. E2Fc, CYCLIN D3;1, SSP, MKK4, AUXIN RESPONSE FACTOR 10 (ARF10) and INDOLEACETIC ACID-INDUCED PROTEIN 8 (IAA8) were among the new candidates, which showed interaction with YDA-MPK6 (Fig. 25). CYCLIN D4:1, MAP65-5 and E2Fa showed stronger interaction with YDA in presence of MPK6. MPK6 (bridge) and YDA (bait) together already showed a weak interaction with the NubG (negative control) suggesting that the candidates identified from the interaction study with YDA and in presence of bridge MPK6 could also be an artifact. All these candidates were selected based on their expression in the embryo and their probable function in cell elongation and cell fate determination. However this biased selection does not represent all the proteins present in the embryo. Therefore, we decided to conduct a SUS screen on an expression library to study the components of the SSP signaling cascade.





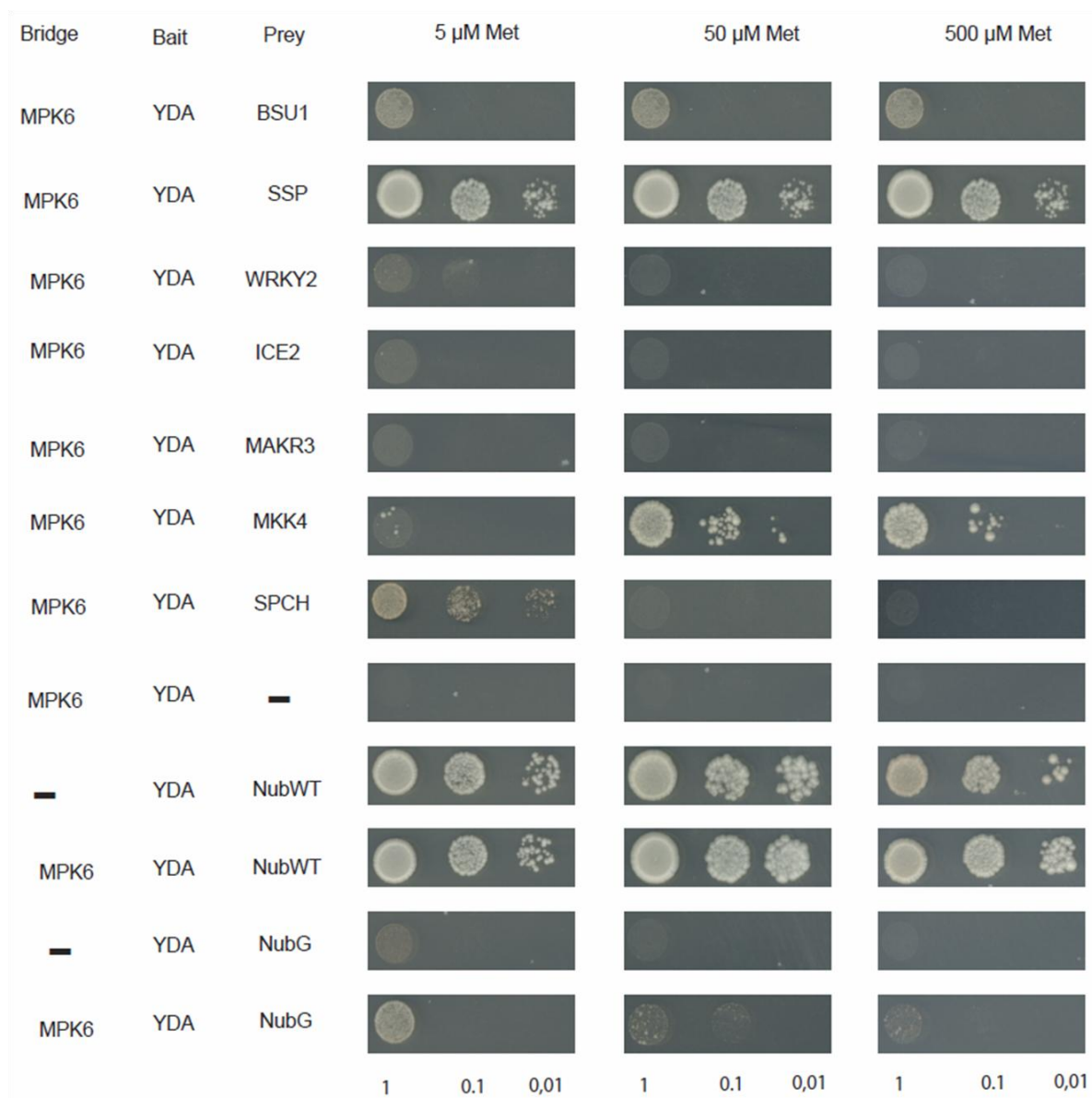


**Figure 25. Split-ubiquitin assay with YDA (bait) with (bridge).** NubWT (positive control) and NubG (negative control) positive colonies were replated after dilution (1/10, 1/100) onto minimal media with increasing methionine (Met) concentrations (5, 50, 500 $\mu$ M).

#### 5.14 cDNA library construction and screening for interacting proteins of YDA and MPK6

Since we wanted to study the SSP signaling cascade in embryogenesis, it was necessary to prepare a library from isolated embryos. To prepare this library, we required at least 1 $\mu$ g of mRNA from embryos, making the task very laborious. As an alternative, we prepared a library from entire ovules isolated from siliques one to two days after pollination. The ovules were isolated from WT Col-0 siliques and stored in RNA Later<sup>TM</sup> until the total RNA was extracted (Qiagen plant mini kit). The total RNA

was analyzed with an Agilent Bioanalyzer™ for 28S and 18S peaks and the RNA integrity number (RIN). The total RNA was used to enrich specifically mRNA which ranges from 0.5 to 2% depending on the tissue type. We used the Oligotex mRNA Mini Kit from Qiagen™ which yielded 198µg of total RNA from 14400 ovules and after mRNA enrichment the yield was 1µg of mRNA (Fig. 26). From this starting material of mRNA, we constructed a gateway-compatible cDNA library using CloneMiner™ II cDNA Library Construction Kit. This library was then sub-cloned into the prey vector converting it into an expression library. In a similar way, we also prepared an expression library from isolated pollen grains.

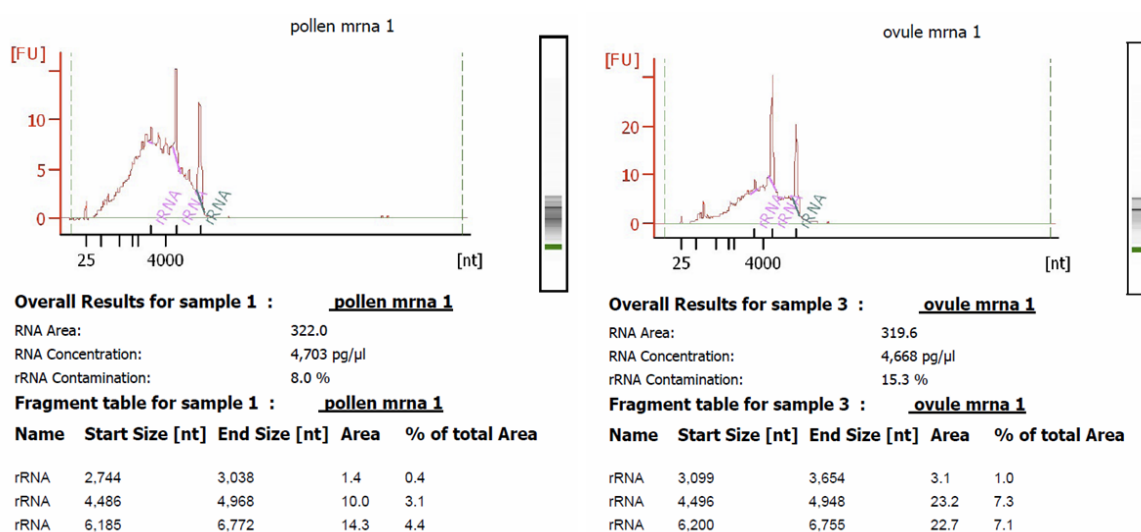


**Figure 26. A plot representing mRNA peaks of pollen and ovule mRNA used for library preparation.**

We used this expression library and performed a SUS screen with YDA (bait) and MPK6 (bridge). From this screen, we identified numerous interacting proteins (Tab. 4). The candidates will be analyzed by performing interaction assays with full length clones and bimolecular fluorescence complementation (BiFC), in the future.

Gene	Gene Model Description
AT1G02780	emb2386   Ribosomal protein L19e family protein
AT1G08820	VAMP/SYNAPTOBREVIN-ASSOCIATED PROTEIN 27-2, VAP27-2
AT1G19310	RING/U-box superfamily protein
AT1G21750	ARABIDOPSIS THALIANA PROTEIN DISULFIDE ISOMERASE 5, ATPDI5, ATPDIL1-1, PDI-LIKE 1-1, PDI5, PDIL1-1, PROTEIN DISULFIDE ISOMERASE 5
AT1G22300	14-3-3 PROTEIN G-BOX FACTOR14 EPSILON, 14-3-3EPSILON, GENERAL REGULATORY FACTOR 10, GF14 EPSILON, GRF10
AT1G22882	Galactose-binding protein
AT1G25540	PFT1   phytochrome and flowering time regulatory protein

AT1G26630	ATELF5A-2, ELF5A-2, EUKARYOTIC ELONGATION FACTOR 5A-2, FBR12, FUMONISIN B1-RESISTANT12
AT1G34640	peptidases
AT1G35160	14-3-3 PROTEIN G-BOX FACTOR14 PHI, 14-3-3PHI, GENERAL REGULATORY FACTOR 4, GF14 PHI, GF14 PROTEIN PHI CHAIN, GRF4
AT1G62333	unknown protein
AT1G62790	Bifunctional inhibitor/lipid-transfer protein/seed
AT1G63220	Calcium-dependent lipid-binding (CaLB domain) family
AT1G65270	unknown protein
AT1G71780	unknown protein
AT1G74060	Ribosomal protein L6 family protein
AT1G75630	AVA-P4, VACUOLAR H <sup>+</sup> -PUMPING ATPASE 16 KDA PROTEOLIPID SUBUNIT 4
AT1G76180	EARLY RESPONSE TO DEHYDRATION 14, ERD14
AT1G77710	ATCCP2, CCP2, CONSERVED IN CILIATED SPECIES AND IN THE LAND PLANTS 2
AT1G79040	PHOTOSYSTEM II SUBUNIT R, PSBR
AT1G80230	Rubredoxin-like superfamily protein; FUNCTIONS IN: cytochrome-c oxidase activity;
AT2G03680	SKU6, SPIRAL1, SPR1
AT2G20920	Protein of unknown function
AT2G22425	Microsomal signal peptidase 12 kDa subunit
AT2G23090	Uncharacterised protein family SERF
AT2G27140	HSP20-like chaperones superfamily protein
AT2G33810	SPL3, SQUAMOSA PROMOTER BINDING PROTEIN-LIKE 3
AT2G38540	ARABIDOPSIS THALIANA LIPID TRANSFER PROTEIN 1, ATLTP1, LIPID TRANSFER PROTEIN 1, LP1, LTP1
AT2G44080	ARGOS-LIKE, ARL
AT2G45470	AGP8, ARABINO GALACTAN PROTEIN 8, FASCICLIN-LIKE ARABINO GALACTAN PROTEIN 8, FLA8
AT2G47240	CER8, ECERIFERUM 8, LACS1, LONG-CHAIN ACYL-COA SYNTHASE 1
AT2G47710	Adenine nucleotide alpha hydrolases-like superfamily
AT3G14595	Ribosomal protein L18ae family;
AT3G16370	GDSL-like Lipase/Acylhydrolase superfamily protein
AT3G17000	UBC32, UBIQUITIN-CONJUGATING ENZYME 32
AT3G20520	GDPDL5, GLYCEROPHOSPHODIESTER PHOSPHODIESTERASE (GDPD) LIKE 5, SHV3-LIKE 3, SVL3
AT3G51510	unknown protein
AT3G52590	EARLY-RESPONSIVE TO DEHYDRATION 16, EMB2167, EMBRYO DEFECTIVE 2167, ERD16, HAP4, HAPLESS 4, UBIQUITIN EXTENSION PROTEIN 1, UBIQ1
AT3G55360	CER10, ECR, ATTSC13, TSC13   3-oxo-5-alpha-steroid
AT3G60600	VAP27-1, VAP, (AT)VAP, VAP27
AT4G01400	unknown protein
AT4G05050	UBQ11   ubiquitin 11
AT4G27500	PPI1, PROTON PUMP INTERACTOR 1

AT4G32520	ATSHMT3, SERINE HYDROXYMETHYLTRANSFERASE 3, SHM3
AT4G32530	ATPase, F0/V0 complex
AT5G02490	ATHSP70-2, HSP70-2
AT5G04750	F1F0-ATPase inhibitor protein, putative
AT5G08290	YELLOW-LEAF-SPECIFIC GENE 8, YLS8, Encodes Dim1 homolog.
AT5G10450	14-3-3 PROTEIN G-BOX FACTOR14 LAMBDA, 14-3-3LAMBDA, AFT1, G-BOX REGULATING FACTOR 6, GRF6
AT5G15200	Ribosomal protein S4;
AT5G21990	ATTPR7, OEP61, OUTER ENVELOPE PROTEIN 61, TETRATRICOPEPTIDE REPEAT 7, TPR7
AT5G24580	Heavy metal transport/detoxification superfamily protein
AT5G25940	early nodulin-related
AT5G39950	ARABIDOPSIS THIOREDOXIN H2, ATH2, ATTRX2, ATTRXH2, THIOREDOXIN 2, THIOREDOXIN H2, TRX2, TRXH2
AT5G42000	ORMDL family protein
AT5G46860	RABIDOPSIS THALIANA SYNTAXIN OF PLANTS 22,
AT5G48810	ARABIDOPSIS CYTOCHROME B5 ISOFORM D, ATB5-B, ATCB5-D, B5 #3, CB5-D, CYTB5-B, CYTOCHROME B5 ISOFORM D
AT5G51510	unknown protein
AT5G54540	unknown protein
AT5G60460	Preprotein translocase Sec, Sec61-beta subunit protein
AT5G62740	ATHIR1, ATHIR4, HIR1, HIR4, HYPERSENSITIVE INDUCED REACTION 4, HYPERSENSITIVE-INDUCED RESPONSE PROTEIN 1
AT5G65430	14-3-3 PROTEIN G-BOX FACTOR14 KAPPA, 14-3-3KAPPA, GENERAL REGULATORY FACTOR 8, GF14 KAPPA, GRF8
AT5G67590	FRO1, FROSTBITE1
AT5G67600	WIH1, WINDHOSE 1
AT1G01100	60S acidic ribosomal protein family
AT1G04440	CASEIN KINASE LIKE 13, CKL13
AT1G04750	AT VAMP7B, ATVAMP721, VAMP721, VAMP7B, VESICLE-ASSOCIATED MEMBRANE PROTEIN 721, VESICLE-ASSOCIATED MEMBRANE PROTEIN 7B
AT1G05210	Transmembrane protein 97, predicted
AT1G09070	(AT)SRC2, ATSRC2, SOYBEAN GENE REGULATED BY COLD-2, SRC2
AT1G19360	REDUCED RESIDUAL ARABINOSE 3, RRA3
AT1G29850	double-stranded DNA-binding family protein
AT1G58380	XW6   Ribosomal protein S5 family protein
AT1G72370	P40, AP40, RP40, RPSAA   40s ribosomal protein SA
AT2G22670	IAA8, INDOLEACETIC ACID-INDUCED PROTEIN 8
AT2G23170	ncodes an IAA-amido synthase that conjugates Asp and other amino acids to auxin in vitro.
AT2G26300	ARABIDOPSIS THALIANA G PROTEIN ALPHA SUBUNIT 1, ATGPA1, G PROTEIN ALPHA SUBUNIT 1, GP ALPHA 1, GPA1
AT2G29960	ARABIDOPSIS THALIANA CYCLOPHILIN 5, ATCYP5, CYCLOPHILIN 19-4, CYCLOPHILIN 5, CYP19-4, CYP5
AT2G32950	COP1, ATCOP1, DET340, FUS1, EMB168   Transducin/WD40

AT2G40950	ATBZIP17, BZIP17
AT2G48010	RECEPTOR-LIKE KINASE IN FLOWERS 3, RKF3
AT3G04840	Ribosomal protein S3Ae;
AT3G10800	Encodes bZIP28, a putative membrane-tethered transcriptional factor.
AT3G11660	NDR1/HIN1-LIKE 1, NHL1
AT3G13882	Ribosomal protein L34
AT3G15580	ATG8I, APG8H   Ubiquitin-like superfamily protein
AT3G15820	REDUCED OLEATE DESATURATION 1, ROD1
AT3G18030.	ATHAL3A, HAL3A, HAL3, ATHAL3   HAL3-like protein A
AT3G54820	PIP2;5, PIP2D, PLASMA MEMBRANE INTRINSIC PROTEIN 2;5, PLASMA MEMBRANE INTRINSIC PROTEIN 2D
AT3G57880	Calcium-dependent lipid-binding (CaLB domain)
AT3G58700	Ribosomal L5P family protein;
AT4G24770	31-KDA RNA BINDING PROTEIN, ARABIDOPSIS THALIANA RNA BINDING PROTEIN, APPROXIMATELY 31 KD, ATRBP31, ATRBP33, CP31, RBP31
AT4G28440	Nucleic acid-binding, OB-fold-like protein
AT4G37930	SERINE HYDROXYMETHYLTRANSFERASE 1, SERINE TRANSHYDROXYMETHYLTRANSFERASE, SERINE TRANSHYDROXYMETHYLTRANSFERASE 1, SHM1, SHMT1, STM
AT5G03520	ARABIDOPSIS RAB HOMOLOG E1D, ATRAB-E1D, ATRAB8C, ATRABE1D, RAB GTPASE HOMOLOG 8C, RAB HOMOLOG E1D, RAB-E1D, RAB8C
AT5G17170	ENH1, ENHANCER OF SOS3-1
AT5G19440	NAD(P)-binding Rossmann-fold superfamily protein
AT5G41520	RNA binding Plectin/S10 domain-containing protein
AT5G42980	ATH3, ATTRX3, ATTRXH3, THIOREDOXIN 3, THIOREDOXIN H-TYPE 3, THIOREDOXIN H3, TRX3, TRXH3
AT5G48580	FK506- and rapamycin-binding protein 15 kD-2
AT5G55230	ATMAP65-1, MAP65-1, MICROTUBULE-ASSOCIATED PROTEINS 65-1

**Table 4. Genes which were isolated from the split ubiquitin based three hybrid assay (YDA-MPK6-prey).**

## Discussion

### 6.1 NMA and suspensor cell elongation

The extra-embryonic cells of the suspensor have been ascertained with numerous functions, but nutrient and hormone translocation has been their major function in many plant species. Suspensor morphology is highly diverse, varying from a single cell to a complex multicellular structure according to their adaptation to the environment (Raghavan 2006). In some cases the suspensor even functions by complementing endosperm cells and providing nutrients to the developing embryos (Nagl, 1976). However, the impact of suspensor length on embryo development has not been studied. Here we describe a mutant (*nma*) where the suspensor cells fail to elongate resulting in a short suspensor. In consequence to this phenotype, *nma* mutant embryos develop slower when compared to WT, suggesting suspensor length is one of the determinants for the developmental progression of the embryo. This result was also verified by studying another mutant (*ssp*) with a short suspensor phenotype which results from a reduced number of suspensor cells rather than their smaller size (Bayer et al., 2009). At least in *Arabidopsis* it can be clearly stated that a short suspensor leads to slower development of the embryo. From an ecological adaptation point of view, suspensor length could play an important role in *Arabidopsis* since it is a weed with a short life span and it has to complete its life cycle within a season. Even within one silique, all developing embryos are in competition with each other for nutrients and hormone allocation during early embryo development. In this perspective, faster development is also an advantage for an embryo which might be accomplished by a longer suspensor.

There might be two reasons that explain how the suspensor length determines the developmental progression. Firstly, the embryo needs space in the embryo sac for its growth and development; this is achieved by stretching the suspensor by cell elongation. When the suspensor is shorter, the embryo still resides in the micropylar niche between the integuments where space is a constraint for its development. Secondly, as suspensors are shorter in the two mutants described (*nma* and *ssp*) thus the surface area required for hormone and nutrient transport is reduced which might result in developmental delay of the embryos.

Although *NMA* expression was detected in both female and male gametophytic cells there was no mutant effect on pollen tube growth or the fertilization event itself. This evidence further suggested that the developmental delay occurs only after fertilization. Furthermore, the function of *NMA* in suspensor cell elongation was shown to be cell-autonomous. Additionally, suspensor-specific activity of *NMA* is sufficient to partially rescue the developmental delay observed in *nma* mutants. The partial rescue might be due to the promoter used, whose expression is activated in embryos around four to eight cell stage and this might be too late to fully rescue the developmental delay at early embryonic stages. However, when characterized at transition stage all embryos were fully rescued. All these results suggest that the *NMA* protein functions in suspensor cell elongation is necessary for early embryo development.

*NMA* encodes a putative exo-polygalacturonase. Polygalacturonases in general cleave pectin polysaccharides thereby loosening the cell wall and allowing for cell elongation (Caffall and Mohnen 2009). In *Arabidopsis*, the *QUARTET2* (*QRT2*) gene encodes an endo-polygalacturonase and was shown to be involved in the tetrad cell-separation event during pollen development (Ogawa et al., 2009). *ARABIDOPSIS DEHISCENCE ZONE POLYGALACTURONASE1* (*ADPG1*) and *ADPG2* which are closely related to *QRT2*, are also required for anther dehiscence. Additionally, *ADPG2* and *QRT2* are involved in floral organ abscission, which implicates that these three polygalacturonases are involved in cell separation events (Ogawa et al., 2009). Another endo-polygalacturonase *POLYGALACTURONASE INVOLVED IN EXPANSION1* (*PGX1*) was recently shown to be involved in cell elongation during flower and hypocotyl development (Xiao et al., 2014). The contrasting phenotypes observed between these polygalacturonases suggest that their expression and the composition of the pectin polysaccharides in the given tissue will also determine the enzymatic effect on the cell wall. We also conducted a functional analysis to study the catalytic activity of *NMA* by heterologously expressing it in *E. coli*. The soluble *NMA* protein which we obtained did not show enzymatic activity when we tested it with different substrates such as tri-galacturonic acid, sodium poly-pectate or even oligogalacturonic acid. This lack of activity in our experiments was likely due to two reasons. As *NMA* is an exo-polygalacturonase, its posttranslational modification such as glycosylation might be essential for the activity however, *E. coli* does not post-translationally glycosylate proteins. This could be achieved by expressing *NMA* in



eukaryotic organisms such as yeast or even in tobacco BY2 cells. Another reason could be because of the inappropriate substrate used in these assays. The pectin composition of the zygote cell wall might be specifically modified for elongation and NMA might need modified pectins for its function *in vitro*.

Cell elongation defects in *nma* mutants can only be seen during early embryogenesis and during internode elongation. Although the internode length in *nma* mutant plants is shorter when compared to WT the overall plant height was not affected in general. Overall, loss of function of *nma* does not affect the growth and development of the adult plant other than the internode elongation. This case might be observed because of two reasons. Even though polygalacturonases are redundantly expressed in *Arabidopsis*, *NMA* expression during early embryogenesis might break this redundancy and cause an effect specific for cell elongation. This phenotype could then be complemented by other polygalacturonases at later stages of embryogenesis. Alternatively, the composition of pectin polysaccharides in the zygote and later in the suspensor cell wall could only be modified by a NMA-specific function. Later as the embryo develops, the pectin composition in the pro-embryo might also change which could then be modified by other polygalacturonases for proper cell elongation to occur.

The action of polygalacturonases on pectins (homogalacturonans) results in their modification and the pectin matrix in the cell wall will be disturbed by these modifications (Caffall and Mohnen 2009). We were not able to notice any changes in the pectin matrix by immunolocalization studies in *nma* embryos in comparison WT. This could be either because the function of NMA does not produce such major changes to the pectin matrix or the embryos used for these experiments were too old.

Function of *NMA* is spatially restricted by its expression. *NMA* is predominantly expressed in reproductive tissue; this is not surprising as it belongs to clade C of the glycosyl hydrolase family 28 where all the members in this clade are defined as pollen and flower polygalacturonases (Markovic and Janecek, 2001). *NMA* is also expressed in female gametophytic cells, however there was no phenotype observed probably because of redundant gene function in this family. It is expressed at lower levels in vegetative tissues such as the expanding leaf, the root, and certain parts of the stem and also in columella cells.

The *nma* mutant was identified in a screen for paternal effect mutants. The analysis of offspring from reciprocal crosses did not show a fully penetrant paternal effect of *nma* on suspensor cell elongation. However, unequal parental contribution was noticed whereby with respect to suspensor elongation the paternal allele was stronger than the maternal. This might be simply due to the different expression strengths observed in the sperm and egg cell. Although there was no direct quantitative measurement conducted, the promoter analysis suggested this unequal expression (Fig.14). The cell elongation defects in the *nma* mutant were severe at early embryonic stages suggesting that parental contribution is necessary for zygote elongation. The unequal contribution of protein or transcripts between sperm and egg cell might have a more profound effect than the de novo synthesis on zygote elongation. This might be a similar case in *NMA* and suspensor cell elongation. Interestingly, the *short suspensor* mutant also shows a paternal effect (Bayer et al., 2009). These results on paternal effect in both *ssp* and *nma* might suggest that there is a common theme to bring suspensor cell elongation under paternal control. This might be advantageous in small herbs where cross-pollination can affect embryo development indirectly.

## 6.2 SSP signaling cascade in Arabidopsis embryogenesis

As SSP signaling cascade mediated by YDA determines aspects of suspensor cell fate determination (Lukowitz et al., 2004; Bayer et al., 2009). MPK3/6 which acts downstream to ERECTA family signaling in stomata development was also shown to play a role in embryo development (Wang et al., 2007; Lampard et al., 2008; Bush and Krysan 2007). A list of selected genes was prepared considering three criteria; they should be expressed in embryo according to publicly available expression data, they should contain the short consensus L/PXSPR/K and their function in cell elongation or cell fate determination. In an attempt to identify substrates for MPK3 and MPK6 in SSP signaling in embryogenesis, these candidate genes were analyzed by generating their phospho-mutants (Sörensson et al., 2012). This was achieved by mutating a single serine residue in the consensus of these target genes to either glutamic acid or to alanine, rendering the site a phospho-mimic or non-phosphorylatable version, respectively. Most of the phospho-mutants failed to produce any effects on embryogenesis and only two of them produced over-expression phenotypes (PID and PP2C5a). This might have resulted because mutating a single

residue did not produce any effect on protein stability or activity in these target proteins. Some of the target proteins contain one or more of serine and threonine residues in their amino acid sequence, may be mutating all of them will produce additive or significant effect on the protein activity. Where as in SPCH for example which is one of the known phosphorylation targets of MPK3 and MPK6, phospho-mimic versions of single or multiple serine or threonine residues affect stomata development (Lampard et al., 2008). SPCH amino acid sequence contains a stretch where the above mentioned consensus is repeated several times, this stretch is absent in both MUTE and FAMA which coincidentally seem not to be regulated directly by MPK3/6 during stomata development. This might further imply that single serine residue might not be enough to decide that it is a target of MPK3/6 for phosphorylation. Alternatively, these genes may not be targets of MPK3 or MPK6 in the embryo.

As an alternative approach we used a split ubiquitin based yeast two hybrid assay to test or to identify the components of the SSP signaling cascade. Novel candidates were identified from this screen to directly interact with YDA or with YDA and MPK6 (as a bridge in a three component system). MPK3 and MPK6 were shown to directly interact with YDA, suggesting that YDA and MPK3/6 might form a scaffold in which YDA can specify the interaction with the target for phosphorylation. Additionally, cell cycle genes such as CYCLIN D4:1 and E2Fa were shown to directly interact with YDA, which suggests that the YDA pathway might regulate the entry into cell division during embryo development. In order to orient these divisions YDA might require a cytoskeleton regulator such as MICROTUBULE ASSOCIATED PROTEIN (MAP65). MAP65-5 was shown to interact with YDA directly (this study) and in addition YDA was recently shown to regulate MAP65-1 which in turn is important for orientation of the plane of cell division during root development (Smékalová et al., 2014). Interestingly, we also identified MAP65-1 in a screen with the YDA-MPK6 scaffold (Tab.4). Among the proteins which showed to interact with YDA-MPK6 are E2Fc, CYCLIN D3;1, SSP, MITOGEN ACTIVATED KINASE KINASE4 (MKK4), IAA8 and an auxin response factor (ARF10)(Fig. 23, 25 and Tab. 4). Additionally, the presence of MPK6 also strengthened the interaction of proteins with YDA such as CYCLIN D4;1, MAP65-5 and E2Fa (Fig. 25). SSP which is upstream of YDA was shown to interact with the YDA-MPK6 scaffold (Fig. 25), suggesting a possibility that SSP directly regulates YDA or that it might be associated with the YDA scaffold during

signal transduction. As auxin plays an important role in plant growth and development, it was not surprising to find an auxin response factor (ARF10) to interact with the YDA-MPK6 scaffold (Fig. 25). Along with ARF10, IAA8 was also isolated in a later screen with YDA-MPK6 (Tab. 4) which further suggests that localized auxin accumulation and auxin response might influence cell fate determination in the daughter cells of the zygote. We also showed the interaction of MKK4 with YDA-MPK6 (Fig. 25) which was shown to be an immediate downstream target of YDA (Wang et al., 2007). However some of the candidates which were shown to interact with YDA-MPK6 should also be tested with YDA alone. These interactions should be retested again in yeast or with direct protein-interaction studies as should all these interactions be retested in another system and also by an *in vitro* kinase assay.

In order to broaden the pool of candidates, an ovule library was used to screen proteins interacting with YDA in presence of MPK6 (as a bridge). In this screen we identified several proteins which function in brassinosteroid signaling, stress response, organelle growth, cytoskeleton regulating proteins, vesicular proteins and others (Tab. 4). However, the expression library used does not always contain full-length proteins, so the positive candidates should be first tested with full-length proteins. Overall, the split ubiquitin system has been successful in identifying components of SSP signaling. Additional verification in another system is essential to state this interaction and the functional importance of these interactions should also be tested in embryo development. Novel potential candidates isolated will broaden our knowledge about cell fate determination of suspensor and early embryo development.

## Materials and Methods

### Plant growth conditions

*Arabidopsis thaliana* Col-0 and Ler-0 ecotypes were used in this study. All seeds were surface-sterilized with 95% ethanol and 70% ethanol and placed on half Murashige and Skoog (MS) medium with or without 1% sucrose. The seedlings were grown in a chamber with long-day conditions 16 h at 3-kilolux illumination, 8-h-dark at 65% relative humidity and at 23°C.

Two T-DNA alleles of *nma* (*nma-2*, SALK\_126968; *nma-3*, SALK\_015991) and one *ssp* allele (*ssp-2*, SALK\_051462) were ordered from the Nottingham Arabidopsis Stock Center NASC United Kingdom (Alonso et al., 2003). Genotyping of T-DNA lines were performed with a gene-specific primer 160-3 R for *nma-3*, 160.2 R for *nma-2* and left boarder primer LBb1.3 (Appendix Tab.1). The wild type alleles were genotyped with 160-3 WT LP and 160-3 WT RP for *nma-3* and 160-2 WT LP and 160-3 WT RP for *nma-2* (Appendix Tab.1). *ssp-2* plants were genotyped as described in Bayer et al., 2009.. We designed a derived cleaved amplified polymorphic sequence from dCAPS Finder 2.0 (Neff et al., 2002) for genotyping *nma-1* allele with Swal restriction site, where *nma-1* allele is cleaved. For selecting plants expressing PGIIIB constructs BASTA (Bayer cropscience, Germany) was sprayed according to manufacturer's instructions.

### Plant transformation

Plant transformation was performed by floral-dip method mediated through GV3101 strain of *Agrobacterium tumefaciens* (Clough and Bent 1998). Plasmids were transformed into GV3101 *Agrobacterium* strain harboring pSoup and selected on LB-plates containing 50µg/ml kanamycin, 25µg/ml gentamycin, 25µg/ml rifampicin. Several colonies were inoculated into 200ml LB medium with the above mentioned antibiotics and grown overnight at 30°C. The cell culture was pelleted down and resuspended in a 5% sucrose solution with 0.03% silvett L-77. The flowers were dipped in this solution and later placed in a covered tray to maintain humidity for one day.

## Light Microscopy

The immature seeds were cleared in modified Hoyer's solution (70% w/v chloralhydrate, 4% w/v glycerol, 5% w/v gum arabic) (Bayer et al., 2009) for one hour to two days depending on the stage of the embryo. The cleared seeds were observed under Zeiss Axio Imager.Z1 (with Differential Interference Contrast settings). The measurements were performed with length tool in Axiovision 4 software. GUS images were obtained from Carl Zeiss SteREO Discovery.V12 with the dark field settings for inflorescence and bright field settings for seedling. For fluorescence imaging dissected seeds were mounted on 4%PFA or water and gently squeezed over the cover slip and observed under Olympus FV1000 confocal microscope. For imaging pollen, the pollen were dispersed in DAPI solution in 10% glycerol and observed under Carl Zeiss LSM 780 NLO. 1:1000 dilution of DAPI stock was used to stain the nucleus. The images were then processed in Adobe Photoshop and Adobe Illustrator CS4.

## GUS staining

For GUS staining, the tissue was fixed for 20 minutes in 90% acetone and then washed with GUS washing solution (0.1M phosphate buffer pH7.0, 10mM EDTA and 2mM potassium ferricyanide) for 10 minutes two times. The fixed tissue were stained with GUS staining solution (0.1M phosphate buffer pH7.0, 10mM EDTA, 1mM potassium ferricyanide, 1mM potassium ferrocyanide and 1mg/ml x-glucose) in vacuum for 10 minutes and then incubated at 37°C for 24 hours. The staining was stopped by incubating the tissue in a solution of acetic acid and ethanol 3:1 for one hour. The serial washing was performed with 75%, 50% and 25% ethanol on the tissues, later the tissue was mounted on 10% glycerol or chlorohydrate solution.

## Molecular cloning

To rescue the *nma* mutant phenotype genomic version of 2.5kbp promoter elements and 1.6kbp length *NIMNA* was cloned including promoter region with At2g33160P-FC and At2g33160-RC primers into PGII::Kanamycin vector. The first intron was removed by overlap extension PCR from the *NMA* genomic version with Mutagenesis

F and Mutagenesis R primers. The dCAPS marker was designed including the first intron where the mutant allele is cut by *SwaI* giving 300 and 20 bp fragments.

*AscI* and *PacI* restriction sites were inserted at position -1 and again right after the predicted signal peptide (SP) +78b respectively by site directed mutagenesis. These two restriction sites were used to insert the mCitrine YFP coding sequence at both of these sites to generate *PGIIK::SP:YFP:NMAPG* and *PGIIK::YFP:SP:NMAPG*. For expression analysis of the *NMA* promoter element was cloned into *pGIIb::3xVenus-N7:ocs3'* and to *pHyg::GUS* with the *At2g33160P-FC* and *At2g33160P-RC*. For over expression *CaMV 35S* promoter and for mis-expression of *NMA*, *SUC5* (Baud et al., 2005), OBF BINDING PROTEIN 1(OBP1) (Skirycz et al., 2008) and *At5g42200* promoters (personal communication with Jixiang Kong) were substituted for *NMA* promoter between -1369bp to -23b region with the use of restriction sites *XhoI* and *BstEII* at this respective position within *pNMA::SP:YFP:NMA PG* vector. To generate phospho mutants, the genomic version of the interested gene was cloned into *pGII:UAS* vector using *EcoRI* and *BamHI* restriction sites. The serine residues were mutated to alanine or to aspartic acid by PCR mutagenesis.

### **RNA extraction and cDNA synthesis**

RNA was extracted from various tissues of the plant with RNeasy Plant Mini Kit (Qiagen) and the cDNA synthesis was carried out as per manufacturer's instruction on cDNA synthesis kit (RevertAid First Strand cDNA Synthesis Kit, Thermo scientific). Later on Quantitative Real-Time PCR was conducted on these samples per manufacturer's instruction (SYBR® Select Master Mix, Life technologies) with *NqRT-PCR-F4* and *NqRT-PCR-R4* primers. For analyzing the transcript of *nma-2* and *nma-3* different set of primers were used; *RT-5F* and *RT-5R* primers were used to amplify the region before T-DNA insertion and *NRT-F3* and *NRT-R4* for the region after the insertion in *nma-3*. While *NRT-F3* and *NRT-R4* primers were used to amplify the region before and *RT 160.2 F* and *RT 160.2 R* primers for the region after the insertion in *nma-2*.

### **cDNA library construction**

The ovules were collected from siliques which were one or two day after pollination old in *RNA Later* (Qiagen, Germany). And the RNA was extracted right after collection as mentioned above. Inflorescences were collected in a 50ml Falcon tubes and later

12% sucrose solution was used to precipitate the pollen grains. The precipitate was washed two to three times to remove the floral debris with the same solution. The precipitate was directly used for RNA extraction. Around 200µg of total RNA was extracted for both pollen and ovule. Entire amount was used for mRNA enrichment (Oligotex mRNA Mini Kit, Qiagen). The quality of mRNA was analyzed in Agilent 2100 Bioanalyzer system (Fig.24). The mRNA was concentrated in a speedVac (Eppendorf) and used for cDNA library construction using CloneMiner™ II cDNA Library Construction Kit. During the library preparation, the third fractionate was also used as the mRNA content was low in both of these difficult samples.

### **Split Ubiquitin Assay and screen**

Bait vectors and prey vectors were transformed into THY AP4 and THY AP5 yeast strains respectively using YEAST Transformation kit (Sigma-Aldrich). The transformed yeast cells were plated on synthetic complete (SC) drop-out plates – leucine for bait and – (tryptophan and uracil) for prey. Few colonies were inoculated into a liquid culture and grown over night at 30°C with shaking. 1ml of the culture was pelleted and resuspended in 200µl of YPD. 20µl each of bait and prey were mixed in a 96 well plate according to required combinations and plated on YPD plates. After 8 hours the colonies were replica plated on SC drop-out plates (-adenine-histidine). To observe the interaction between bait and prey the colonies were plated on minimal medium with varying concentration of methionine and along with the dilutions (1/10, 1/100).

To transform a library into yeast cells we used yeast transformation kit from Clontech™. In a screen where yeast cells contain bait+bridge+prey the minimal media was used. When only prey library was transformed into yeast cells bait, uracil synthetic complete drop-out plates were used.

### **Heterologous expression of *NMA*.**

The coding sequence of *NMA* was cloned into pETM20 with NcoI and BamHI restriction sites. BL21 and RosettaGami™ strains were used for *NMA* expression. Pre culture of 20ml LB medium containing appropriate antibiotics such as 15 µg/ml kanamycin (pETM20) and 34 µg/ml chloramphenicol (pRARE2) for BL21; kanamycin(pETM20), chloramphenicol (pRARE2) and 12.5 µg/ml tetracycline (*gor* mutation for disulfide bond formation in the cytoplasm) for RosettaGami™. The whole



of preculture was used to inoculate main culture of one liter. The cells were grown till 0.5 to 0.8 OD and later the expression was induced by 500 $\mu$ M IPTG. After induction the cells were continued to grow overnight but at 18-20°C. The purification protocol and the assistance were provided from Ancilla Neu and Remco Spranger. Cells were harvested by centrifuging at 4000rpm for 15 minutes. The pellet was then resuspended in 10 ml of lysis buffer per gram of cell pellet. A small amount of lysozyme was added to the suspension and incubated on ice for 15 minutes. Suspension was then passed through the french press (emulsiflex). All the debris was pelleted by centrifuging the lysate for 45 minutes at 18 krpm. Ni-NTA Agarose (Qiagen) was placed in a column and stored in 20% ethanol, while the centrifuging step is on progress; the ethanol was removed from the column. And then the column was washed with 10 column volumes (CV) and later equilibrated with 10 CV of lysis buffer. The supernatant from the centrifuging step was filtered with syringe fitted with 1.2  $\mu$ m filter. Now this filtrate is passed through the column and the flow through can be saved for further analysis. The column is then washed until the flow-through does not appear blue in the Bradford test. Also save the wash, and now start to elute with elution buffer until it doesn't turn blue in the Bradford test any more. A small aliquot or sample should be saved from all the steps and analysed by SDS-PAGE. The purified protein can be tested by cleaving the 6X HIS tag from the protein using TEV protease.

#### Lysis buffer

50 mM Na<sub>2</sub>HPO<sub>4</sub>/NaH<sub>2</sub>PO<sub>4</sub> pH 8.0

300 mM NaCl

10 mM Imidazole

1 mM DTT (add just before use)

1:1000 Triton-X 100

#### Wash buffer:

50 mM Na<sub>2</sub>HPO<sub>4</sub>/NaH<sub>2</sub>PO<sub>4</sub> pH 8.0

300 mM NaCl

20 mM Imidazole

1 mM DTT (add just before use)

Elution buffer:

50 mM Na<sub>2</sub>HPO<sub>4</sub>/NaH<sub>2</sub>PO<sub>4</sub> pH 8.0

300 mM NaCl

200 mM Imidazole

1 mM DTT (add just before use)

### **Polygalacturonase assay**

#### **2-cyanoacetamide method (Gross 1982)**

It is one of the simple methods to analyze polygalacturonases activity. 100µg of purified THR-His-NMA protein was incubated with 0.4% polygalacturonic acid (PGA) (Sigma-Aldrich) in sodium acetate buffer pH 5.0 at 30°C. The reactions were terminated two hours after incubation with cold 1.0ml 100mM borate buffer and with 0.2ml of 1% 2-cyanoacetamide. And the absorbance was measured to quantify the released reducing groups at 276nm after blanking the spectrophotometer with a reaction at zero time.

#### **Nelson and Somogyi method**

500µg of HIS-NMA was incubated with substrate 0.5% PGA in sodium acetate buffer pH4.5 for at least one hour. The reactions were terminated with equal volume of cupralkaline solution by immersing the tubes in boiling water for 15 minutes and then cooled it room temperature. Half volume of arsenomolybdate solution was added to the solution to measure the absorbance at 540nm. We used a polygalacturonase (Sigma-Aldrich) as a positive control and BSA as negative control. A curve was plotted between Standard  $\Delta A_{540nm}$  readings and µmoles of D-galacturonic acid. We determined the µmoles of D-galacturonic acid liberated using the standard curve and enzymatic units were calculated. Oligo-galacturonic acid substrate was prepared by autoclaving the polygalacturonases two times at 121°C for 15 minutes and the substrate was precipitated using speed vac.

#### **Nuclear Magnetic Resonance (NMR)**

All NMR spectra were recorded at 298 K on a Bruker AVIII-600 spectrometer equipped with a room temperature probehead. 1D spectra of 1H trigalacturonic acid were obtained from samples containing 1 mM TGA in buffer containing either 25 mM acetate pH 5.0, 100 mM NaCl and 100 % D<sub>2</sub>O

or buffer containing 25 mM phosphate pH 5.8, 100 mM NaCl and 100 % D<sub>2</sub>O. For positive control experiments, the reaction was started by addition of 2.5 µg pectinolyase. The sample was incubated at room temperature and spectra were recorded at various time points. For NMA degradation experiments, 10 µl of NMA preparation purified either from *E. coli* or from baculo virus culture were added to the reaction. After incubation at room temperature, spectra were recorded at indicated time points.

## References

- Abbott, D.W. and Boraston, A.B.** (2007a) A family 2 pectate lyase displays a rare fold and transition metal-assisted beta-elimination. *The Journal of biological chemistry*, **282**, 35328–36.
- Abbott, D.W. and Boraston, A.B.** (2007b) The structural basis for exopolygalacturonase activity in a family 28 glycoside hydrolase. *Journal of molecular biology*, **368**, 1215–22.
- Alonso, José M, Stepanova, A.N., Leisse, T.J., et al.** (2003) Genome-wide insertional mutagenesis of *Arabidopsis thaliana*. *Science (New York, N.Y.)*, **301**, 653–7.
- Anderson, C.T., Carroll, A., Akhmetova, L. and Somerville, C.** (2010) Real-time imaging of cellulose reorientation during cell wall expansion in *Arabidopsis* roots. *Plant physiology*, **152**, 787–96.
- Babu, Y., Musielak, T., Henschen, A. and Bayer, M.** (2013) Suspensor length determines developmental progression of the embryo in *Arabidopsis*. *Plant physiology*, **162**, 1448–58.
- Baskin, T.I., Beemster, G.T.S. and Judy-march, J.E.** (2004) Disorganization of Cortical Microtubules Stimulates Tangential Expansion and Reduces the Uniformity of Cellulose Microfibril Alignment among Cells in the Root of *Arabidopsis* 1. , **135**, 2279–2290.
- Baud, S., Wuillème, S., Lemoine, R., Kronenberger, J., Caboche, M., Lepiniec, L. and Rochat, C.** (2005) The AtSUC5 sucrose transporter specifically expressed in the endosperm is involved in early seed development in *Arabidopsis*. *The Plant journal* □: for cell and molecular biology, **43**, 824–36.
- Bayer, M., Nawy, T., Giglione, C., Galli, M., Meinel, T. and Lukowitz, Wolfgang** (2009) Paternal control of embryonic patterning in *Arabidopsis thaliana*. *Science (New York, N.Y.)*, **323**, 1485–8.
- Bergmann, D.C., Lukowitz, Wolfgang and Somerville, Chris R** (2004) Stomatal development and pattern controlled by a MAPKK kinase. *Science (New York, N.Y.)*, **304**, 1494–7.
- Bozhkov, P.V., Suarez, M.F., Filonova, L.H., Daniel, G., Zamyatnin, A. a, Rodriguez-Nieto, S., Zhivotovsky, B. and Smertenko, A.** (2005) Cysteine protease mcll-Pa executes programmed cell death during plant embryogenesis. *Proceedings of the National Academy of Sciences of the United States of America*, **102**, 14463–8.
- Bozhkov, P, V., Filonova, L, H., Suarez, M, F (2005b)** Programmed Cell Death in Plant Embryogenesis *Current Topics in Developmental Biology* **67**, 135-179
- Brett, C, T (2000)** Cellulose microfibrils in plants: Biosynthesis, deposition, and integration into the cell wall *International Review of Cytology* **199**, 161-199

- Brown, R.M.** (2003) Cellulose Structure and Biosynthesis□: What is in Store for the 21st Century□? , 487–495.
- Bush, S.M. and Krysan, P.J.** (2007) Mutational evidence that the Arabidopsis MAP kinase MPK6 is involved in anther, inflorescence, and embryo development. *Journal of experimental botany*, **58**, 2181–91.
- Caffall, K.H. and Mohnen, D.** (2009) The structure, function, and biosynthesis of plant cell wall pectic polysaccharides. *Carbohydrate research*, **344**, 1879–900.
- Ceccarelli, N., Lorenzi, Roberto and Alpi, A.** (1981a) Gibberellin Biosynthesis in *Phaseolus coccineus* Suspensor. *Zeitschrift für Pflanzenphysiologie*, **102**, 37–44.
- Chanliaud, E., Burrows, K.M., Jeronimidis, G. and Gidley, M.J.** (2002) Mechanical properties of primary plant cell wall analogues. *Planta*, **215**, 989–96.
- Cheng, Y., Dai, X. and Zhao, Y.** (2007) Auxin synthesized by the YUCCA flavin monooxygenases is essential for embryogenesis and leaf formation in Arabidopsis. *The Plant cell*, **19**, 2430–9.
- Cosgrove, D.J.** (2005) Growth of the plant cell wall. *Nature reviews. Molecular cell biology*, **6**, 850–61.
- David, H., Bade, P., David, A., et al.** (1995) Pectins in walls of protoplast-derived cells imbedded in agarose and alginate beads. , 122–130.
- Delmer, D.P.** (1999) Cellulose Biosynthesis: Exciting Times for A Difficult Field of Study. *Annual review of plant physiology and plant molecular biology*, **50**, 245–276.
- Donaldson, L. A and Knox, J Paul** (2012) Localization of cell wall polysaccharides in normal and compression wood of radiata pine: relationships with lignification and microfibril orientation. *Plant physiology*, **158**, 642–53.
- Friml, Jirí, Vieten, A., Sauer, M., Weijers, D., Schwarz, H., Hamann, T., Offringa, R. and Jürgens, G.** (2003) Efflux-dependent auxin gradients establish the apical-basal axis of Arabidopsis. *Nature*, **426**, 147–53.
- Friml, Jirí, Yang, X., Michniewicz, M., et al.** (2004) A PINOID-dependent binary switch in apical-basal PIN polar targeting directs auxin efflux. *Science (New York, N.Y.)*, **306**, 862–5.
- Grefen, C.** (2014) Arabidopsis Protocols J. J. Sanchez-Serrano and J. Salinas, eds. , **1062**, 659–678.
- Grefen, C., Lalonde, S. and Obrdlik, P.** (2007) Split-ubiquitin system for identifying protein-protein interactions in membrane and full-length proteins., *Curr Protoc Neurosci* Oct;Chapter 5:Unit 5.27
- Gross, K. C. (1982)** A rapid and sensitive spectrophotometric method for assaying polygalacturonases using 2-cyanoacetamide *HortScience* **17**, 933-934

- Ha, M. a, Apperley, D.C., Evans, B.W., Huxham, I.M., Jardine, W.G., Viëtor, R.J., Reis, D., Vian, B. and Jarvis, M.C.** (1998) Fine structure in cellulose microfibrils: NMR evidence from onion and quince. *The Plant journal*: for cell and molecular biology, **16**, 183–90.
- Hellens RP, Edwards EA, Leyland NR, Bean S, Mullineaux PM** (2000)pGreen: a versatile and flexible binary Ti vector for Agrobacterium mediated plant transformation. *Plant Mol Biol* 42: 819–832
- Henrissat, B., Vegetales, M. and Grenoble, F.-** (1991) A classification of glycosyl hydrolases based sequence similarities amino acid. *Biochem J* , **280**, 309–316.
- Hu, J., Mitchum, M.G., Barnaby, N., et al.** (2008) Potential sites of bioactive gibberellin production during reproductive growth in Arabidopsis. *The Plant cell*, **20**, 320–36.
- Irshad, M., Canut, H., Borderies, G., Pont-Lezica, R. and Jamet, E.** (2008) A new picture of cell wall protein dynamics in elongating cells of Arabidopsis thaliana: confirmed actors and newcomers. *BMC plant biology*, **8**, 94.
- Jeong, S., Volny, M. and Lukowitz, Wolfgang** (2012) Axis formation in Arabidopsis - transcription factors tell their side of the story. *Current opinion in plant biology*, **15**, 4–9.
- Johnsson, N. and Varshavsky, a** (1994) Split ubiquitin as a sensor of protein interactions in vivo. *Proceedings of the National Academy of Sciences of the United States of America*, **91**, 10340–4.
- Kanaoka, M.M., Pillitteri, L.J., Fujii, H., Yoshida, Y., Bogenschutz, N.L., Takabayashi, J., Zhu, J.-K. and Torii, K.U.** (2008) SCREAM/ICE1 and SCREAM2 specify three cell-state transitional steps leading to arabidopsis stomatal differentiation. *The Plant cell*, **20**, 1775–85.
- Kataoka, Y. and Kondo, T.** (1998) FT-IR Microscopic Analysis of Changing Cellulose Crystalline Structure during Wood Cell Wall Formation. *Macromolecules*, **31** 760–764.
- Kawashima, T. and Goldberg, R.B.** (2010) The suspensor: not just suspending the embryo. *Trends in plant science*, **15**, 23–30.
- Kim, T.-W., Michniewicz, M., Bergmann, D.C. and Wang, Z.-Y.** (2012) Brassinosteroid regulates stomatal development by GSK3-mediated inhibition of a MAPK pathway. *Nature*, **482**, 419–22.
- Lampard, G.R., Lukowitz, Wolfgang, Ellis, B.E. and Bergmann, D.C.** (2009) Novel and expanded roles for MAPK signaling in Arabidopsis stomatal cell fate revealed by cell type-specific manipulations. *The Plant cell*, **21**, 3506–17.
- Langdale, J. a** (2008) Evolution of developmental mechanisms in plants. *Current opinion in genetics & development*, **18**, 368–73.

- Lau, S., Slane, D., Herud, O., Kong, J. and Jürgens, G.** (2012) Early embryogenesis in flowering plants: setting up the basic body pattern. *Annual review of plant biology*, **63**, 483–506.
- Lennon, K.A., and Lord, E.M.** (2000). The in vivo pollen tube cell of *Arabidopsis thaliana*. I. Tube cell cytoplasm and wall. *Protoplasma* **214**, 45–56.
- Li, Y.-Q., Mareck, A., Faleri, C., Moscatelli, A., Liu, Q. and Cresti, M.** (2002) Detection and localization of pectin methylesterase isoforms in pollen tubes of *Nicotiana tabacum* L. *Planta*, **214**, 734–40.
- Lombardi, L., Ceccarelli, N., Picciarelli, Piero and Lorenzi, Roberto** (2007) DNA degradation during programmed cell death in *Phaseolus coccineus* suspensor. *Plant physiology and biochemistry*, **45**, 221–7.
- Lukowitz, W, Gillmor, C.S. and Scheible, W.R.** (2000) Positional cloning in *Arabidopsis*. Why it feels good to have a genome initiative working for you. *Plant physiology*, **123**, 795–805.
- Lukowitz, Wolfgang, Roeder, A., Parmenter, D. and Somerville, C.** (2004) A MAPKK kinase gene regulates extra-embryonic cell fate in *Arabidopsis*. *Cell*, **116**, 109–19.
- López-Bucio, J.S., Dubrovsky, J.G., Raya-González, J., Ugartechea-Chirino, Y., López-Bucio, J., Luna-Valdez, L. a de, Ramos-Vega, M., León, P. and Guevara-García, a a** (2014) *Arabidopsis thaliana* mitogen-activated protein kinase 6 is involved in seed formation and modulation of primary and lateral root development. *Journal of experimental botany*, **65**, 169–83.
- Maheshwari, P and Singh, B.** (1952) Embryology of *Macrosolen cochinchinensis* *Bot. Gaz.* **114**, 20-32
- Mansfield S.G., Briar'd' L.G:** (1991) Early Embryogenesis in *Arabidopsis thaliana*. II. The Developing Embryo. *Can J Bot*, **69**:461-476.
- Marin-Rodriguez, M.C.** (2002a) Pectate lyases, cell wall degradation and fruit softening. *Journal of Experimental Botany*, **53**, 2115–2119.
- Markovic, O. and Janecek, S.** (2001) Pectin degrading glycoside hydrolases of family 28: sequence-structural features, specificities and evolution. *Protein engineering*, **14**, 615–31
- Mccann, M C, Wells, B and Roberts, K** (1990) Direct visualization of cross-links in the primary plant cell wall. *J Cell Sci* **96**, 323–334.
- Meinke, D.W.** (1991) Perspectives on Genetic Analysis of Plant Embryogenesis. *The Plant cell*, **3**, 857–866.
- Meyer, S, Melzer, M., Truernit, E., Hümmer, C., Besenbeck, R., Stadler, R and Sauer, N** (2000) AtSUC3, a gene encoding a new *Arabidopsis* sucrose

- transporter, is expressed in cells adjacent to the vascular tissue and in a carpel cell layer. *The Plant journal*, **24**, 869–82.
- Meyer, Stefan, Lauterbach, C., Niedermeier, M., Barth, I., Sjolund, R.D. and Sauer, Norbert** (2004) Wounding Enhances Expression of AtSUC3 , a Sucrose Transporter from Arabidopsis Sieve Elements and Sink Tissues. *Plant Physiology*, **134**, 684–693.
- Nagl, W and Ktihner, S.** (1976) Early Embryogenesis in *Tropaeolum majus* L.: Diversification of Plastids. *Planta.* , **19**, 15–19.
- Nagl, Walter** (1990) Translocation of Putrescine in the Ovule, Suspensor and Embryo of *Phaseolus coccineus*. *Journal of Plant Physiology*, **136**, 587–591.
- Nelson N** (1944) A photometric adaptation of the Somogyi method for the determination of glucose. *Journal of Biological chemistry* 375-380
- Newcomb W, and Fowke L.C.** (1974). *Stellaria media* embryogenesis:the development and ultrastructure of the suspensor.*Canadian Journal of Botany* **52**: 607–614.
- Nishiyama, Y., Langan, P. and Chanzy, H.** (2002) Crystal structure and hydrogen-bonding system in cellulose I $\beta$  from synchrotron X-ray and neutron fiber diffraction. *Journal of the American Chemical Society*, **124**, 9074–82.
- Normanly, J.** (2010) Approaching cellular and molecular resolution of auxin biosynthesis and metabolism. *Cold Spring Harbor perspectives in biology*, **2**, a001594.
- Obrdlik, P., El-bakkoury, M., Hamacher, T., et al.** (2004) K<sup>+</sup> channel interactions detected by a genetic system optimized for systematic studies of membrane. , *Proc Natl Acad Sci U S A.* **101**. 12242-7
- Ogawa, M., Kay, P., Wilson, S. and Swain, S.M.** (2009) ARABIDOPSIS DEHISCENCE ZONE POLYGALACTURONASE1 (ADPG1), ADPG2, and QUARTET2 are Polygalacturonases required for cell separation during reproductive development in Arabidopsis. *The Plant cell*, **21**, 216–33.
- O'Neill and York (2003).** The composition and structure of primary cell walls. In *The Plant Cell Wall* (JKC Rose ed) Blackwell, pp. 1-54.
- Palusa, S.G., Golovkin, M., Shin, S.-B., Richardson, D.N. and Reddy, A.S.N.** (2007) Organ-specific, developmental, hormonal and stress regulation of expression of putative pectate lyase genes in Arabidopsis. *The New phytologist*, **174**, 537–50.
- Parisot, J., Langlois, V., Sakanyan, V. and Rabiller, C.** (2003) Cloning expression and characterization of a thermostable exopolygalacturonase from *Thermotoga maritima*. *Carbohydrate Research*, **338**, 1333–1337.



- Peter, S.** (2006) Biomechanics of plant growth . *American Journal of Botany*, **93**, 1415–1425.
- Petersen TN, Brunak S, von Heijne G, Nielsen H** (2011) SignalP 4.0: discriminating signal peptides from transmembrane regions. *Nat Methods* **8**: 785–786
- Petrásek, J., Mravec, J., Bouchard, R., et al.** (2006) PIN proteins perform a rate-limiting function in cellular auxin efflux. *Science (New York, N.Y.)*, **312**, 914–8
- Piaggese, a, Picciarelli, P, Lorenzi, R and Alpi, a** (1989) Gibberellins in Embryo-Suspensor of Phaseolus coccineus Seeds at the Heart Stage of Embryo Development. *Plant physiology*, **91**, 362–6.
- Pickersgill R1, Jenkins J, Harris G, Nasser W, R.-B.J.** (1994) The structure of Bacillus subtilis pectate lyase in complex with calcium. *Nat Struct Biol*, **1**, 717–723.
- Raghavan V. 2006.** Double Fertilization – Embryo and Endosperm Development in Flowering Plants. Springer, Berlin
- Robert, H.S., Grones, P., Stepanova, A.N., Robles, L.M., Lokerse, A.S., Alonso, Jose M, Weijers, D. and Friml, Jiří** (2013) Local auxin sources orient the apical-basal axis in Arabidopsis embryos. *Current biology*: *CB*, **23**, 2506–12.
- Robles, L.M., Lokerse, A.S., Alonso, Jose M and Weijers, D.** (2013) Report Local Auxin Sources Orient the Apical-Basal Axis in Arabidopsis Embryos. , 2506–2512.
- Rojo, E., Gillmor, C.S., Kovaleva, V., Somerville, C R and Raikhel, N.V.** (2001) VACUOLELESS1 is an essential gene required for vacuole formation and morphogenesis in Arabidopsis. *Developmental cell*, **1**, 303–10.
- Sanderson, M.J.** (2003) r8s: inferring absolute rates of molecular evolution and divergence times in the absence of a molecular clock, *Bioinformatics* **19**, 301–302.
- Scheres, B., Wolkenfelt, H., Willemsen, V., Terlouw, M., Lawson, E., Dean, C. and Weisbeek, P.** (1994) Embryonic origin of the Arabidopsis primary root and root meristem initials. , **2487**, 2475–2487.
- Shea, E.M., Gibeaut, D.M. and Carpita, N.C.** (1989) Structural analysis of the cell walls regenerated by carrot protoplasts. *Planta*, **179**, 293–308.
- Sinnott, M.L.** (1990) Catalytic mechanisms of enzymic glycosyl transfer. *Chem. Rev.*, **90**, 1171–1202
- Sitrit, Y., Hadfield, K. a, Bennett, a B., Bradford, K.J. and Downie, a B.** (1999) Expression of a polygalacturonase associated with tomato seed germination. *Plant physiology*, **121**, 419–28.

- Skiryecz, A., Radziejwoski, A., Busch, W., et al.** (2008) The DOF transcription factor OBP1 is involved in cell cycle regulation in *Arabidopsis thaliana*. *The Plant journal*: for cell and molecular biology, **56**, 779–92.
- Smékalová, V., Luptovčiak, I., Komis, G., et al.** (2014) Involvement of YODA and mitogen activated protein kinase 6 in *Arabidopsis* post-embryogenic root development through auxin up-regulation and cell division plane orientation. *The New phytologist*.
- Somerville, C., Bauer, S., Brininstool, G., et al.** (2004) Toward a systems approach to understanding plant cell walls. *Science (New York, N.Y.)*, **306**, 2206–11.
- Stacey, Nicola, J., Roberts, Keith, Carpita, Nicholas, C., Wells, Brian and Mccann, Maureen C** (1995) Dynamic changes in cell surface molecules are very early events in the differentiation of mesophyll cells from *Zinnia elegans* into tracheary elements. *The Plant Journal*, **8**, 891–906.
- Stadler, Ruth, Wright, K.M., Lauterbach, C., Amon, G., Gahrtz, M., Feuerstein, A., Oparka, K.J. and Sauer, Norbert** (2005a) Expression of GFP-fusions in *Arabidopsis* companion cells reveals non-specific protein trafficking into sieve elements and identifies a novel post-phloem domain in roots. *The Plant journal*: for cell and molecular biology, **41**, 319–31.
- Stadler, R., Lauterbach, C , and Sauer, Norbert.** (2005b) Cell-to-Cell Movement of Green Fluorescent Protein Reveals Post-Phloem Transport in the Outer Integument and Identifies Symplastic Domains in *Arabidopsis* Seeds and Embryos 1. *Plant Physiology* , **139**, 701–712.
- Sugiyama, J., Persson, J., Chanzy, H., Recherche, C.D. and Vbgktales, M.** (1991) Combined Infrared and Electron Diffraction Study of the Polymorphism of Native Celluloses. , 2461–2466.
- Sörensson, C., Lenman, M., Veide-Vilg, J., Schopper, S., Ljungdahl, T., Grøtli, M., Tamás, M.J., Peck, S.C. and Andreasson, E.** (2012) Determination of primary sequence specificity of *Arabidopsis* MAPKs MPK3 and MPK6 leads to identification of new substrates. *The Biochemical journal*, **446**, 271–8.
- Swamy, BGL.** (1949) Embryological studies in the Orchidaceae II. Embryogeny. *Am Midl. Nat.* **41**, 202-232
- Somogyi M** (1952) Notes on sugar determination *Journal of Biological chemistry* 375-380
- Tanaka, H., Dhonukshe, P, Brewer, P.B. and Friml, J** (2006) Spatiotemporal asymmetric auxin distribution: a means to coordinate plant development. *Cellular and molecular life sciences*, **63**, 2738–54.
- Torki, M., Mandaron, P., Thomas, F., Quigley, F., Mache, R. and Falconet, D.** (1999) Differential expression of a polygalacturonase gene family in *Arabidopsis thaliana*. *Molecular & general genetics*, **261**, 948–52

- Ueda, M., Zhang, Z. and Laux, T.** (2011) Transcriptional activation of Arabidopsis axis patterning genes *WOX8/9* links zygote polarity to embryo development. *Developmental cell*, **20**, 264–70.
- Wang, H., Ngwenyama, N., Liu, Y., Walker, J.C. and Zhang, S.** (2007) Stomatal development and patterning are regulated by environmentally responsive mitogen-activated protein kinases in Arabidopsis. *The Plant cell*, **19**, 63–73.
- Ward J. M. , Kühn, C. , Tegeder, M. , Frommer, W. B., (1998)** Sucrose Transport in Higher Plants *International Review of Cytology* **178** 41-56
- Wardlaw, C.W.** (1955). Embryogenesis in Plants. (London: Methuen)
- Whitney, S.E.C., Wilson, E., Webster, J., Bacic, A., Reid, J.S.G. and Gidley, M.J.** (2006) Effects polymers on interactions with bacterial cellulose. *American Journal of Botany* , **93**, 1402–1414.
- Willats, W.G., Orfila, C., Limberg, G., et al.** (2001) Modulation of the degree and pattern of methyl-esterification of pectic homogalacturonan in plant cell walls. Implications for pectin methyl esterase action, matrix properties, and cell adhesion. *The Journal of biological chemistry*, **276**, 19404–13
- Wilson, S.M., Burton, R. a, Collins, H.M., Doblin, M.S., Pettolino, F. a, Shirley, N., Fincher, G.B. and Bacic, A.** (2012) Pattern of Deposition of Cell Wall Polysaccharides and Transcript Abundance of Related Cell Wall Synthesis Genes during Differentiation in Barley Endosperm. *Plant physiology*, **159**, 655–70.
- Wing, R. a, Yamaguchi, J., Larabell, S.K., Ursin, V.M. and McCormick, S.** (1990) Molecular and genetic characterization of two pollen-expressed genes that have sequence similarity to pectate lyases of the plant pathogen *Erwinia*. *Plant molecular biology*, **14**, 17–28.
- Wolf, S. and Greiner, S.** (2012) Growth control by cell wall pectins. *Protoplasma*, **249 Suppl** , S169–75.
- Word, K.** (1979) Kaurene and kaurenol biosynthesis in cell-free system of phaseolus coccineus suspensor. , **18**, 1657–1658.
- Xiao, C., Somerville, C. and Anderson, C.T.** (2014) POLYGALACTURONASE INVOLVED IN EXPANSION1 Functions in Cell Elongation and Flower Development in Arabidopsis. *The Plant cell*, **26**, 1018–35.
- Yang, H. and Murphy, A.S.** (2009) Functional expression and characterization of Arabidopsis ABCB, AUX 1 and PIN auxin transporters in *Schizosaccharomyces pombe*. *The Plant journal* □: for cell and molecular biology, **59**, 179–91.
- Yeung, E. C. and Meinke, D.W.** (1993a) Embryogenesis in Angiosperms: Development of the Suspensor. *The Plant cell*, **5**, 1371–1381.

- Yeung, Edward C.** (1980) Embryogeny of Phaseolus: the Role of the Suspensor. *Zeitschrift für Pflanzenphysiologie*, **96**, 17–28.
- Yoneda, A., Ito, T., Higaki, T., et al.** (2010) Cobtorin target analysis reveals that pectin functions in the deposition of cellulose microfibrils in parallel with cortical microtubules. *The Plant journal*: for cell and molecular biology, **64**, 657–67.
- Zablackis, E., Huang, J., Müllerz, B., Darvill, A.C. and Albersheim, P.** (1995) Characterization of the Cell-Wall Polysaccharides of Leaves, Arabidopsis. *Plant Physiology*, **107**, 1129–1138.
- Zhang, C., Yao, J., Zhou, C., Mao, L., Zhang, G. and Ma, Y.** (2013) The alkaline pectate lyase PEL168 of *Bacillus subtilis* heterologously expressed in *Pichia pastoris* is more stable and efficient for degumming ramie fiber. *BMC biotechnology*, **13**, 26.
- Zhang, L., Kars, I., Essenstam, B., et al.** (2014) Fungal endopolygalacturonases are recognized as microbe-associated molecular patterns by the arabidopsis receptor-like protein RESPONSIVENESS TO BOTRYTIS POLYGALACTURONASES1. *Plant physiology*, **164**, 352–64.

## Appendix

Table 1. Primers

Primer name	Primer sequence
160-3, R	ctctcttcttctcctcgcc
At2g33160P-FC	cggatctgtgtttttctcag
At2g33160P-RC	tctctcttcttggttgg
At2g33160-RC	aagtagaggacgatgtgattc
160-3, WT LP	ttccaggactatcacattgcc
160-3, WT RP	caaagagataacgctttgcg
160-2, WT LP	tgactcaatctcactagctgtgc
160-2, WT RP	aagctaaagatgattcgtaacg
LBb1.3	atthtgccgatttcggaac
NMA dC-F	aacaaacttgaatgagctgtaat
NMA dC-R	tgcgatacggacttagccatgtcttgatattaaa
NMAi1 AP-F	accaaaccaaagaagagagaggcgccgcaaaaattaattaagcgtctagggttctctgat
NMAi1 AP-R	atcagaagaaccctagacgcttaattaattttggcgcgccctctcttcttggtttgg
NMAi1 ASP-F	ccacgaaggaatatacccgcgccagtcgacttaattaataatcttgacgtcagaaa
NMAi1 ASP-R	ttctgacgtcaaagatttaattaagtcgactggcgcgccgggatattccttcgtgg
NMAi1-F	ttggatatctctgatgtcagatgacggaccagggcatggta
NMAi1-R	taccatgccctggcgcacatcgacatcagagatatccaa
NqRT-PCR-F4	tgcttctcttcttcttct
NqRT-PCR-R4	ttatctcttggctatctg
NRT-F3	gtcgtacactagctatgaa
NRT-R4	aatgacgatagggttccaa
p35Sas	aaaaaaggtaacccccgtgttctctccaaatg
p35Ss	tttttctcgagtcgacctgcaggcggccgca
pJ10as	aaaaaagggtaccctttacaccgtctcttgcctc
pJ10s	tttttctcgagggtccatgttctctatattct
pOBP1as	aaaaaagggtaccatcggagaaagggtgaagctt
pOBP1s	tttttctcgagcatagatttgggtgatgtgg
pSUC5as	aaaaaagggtaccctatgaaaagaaaaacgagcag
pSUC5s	tttttctcgagtgagtaagaacaggtagtc
RT 160.2 F	ttgtgtgagaacgttgg
RT 160.2 R	ggtttagtagcctcagta
RT-5F	tttgtgtgtgccttctc
RT-5R	aagtaatccaccgccagtaa
SSP1-I	ttagagaccacacgagaaggc
SSP1-R	taacatggcttggctgatcc
attB1F MPK3	ggggacaagttgtacaaaaaagcaggctcatgaacaccggcgggtggccaat
attB2 R MPK3	ggggaccactttgtacaagaaagctgggtcaccgtatgttgattgagtgct
attB1F MPK6	ggggacaagttgtacaaaaaagcaggctcatggacgggtgggtcaggtcaac
attB2 R MPK6	ggggaccactttgtacaagaaagctgggtcttctgatattctggattgaaa
attB1F SPCH	ggggacaagttgtacaaaaaagcaggctcatgcaggagataataaccggatt

attB2 R SPCH	ggggaccactttgtacaagaaagctgggtcgcagaatgtttgctgaattgt
attB1F BIN2	ggggacaagttgtacaaaaaagcaggctcatggctgatgataaggagatgc
attB2 R BIN2	ggggaccactttgtacaagaaagctgggtcagttccagattgattcaagaag
attB2 R SCRM1	ggggaccactttgtacaagaaagctgggtcgcataaccagcataccctgct
attB1F SCRM1	ggggacaagttgtacaaaaaagcaggctcatgggtcttgacggaaacaatg
attB2 R MAP65-5	ggggaccactttgtacaagaaagctgggtcatcgtcttctgaagagcaaca
attB1F MAP65-5	ggggacaagttgtacaaaaaagcaggctcatgtctccgtctcaaccacta
attB2 R SSP	ggggaccactttgtacaagaaagctgggtcttcttacttcaagaagagct
attB1F SSP	ggggacaagttgtacaaaaaagcaggctcatgggtgtgttactcactat
attB2 R YODA	ggggaccactttgtacaagaaagctgggtcgggtcctctgtttgtgatccg
attB1F YODA	ggggacaagttgtacaaaaaagcaggctcatgccttggaggagtaaataca
NX-35 sF3	caggatccacaagtttga
NX-35 R1	ggtagaggtgtggtaataag

## Curriculum vitae

### Personal details

Name: Yashodar Babu  
Date of Birth: 14<sup>th</sup> March 1985  
Place of Birth: Tumkur/India

### School

1991-1998 St. Mary's School-Tumkur, India  
1998-2001 Sarvodaya Boys High School- Tumkur, India  
2001-2003 Vidya Pre-University College- Tumkur, India

### University

2003-2007 Bachelor of Science in Agriculture, University of Agricultural Sciences, Bangalore, India  
2008-2010 Master of Science in Horticulture, Erasmus Mundus International Master program jointly offered by University of Bologna, Bologna, Italy., Technical University of Munich, Munich, Germany., University of Natural Resources and Applied Sciences, Vienna, Austria  
2010-2014 Doctorate , University of Tübingen, Max Planck Institute for Developmental Biology, Tübingen, Germany under the guidance of Martin Bayer/ Prof. Gerd Jürgens.